

*Synthesis of Fine Chemicals From Renewables using
Supported Metal Oxides as Catalysts*

A thesis submitted to the University of Pune

*for the award of
Doctor of Philosophy in Chemistry*

*by
Trupti V. Kotbagi*

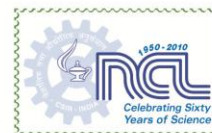
*Under the guidance of
Dr. M. K. Dongare*

*Catalysis & Inorganic Chemistry Division
National Chemical Laboratory
Pune - 411 008, India*

April, 2013



राष्ट्रीय रासायनिक प्रयोगशाला
(वैज्ञानिक तथा औद्योगिक अनुसंधान परिषद)
डॉ. होमी भाभा रोड, पुणे - 411 008. भारत
NATIONAL CHEMICAL LABORATORY
(Council of Scientific & Industrial Research)
Dr. Homi Bhabha Road, Pune - 411008. India



Certificate of the Guide

Certified that the work incorporated in the thesis, “*Synthesis of Fine Chemicals from Renewables using Supported Metal Oxides as Catalysts*” submitted by *Trupti Kotbagi*, for the Degree of *Doctor of Philosophy*, was carried out by the candidate under my supervision in the Catalysis and Inorganic Chemistry Division, National Chemical Laboratory, Pune - 411008, India. Such material as has been obtained from other sources has been duly acknowledged in the thesis.

(Dr. M. K. Dongare)

Research Guide

(Dr. S. B. Umbarkar)

Research Co-guide

Date:

Communications Channels
+91 20 25902000
+91 20 25893300
+91 20 25893400

Fax +91 20 25902601 (Director)
+91 20 25902660 (Admin.)
+91 20 25902639 (Business Development)

URL : www.ncl-india.org

Declaration by the Candidate

I, hereby declare that the thesis entitled “*Synthesis of fine chemicals from renewables using supported metal oxides as catalysts*” submitted by me for the degree of *Doctor of Philosophy* to the *University of Pune*, is the record of work carried out by me at *Catalysis and Inorganic Chemistry Division, National Chemical Laboratory, Pune - 411008* under the guidance of *Dr. M. K. Dongare* and has not formed the basis for the award of any degree or diploma to this or any other University. I further declare that the material obtained from other sources has been duly acknowledged in the thesis.

(Trupti V. Kotbagi)

Signature of the Candidate

Date:

dedicated

to

Mother Earth.....



Acknowledgements

At the end of my doctorate I take this opportunity to thank all the people who made this thesis possible and brought this day in my life. This journey in which I have trespassed infinite ways has turned out to be a treasured reminiscence for me.

Foremost I pay all my heartfelt gratitude to my Ph. D. mentor Dr. M. K. Dongare. Without his immense support and encouragement this would have not been possible. Under his guidance I learnt to circumvent many difficulties. I warmly thank him for his valuable advice, constructive criticism and his extensive discussions around my work.

I am also profoundly indebted to my co-guide Dr. S. B. Umbarkar. I acknowledge her for her patience, understanding and attention which provided me with sound and swift basis throughout my Ph.D. tenure. Thanks a million for all that you have done for me. Both will continue to be a sheer source of inspiration in coming times.

I thank Dr. Ankush for his help in the thesis correction. I extend my thanks to all the scientific and non-scientific staff of Catalysis Division, for the help they rendered during my tenure as a research student. I also wish to thank the members of CMC division for carrying out the characterization of my samples. I thank all the members of SAO and accounts section for helping me in one way or the other during my stay at NCL.

My sincere thanks to Dr. S. Pal, Director, National Chemical Laboratory, Pune for providing the infrastructure to carry out the research work and utilize the facilities.

The financial assistance in the form of Senior Research Fellow from Council of Scientific & Industrial Research, New Delhi, is duly acknowledged.

I owe special debt to my school teachers Mrs. Reena Clifton and Mrs. Anita Deshpande and my undergraduate and post graduate teachers Mrs. Dikshit, Mr. Gandhi and specially Dr. (Mr.) Deepak Shendge who showed me an appropriate way to the world of research.

I specially thank the team at UCCS Lille - Dr. Christine, Prof. Edmond, Prof. Franck and all the others whose names I could not mention here for giving me an opportunity to be a part of the collaborative work between NCL and UCCS. I wholeheartedly thank Prof. Kemnitz and group for giving me a chance to work in his group in Germany under CSIR-BMBF collaborative project. I find immense pleasure to thank my lab mates- Swati, Rajesh, Samadhan, Vidhya, Vaibhav, Sumeet, Macchindra, Ashvini, Atul, Pavan, Prakash and Lina for always maintaining a lively and healthy atmosphere in the lab which made me comfortable to carry out my work. I enjoyed working with all of you. A million thanks to Swati for I could depend on her for many things. I thank Rajesh, Vaibhav and Rajesh Varkhedkar to help me in explaining many basic concepts of organic chemistry. I cannot express how gratified I am towards Vidhya for her hospitality and care during my illness. I also wish to thank all the friends in division and friends in NCL.

I owe my deepest gratitude to my mom, dad and brother, for their unfailing love and untiring faith shown in me for whatever decisions I took in life.

And ultimately, I thank the Creator for bestowing me with all the strength and nerve it took during my journey towards the destination. This day would have never arisen in my life without His blessings

Trupti

Contents

Chapter 1:	Introduction	1
1.1	Renewables - Rationale and significance	2
1.2	Biorefinery concept	3
1.3	Biodiesel production	4
1.4	Glycerol - A versatile molecule	5
1.5	Catalytic approaches to the valorization of bio-derived glycerol	6
1.6	Solid catalysts for acid-catalyzed transformations of glycerol	13
1.7	Scope and objective of the thesis	14
1.8	Outline of the thesis	14
1.9	References	15
Chapter 2:	Synthesis and characterization of the MoO₃/SiO₂ catalysts by sol-gel method	19
2.1	Introduction	21
2.1.1	Catalysis	21
2.2	Experimental section	26
2.2.1	Material	26
2.2.2	Catalyst Preparation	26
2.2.3	Characterization	28
a)	Powder X-ray diffraction studies	28
b)	Nitrogen adsorption studies	28
c)	Ammonia temperature programmed desorption	28
d)	FT-IR of adsorbed pyridine	28
e)	Fourier transform infrared spectroscopic studies	28
f)	Raman spectroscopic studies	29
g)	Transmission microscopic studies	29
2.3	Results and Discussion	29
2.3.1	X-ray diffraction studies	31
2.3.2	Textural characterization	32
2.3.3	Acidity measurements	36
2.3.4	FT-IR of adsorbed pyridine	37

2.3.5	FT-IR spectroscopic studies	38
2.3.6	Raman spectroscopic studies	39
2.3.7	Transmission Electron Microscopic Studies	42
2.4	Conclusions	46
2.5	References	46
Chapter 3:	Sol-gel synthesized MoO₃/SiO₂ catalyst for esterification reactions	49
3.1	Introduction	51
3.2	Experimental Section	55
3.2.1	Material	55
3.2.2	Typical esterification reaction	55
	a) Esterification of acetic acid and ethanol in batch mode	55
	b) Esterification of acetic acid and ethanol in continuous mode	55
	c) Esterification of glycerol with acids	55
3.2.3	Catalyst Separation and investigation of the different catalytic species	56
3.2.4	Screening of 20 mol% MoO ₃ /SiO ₂ catalyst under industrial conditions	56
3.2.5	Characterization of catalyst fractions	56
3.3	Results and Discussion	58
3.4	Conclusions	78
3.5	References	78
Chapter 4:	Acetalization and Etherification of glycerol using MoO₃/SiO₂ solid acid catalyst	81
Section 4A:	Acetalization of Glycerol using MoO₃/SiO₂ Solid Acid Catalyst	83
4A.1	Introduction	83
4A.2	Experimental Section	86
4A.2.1	Material	86
4A.2.2	Typical acetalization procedure	86

4A.3	Results and discussion	86
4A.3.1	Catalytic activity	86
4A.3.2	Plausible mechanism for acetalization reaction	91
4A.4	Conclusion	92
Section 4B:	Glycerol etherification using MoO₃/SiO₂ Solid Acid Catalyst	94
4B.1	Introduction	94
4B.2	Experimental section	95
4B.2.1	Material	95
4B.2.2	Typical etherification reactions	95
	a) Open reflux system	95
	b) Closed reflux system	95
4B.3	Results and discussion	95
4B.4	Conclusions	99
4.5	References	100
Chapter 5:	Summary and Conclusions	103

List of publications

Presentations

ABSTRACT OF THE THESIS

SYNTHESIS OF FINE CHEMICALS FROM RENEWABLES USING SUPPORTED METAL OXIDES AS CATALYSTS

Owing to the fast depleting fossil fuels, inflating environmental concerns there is an increasing use of biomass for energy, chemicals and material supply. It is one of the key issues of sustainable development because bio-based resources are renewable and CO₂ neutral in contrast with the fossil fuels. Recently, researchers worldwide are toiling to explore new routes to convert renewable resources like biomass (lignocellulosic material) to range of important organic intermediates. Production of bio fuels (bio-diesel, bioethanol) from non-edible oils has been another important industrial development in the last decade. Glycerol is a 10% by-product of biodiesel production leading to an alarming increase of crude glycerol in the market. The global biodiesel market is estimated to reach 37 billion gallons by 2016. Therefore, it is imperative to find alternative uses for glycerol. Glycerol has many uses in different industries, such as food, paint, pharmaceutical, cosmetic, soap, toothpaste, *etc*, but its surplus is dramatically increasing. It is necessary to develop new and innovative transformations of glycerol into valuable products. Some potential uses for glycerol include: hydrogen gas production, glycerine acetate as a potential fuel additive, composite additive, citric acid production, cosmetic bonding agent for makeup including eye drops and conversion to propylene glycol, acrolein, ethanol and epichlorhydrin, as antifreeze agent and as fuel additives. Dumesic *et al.* has studied the value addition of glycerol to fuels and chemicals by catalytic processing.^[1] Normally most of these catalytic organic transformations are carried out using acid catalyst, base catalyst or oxidation or reduction catalyst. Conventionally, strong mineral acids such as caustic soda, H₂SO₄, *p*-toluenesulfonic acid, HF, AlCl₃ are used for acid catalyzed organic transformations of glycerol. However considering the disadvantages of homogeneous acid catalysts, researchers are trying to find alternative heterogeneous catalysts for the purpose.

Solid, heterogeneous catalysts have the advantages of ease of recovery and recycling and are readily amenable to continuous processing. Heterogeneous catalysis has, moreover, already been widely applied in oil refining and bulk chemicals manufacture. Moreover, solid acids are less corrosive and easier (safer) to handle than mineral acids such as H₂SO₄, and HF. A wide variety of solid-acid catalysts is

available: acidic clays, zeolites, silica-occluded heteropoly acids, sulfonated polysiloxanes, Nafion (sulfonated perfluoroalkyl resin) and Nafion-silica composites, and a variety of hybrid sulfonated mesoporous systems.

Recently, oxides and mixed oxides have attracted remarkable attention in the stream of heterogeneous catalysis, serving either as catalysts or as supports for many catalytically active species (metallic nanoparticles, oxides, organometallic complexes, enzymes, etc). Oxides are preferred for their thermal and chemical stability, and mechanical strength when used as supports and also for their intrinsic activity (acidic, basic, redox) when employed as catalysts. Thus many studies have been devoted to the preparation and characterization of these solids. Metal oxide catalysts (viz., MoO_3 , WO_3) supported on SiO_2 , Al_2O_3 , ZrO_2 and TiO_2 have been extensively investigated because of their catalytic activity in oxidation and acid catalyzed organic reactions.

Considering the overall rationale and significance of the topic, the thesis deals with the use of molybdenum oxide supported on mesoporous SiO_2 as solid acid catalyst for various acid catalyzed transformations of glycerol to value added chemicals.

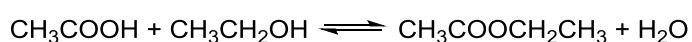
The **first chapter** describes a critical review on worldwide production of glycerol, the available glut of glycerol and its utilisation for various commodity materials. The chapter gives an idea about current scenario in the field of valorization of biorenewables. The chapter briefly describes the biorefinery concept - its rationale and significance. It also gives an overview of the application of heterogeneous catalysis in the field of valorization of biorenewables, especially glycerol.

The **second chapter**, describes the synthesis and characterization of $\text{MoO}_3/\text{SiO}_2$ catalysts using sol-gel technique. A series of $\text{MoO}_3/\text{SiO}_2$ catalysts with varying MoO_3 loadings (1-20 mol%) were prepared by sol-gel technique using ethyl silicate-40 and ammonium heptamolybdate (AHM) as silica and molybdenum source respectively. The sol-gel derived samples were calcined at 500 °C and characterized using various techniques viz., PXRD, BET surface area, NH_3 -TPD, pyridine-FTIR, TEM, Raman and FTIR spectroscopy. The extensive characterization of the catalysts shows presence of various well dispersed entities like SMA, polymolybdate species or molybdenum oxide nanoparticles depending on the Mo loading. The present sol-gel method of preparation allowed us to increase the dispersion and the range of existence of the Mo entities with the Mo loading. It has been shown that the SMA at low Mo loading was not formed during the sol-gel process but by the rehydration of the

calcined catalyst due to the presence of nanosize molybdenum oxospecies supported on high surface mesoporous silica support. This was directly correlated to the ZPC of the silica support, which permits the preservation of this HPA that is only stable in solution at low pH values typically below 2. The increase of the Mo loading induces an increase of the pH of the solution inside the pores and in agreement with literature data, the presence of a well dispersed surface polymolybdate is observed. It has also been shown that the formation of aggregates of α -MoO₃ particles at high Mo loadings originates from the AHM precipitation during the sol-gel preparation. The acidity measurements are in good agreement with this description, well dispersed phases exhibiting only Lewis acidity, whereas molybdenum oxide particles exhibit both Lewis and Brønsted ones. The later aim was to investigate the *in situ* formation of various catalytic species.

The **third chapter** deals with esterification reactions using sol-gel synthesized MoO₃/SiO₂ as solid acid catalyst. The chapter has been divided in two sections-

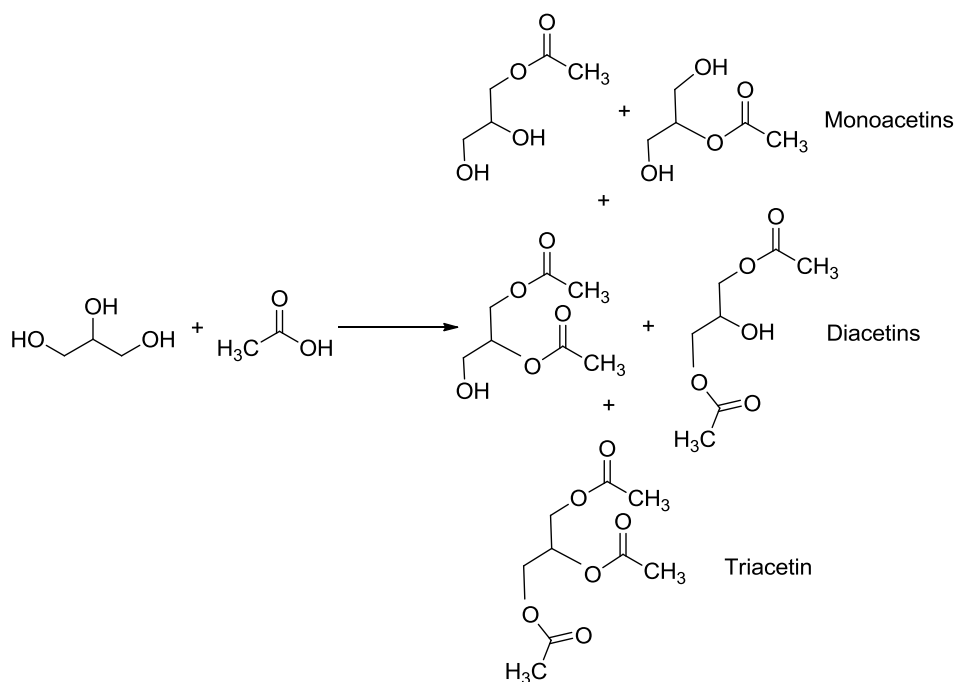
A] Section 3A - This section describes the esterification of ethanol and acetic acid using 20 mol% MoO₃/SiO₂ solid acid catalysts (Scheme 1). The reaction was carried in batch mode as well as continuous mode.



Scheme 1. Esterification of acetic acid and ethanol

The catalyst showed a very high acid conversion (83 %) in 8 h when the esterification was carried out in batch mode. This catalyst was very efficient and stable for continuous esterification of ethanol with acetic acid for ethyl acetate formation. The catalyst was tested for 60 h without any deactivation and without change in the composition of azeotropically distilled fraction (EtOAc/EtOH/H₂O; 93/4/3). During the course of the esterification reaction, the reaction mixture turned blue indicating change in the nature of catalyst under reaction condition. These catalytically active species formed in the reaction mixture were isolated and extensively characterized by FT-IR, Raman, PXRD, BET-Surface area, NH₃-TPD, EDAX and TEM. The characterization results revealed *in situ* formation of silicomolybdic acid on silica surface in presence of water to be catalytically active species responsible for the acid catalyzed reactions.

B] Section 3B - In this section, esterification of glycerol with various acids was investigated using sol-gel synthesized $\text{MoO}_3/\text{SiO}_2$ solid catalysts. Acetylation of glycerol (Scheme 2) with acetic acid was studied in details to achieve maximum conversion of glycerol and high selectivity for triacetin.

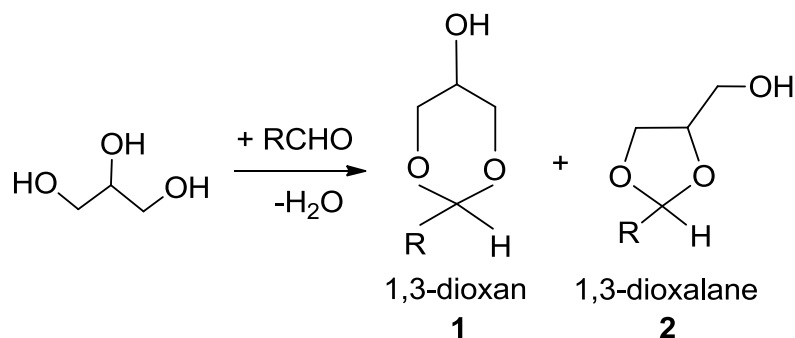


Scheme 2. Acetylation of glycerol with acetic acid

The effects of various parameters such as reaction temperature, molar ratio of AcOH:glycerol, catalyst loading and time-on-stream were studied to optimize reaction conditions so as to achieve the aim of high selectivity for triacetin. Glycerol conversion of 100% was obtained in 2 h and more than 85% selectivity for triacetin was obtained in 20 h at reaction temperature of 118 °C, 10 wt% catalyst loading (w.r.t. wt of glycerol), and AcOH:glycerol molar ratio of 10:1.

In the **Fourth Chapter** acetalization and etherification of glycerol has been studied in details using series of $\text{MoO}_3/\text{SiO}_2$ catalysts. This chapter has been thereby divided into two sections:-

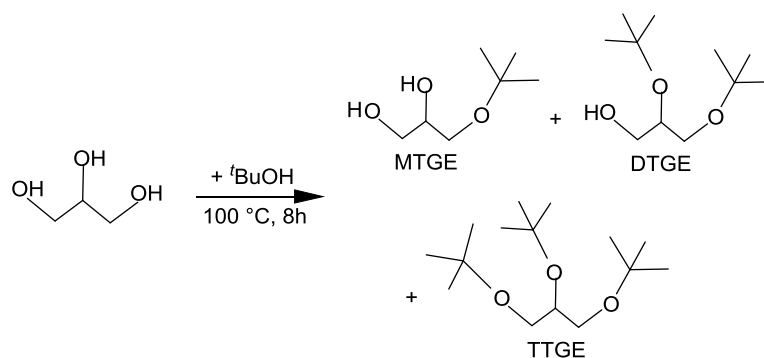
A] Section 4A - In this section, acetalization of glycerol with various aldehydes has been carried out using mesoporous $\text{MoO}_3/\text{SiO}_2$ as a solid acid catalyst (scheme 3).



Scheme 3. Acetalization of aldehyde with glycerol

Acetalization of glycerol with benzaldehyde was carried out using series of $\text{MoO}_3/\text{SiO}_2$ catalysts with varying MoO_3 loadings (1-20 mol%). Among the series, 20 mol% $\text{MoO}_3/\text{SiO}_2$ was found to be the most active catalyst in acetalization under mild conditions. Maximum conversion of benzaldehyde (72%) was obtained in 8 h at 100 °C with 60% selectivity for the six-membered acetal. The high activity of 20 mol% $\text{MoO}_3/\text{SiO}_2$ might be due to a very high Bronsted acidity which can be correlated to the formation of active SMA species on the surface of the catalyst shown by 20 mol% $\text{MoO}_3/\text{SiO}_2$ compared to that of 1 mol% $\text{MoO}_3/\text{SiO}_2$. Owing to the protophilic nature of carbonyl carbon of the aldehyde and the high Bronsted acidity of the 20 mol% catalyst favours the protonation of 'O' atom of the carbonyl which in turn increases the conversion of the reactants. Interestingly, with substituted benzaldehydes under same reaction conditions the conversion of aldehydes decreased with increase in selectivity for six-membered acetals. High conversion up to 78% was obtained for aliphatic aldehydes. Very high selectivity (up to 100%) for six-membered acetal was obtained at lower conversions (10%); however, up to 70% selectivity for six-membered acetal was obtained at 70% conversion for *o*-chloro benzaldehyde. In each case, 6-membered acetal was achieved with maximum selectivity compared to 5-membered acetal. These results indicate the potential of this catalyst for the acetalization of glycerol for an environmentally benign process.

B] Section 4B - This section demonstrated the use of $\text{MoO}_3/\text{SiO}_2$ catalyst for etherification of glycerol (Scheme 4).



Scheme 4. Etherification of glycerol with ^tbutyl alcohol

The reaction was carried in a batch reactor (glass pot) and as well as in autoclave. The objective was to get ^tbutyl alkyl ethers, considering their importance as oxygenate fuel additives. The preliminary study was carried out by etherification of glycerol and ^tbutyl alcohol as a probe reaction. When the reaction was carried out in a batch reactor (glass round bottomed flask) and reflux conditions, the conversion of glycerol was not satisfactory. Although glycerol:^tbutyl alcohol was taken to be 1:5, only 23% glycerol conversion was obtained. Therefore the reaction was carried out at higher temperature (100 °C) and an autoclave. Interestingly a very high glycerol conversion of 72% was obtained with 67% selectivity for tri-^tbutyl-glyceryl ether (TTGE) and the remaining 33% was di-^tbutyl-glyceryl ether (DTGE) and mono-^tbutyl-glyceryl ether (MTGE). A wide range of diols were used to study the etherification using the same reaction conditions.

The **Fifth Chapter** gives an overall summary of all the major conclusions of the present study with respect to the synthesis and characterization of MoO₃/SiO₂ catalysts, isolation, characterization and identification of the *in situ* formed catalytically active species, and the successful attempt in using the acidic properties of the catalyst for acid catalyzed valorization of glycerol to acetins, acetals and glyceryl ethers.

References:

1. R. R. Soares, D. A. Simmonetti, J. A. Dumesic, *Angew Chem Int Ed.* 2006, **45**, 3982.

Chapter 1: Introduction

Chapter 1: Introduction

1.1. Renewables - Rationale and Significance

Energy and materials are pivotal for the sustainable development of our society. Its dependence on fossil fuels contributes significantly to the current environmental problems, such as the greenhouse effect, air pollution and water and soil contamination. These are the main drivers for a worldwide effort toward a reduction in fossil fuel consumption. The challenge is substantial, because fossil fuel resources are an integral part of our economy. Current stock of fossil-based energy resources, viz., petroleum, coal and natural gas, etc. comprise of about three quarters of the world's primary energy consumption, numerically corresponding to 33%, 24% and 19% respectively. Energy resources like nuclear power (5%), hydropower (6%) and biomass (13%) can be alternative options over the earlier mentioned fuels. However, according to the world wide primary energy consumption, the latter energy resources comprise of only one quarter of total consumption. Environmentalists and researchers are toiling towards improved utilization of renewable energy resources. Biomass is an abundant and carbon-neutral, renewable energy resource as well as raw material for the production of fine chemicals required to produce advanced material for the sustainable development of the society. Therefore development of technologies for conversion of renewable resources like biomass for the production of biofuels and valuable chemicals is seen as a promising option.^[1-8] Energy and fine chemicals production from biomass has a prime advantage, that it emits negligible amount of greenhouse gases compared to that of the fossil fuels since the CO₂ generated during the energy conversion is re-consumed during the subsequent regrowth of biomass. In the early 20s, wood-based resources and crops were used to manufacture a range of industrial products such as solvents, dyes and fibres. The severe energy crisis of 1970's focused on the enhanced utilization of bio-based resources for the production of fuels and commodity chemicals. Inclination of world market from fossil based energy resources to renewable sources such as biomass can be considered as a key contribution towards the establishment of favourable climatic conditions and sustainable economy. Therefore, owing to the focus on exploring the novel methodologies for the conversion of biomass, it is necessary to exploit the available bio-renewable resources as raw materials for the development of commodity materials

using various pathways. A biorefinery concept has emerged similar to petroleum refinery which considered as an integral unit that can accept different biological feedstocks and convert them to a range of useful products including chemicals, energy and materials.^[9]

1.2. *Biorefinery Concept*

Biorefinery is a concept that integrates biomass conversion processes and equipments to produce fuels, energy and chemicals. It aims at complete valorization of biomass source by various processes.^[9-11] The biorefinery concept is quite similar to petroleum refineries, which produce fuels and petroleum products. The biorefinery may include thermal, chemical and biological processes and its development. For the multiple product formation, the biorefineries can take advantage of the differences in biomass components and intermediates and maximize the value derived from the biomass feedstock.^[12,13,14] For example, the lignocellulosic biorefinery typically uses 'dry' lignocellulose such as wood, straw, bagasse, etc. However, a biorefinery requires a large throughput to be economical. Moreover, biomass is a low density feedstock that is expensive to transport. There are three types of biorefineries -

1.2a. Type I biorefineries:

They use one feedstock and one process producing single major product. For example biodiesel is produced from oil or fats through transesterification.

1.2b. Type II biorefineries:

Many chemicals, energy and bio-materials are produced using single feedstock through many processes. One example is, the chemical industry producing multitude of carbohydrate derivatives, including native and modified starches, sweeteners, polyol and bio-ethanol from cereal grains.

1.2c. Type III biorefineries:

This is the most developed type of biorefinery. It is able to produce a variety of industrial products using various types of feedstocks and processing technologies. During the multiple product formation some by-products are also formed which might become a key product in the future. In this approach, there is a possibility to select the most profitable combination of raw materials and processes to produce multiple products.

Biorefinery is multidisciplinary in nature. It requires people with different skills

and expertise, e.g. agriculturalists, chemists and biotechnologists for its efficient performance (Figure 1.1).

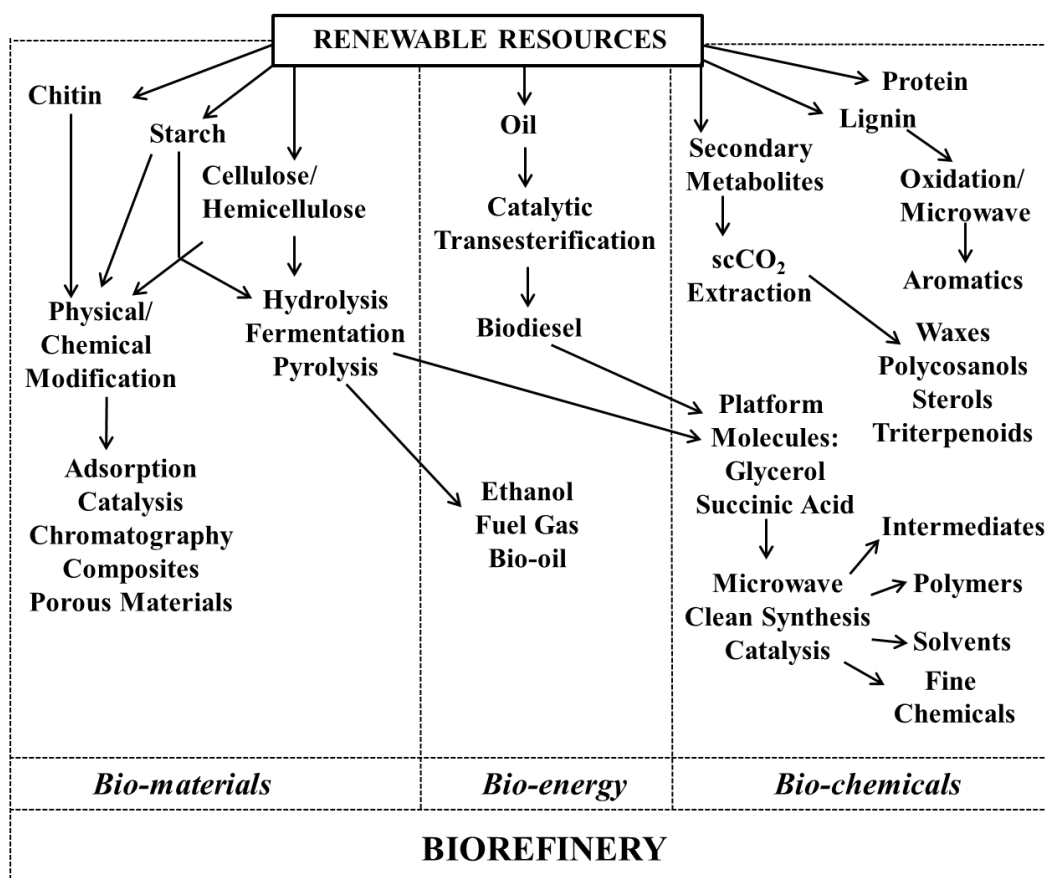
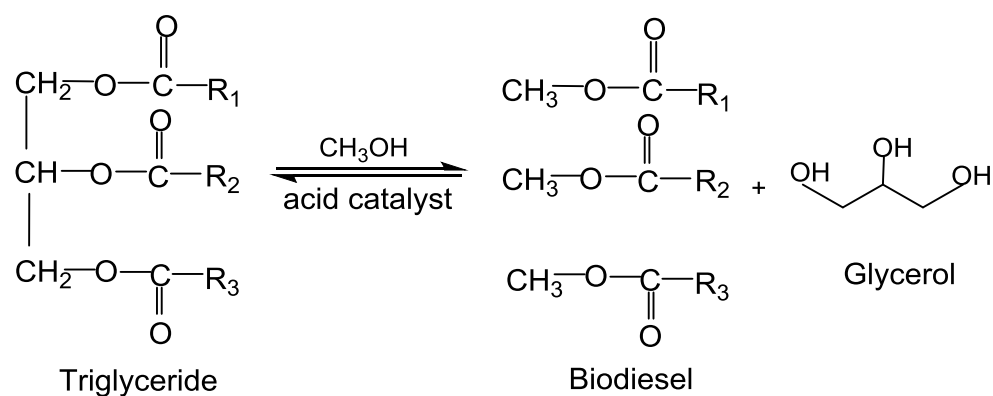


Figure 1.1. Flow chart of a Biorefinery

1.3. Biodiesel Production

The production and application of biofuels (derived from renewable resources) like biodiesel are the corrective measures in context with the fast depleting fossil fuels and increasing dependence on renewable resources.

Biodiesel (FAME, Fatty Acid Methyl Ester) forms the first generation bio-fuels which uses a very simple process of transesterification of fat or oil. In this reaction, a fat or oil (triglyceride) reacts with three moles of light alcohol (C1 to C4) to give three moles of fatty acid alkyl ester (biodiesel) and one mole of glycerol as the by-product (Scheme 1.1).



Scheme 1.1. Biodiesel Production

Glycerol is generated at the rate of 1 mole of glycerol for every 3 moles of methyl esters synthesized and comprises approximately 10 wt% of total product as shown in Scheme 1.1.^[15] In 1992, glycerol was produced in about 6,00,000 tons, whereas in 2012 the production has reached up to 1.1-1.5 million tons.^[16-19] Therefore, glycerol forms a bioresource from the biorefinery type III which appears today as a key raw material for chemists.

1.4. Glycerol a versatile molecule

Glycerol is a highly functionalized molecule compared to hydrocarbons (Figure 1.2), hence it is an advantageous alternative to use it as feedstock for the production of valuable commodity products and important industrial intermediates.

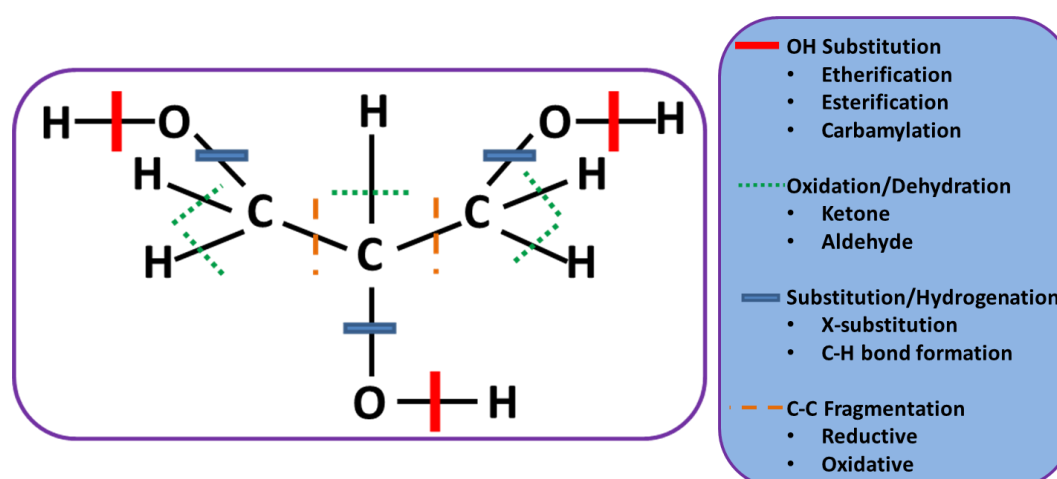


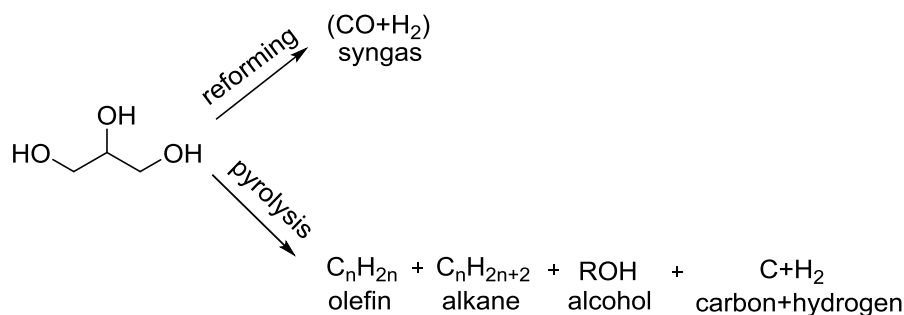
Figure 1.2. Glycerol a versatile molecule

1.5. Catalytic approach for valorization of bio-derived glycerol

Considering the multifunctional structure and properties of glycerol, various reactions can be carried out by several different pathways. Focus on the conversion of glycerol into value-added chemicals is of prime importance as its derivatives find applications in diverse sectors like fuels, chemicals, automotives, drug industries, detergents, etc. In this respect, catalysis represents a critical approach to green chemical technology in the activation and utilization of glycerol. In the near future, the potential conversion of bio-derived glycerol into valuable commodity chemicals can facilitate the replacement of petroleum-based products. Various approaches towards conversion of glycerol using catalysts are illustrated as follows:

a) Glycerol reforming/pyrolysis

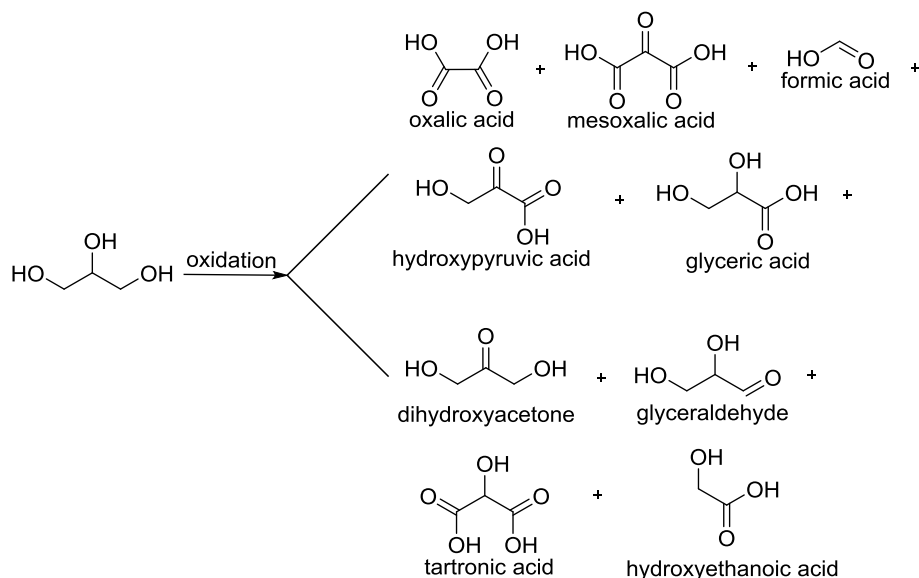
Considering both industrial and innovative approach, an important value addition of glycerol is the reforming process in which glycerol is converted to H₂ and CO (syngas) under mild conditions (225-300 °C) in a single reactor using heterogeneous Pt-supported catalysts.^[20] The process is crucial as syngas can be used as a source for fuels and chemicals by Fisher-Tropsch. The conversion of glycerol to hydrogen or syngas can further contribute to the use of clean renewable energy sources (Scheme 1.2).



Scheme 1.2. Reforming/Pyrolysis of glycerol

b) Selective oxidation of glycerol

Glycerol oxygenates are of high value due to their applications in petroleum based products and pharmaceuticals. Oxidation of glycerol gives number of products like glyceric acid, tartronic acid, glyceraldehyde, dihydroxyacetone (DHA), mesoxalic acid, oxalic acid, formic acid, hydroxypyruvic acid, etc as shown in Scheme 1.3.



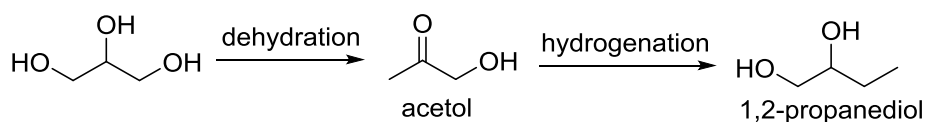
Scheme 1.3. Oxidation of glycerol

All the oxidized products have multitude of applications in various fields like pharmaceuticals, cosmetics, fuel additives, etc. DHA is an important green platform chemical. Glyceric acid, hydroxypyruvic acid, etc can be used as organic building blocks in asymmetric synthesis. These products are the result of oxidation of primary or secondary -OH group. However, due to the presence of similarly reactive hydroxyl groups, the functionalization of triol molecule renders difficulty in selective oxidation of primary or/and secondary alcohol.^[21] The oxidation of primary -OH group of glycerol leads to the formation of glyceric acid and further to tartronic acid. Both the products are commercially important due to their applications in drug industries. Various precious metal based especially Au and Pt based heterogeneous catalysts have been used for the oxidation of terminal -OH groups. For example carbon supported Au and Pt catalysts are reported for very high conversion and selectivity for glyceric acid.^[22-25] CeO₂ supported Pt catalyst gives the oxidation of both primary hydroxyl groups to give tartronic acid.^[26] However, the catalysts pose disadvantages of low stability in oxidative environment, and formation of undesired products. Therefore, the use of organic nitroxyl radical TEMPO (2,2,6,6-tetramethylpiperidin-1-oxyl) has been reported as a selective catalyst for the oxidation of all the hydroxyls to give high yields of ketomalonic acid using NaOCl as stoichiometric oxidant.^[27] Oxidation of secondary hydroxyl group of glycerol mainly gives dihydroxyacetone (DHA) which forms a main ingredient in the various cosmetics and is produced with a scale of 2000 tons per annum (t.p.a.). Industrially, it is produced by

microbial fermentation of glycerol over *Gluconobacter oxydans*. Recently, a green technique for direct conversion of glycerol to DHA has been reported using anodic oxidation method and TEMPO as catalyst.^[28] This process gives comparable yield of DHA and thereby overcoming the cumbersome biotechnological based industrial process. Research is being carried out for the use of heterogeneous catalysts for the production of DHA. The use of various heterogeneous catalysts for oxidation of glycerol has been reviewed recently.^[29]

c) Hydrogenolysis of glycerol to propylene glycol

Propylene glycol (PG, 1,2 propanediol) is used as an antifreeze agent in combination with glycerol (70% PG and 30% glycerol). It is two-step process (Scheme 1.4) which includes dehydration followed by hydrogenation and uses Cu-based catalyst (copper chromite).^[30] The reaction proceeds via formation of acetol as an intermediate.

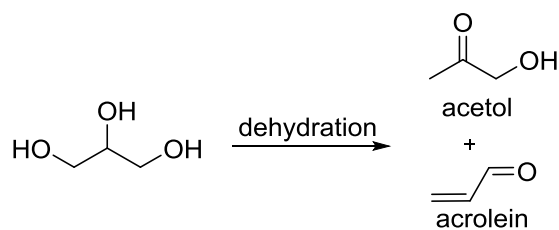


Scheme 1.4. Two-step process for glycerol to 1,2-propanediol

The first step of forming acetol occurs at atmospheric pressure, while subsequent hydrogenation at 200 °C and 10 bar H₂ eventually affords propylene glycol in 73% yield at significantly lower cost than propylene glycol made from petroleum. An important advantage of this process is ability to convert even crude glycerol without purification. The first step of the process also opens up important potential applications of acetol as a monomer for the production of polyols. Supported noble metal catalysts have been used for the conversion of glycerol to 1,2 propanediol. However, poisoning of the catalysts is major drawback in this case.^[31]

d) Dehydration of glycerol to acrolein

Acrolein is another important and versatile value-added product of glycerol which is used in chemical industries in the manufacture of acrylic acid esters, superabsorber polymers and detergents. Glycerol can be used as promising starting material for the production of acrolein by dehydration (Scheme 1.5).

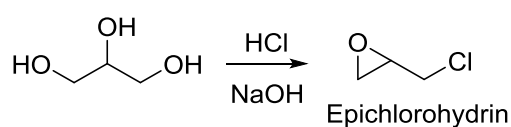


Scheme 1.5. Dehydration of glycerol

Commercially acrolein is produced via oxidation of propylene with Bi/Mo mixed oxide catalyst. Various solid acid catalyst based on supported metal oxides, have been reported for the dehydration of glycerol to acrolein. Recently, the use of supercritical water as a reaction medium has been reported for the dehydration of glycerol. However, the conversion and selectivity is not promising. A worldwide research on the development of promising catalytic process for the dehydration of glycerol to acrolein is ongoing.^[16] Recently, Arkema, France has announced a process for the manufacture of acrylic acid via acrolein from glycerol using mixed oxide containing NbO_x and atleast one element taken from the group of W, Mo and Cr.^[32]

e) Glycerol to epichlorohydrin

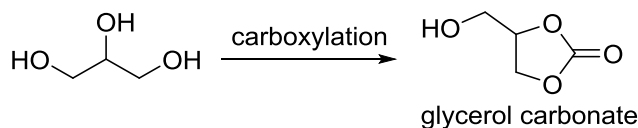
Epichlorohydrin is used in the synthesis of epoxy resins. Commercially, the synthesis of epichlorohydrin from glycerol is catalytically carried out by reaction with HCl and followed by the dechlorination with NaOH (Scheme 1.6). This glycerol-based process is commercialized by Solvay and named as 'Epicerol'.



Scheme 1.6. Glycerol to epichlorohydrin

f) Glycerol to glycerol carbonates

Glycerol carbonates can be a novel component in gas-separation membranes, as solvent and biolubricant. High yields of glycerol carbonates can be directly prepared from renewable glycerol and dimethyl carbonate (DMC) catalyzed by lipase (Scheme 1.7).

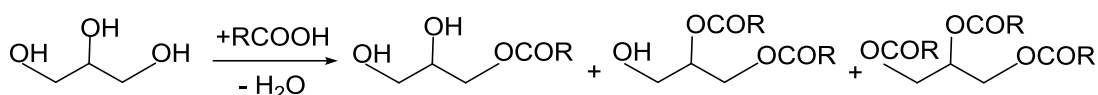


Scheme 1.7. Carboxylation of glycerol to glycerol carbonate

Glycerol carbonate is an important starting material for the synthesis of glycidol which is a high-value component in the production of various polymers. The use of zeolite has been reported for the synthesis of high yield of glycidol from glycerol carbonate. These materials have commercial applications ranging from cosmetics to controlled drug release.^[33]

g) Glycerol to fuel oxygenates

Esterification with acids - Esterification of glycerol with acid gives mono-, di- and triesters as shown in Scheme 1.8.

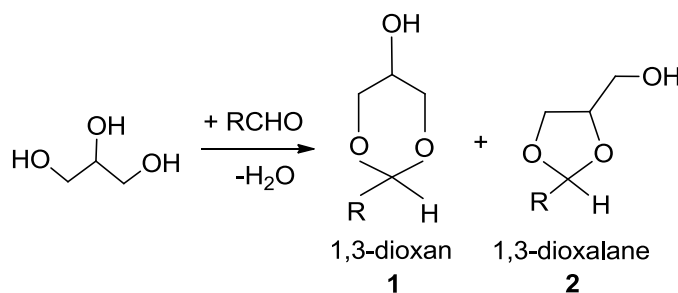


Scheme 1.8. Esterification of glycerol with acid

This is an important industrial reaction because of the applications of esters in synthesis of safe emulsifiers,^[34] fuel additives, and as ‘bio’ organic building blocks in pharmaceuticals.^[35,36] Monoglycerides have significant applications as safe and biodegradable emulsifiers in food, pharmaceutical, cosmetic, and detergent industries. Till date, selective esterification of glycerol to monoglycerides was successfully obtained using conventional organic synthesis routes^[37,38] and enzymatic routes.^[39] Selective esterification of glycerol with various homogeneous catalysts either basic,^[40] such as metal hydroxides, methoxides, or carbonates, or acidic,^[41] such as sulfuric, phosphoric, or organic sulfonic acids has been reported. But a major issue of these homogeneous catalysts is that they are highly corrosive and are poorly selective towards monoglycerides. There are many reports for the esterification of glycerol with fatty acids using heterogeneous catalysts such as cation-exchange resins, zeolites, SiO₂ supported metal oxides. Esterification of glycerol with acetic acid is an important reaction. The products of the reaction are mono-, di- and triacetin which have a numerous applications ranging from cosmetics to fuel additives. Mono- and diacetins have applications in cryogenics and also as raw materials in polymer

industries. Triacetin is an important product as it has interesting applications as fuel additives due to its viscosity and anti-knock properties. It also has wide applications in cosmetic industries. There are many reports on both homogeneous and heterogeneous catalysts which have been used for the acetylation of glycerol. In a few cases acetic anhydride is used as reactant which further leads to the formation of acetic acid as a by-product.^[42] Many solid acids like supported heteropoly acids, zeolites, acidic resins, hydroxylated MgF₂, sulfated CeO₂ and Al₂O₃ based catalysts have been reported for the acetylation of glycerol with acetic acid.^[43] Most of the literature reports suggest the formation of mono- or di- acetin as major products.^[44] The literature reports explain the fact that to achieve high conversion of glycerol and maximum selectivity for triacetin, it is necessary to have a catalyst with high surface area, high pore size and high Brønsted acidity. It is necessary to circumvent these issues in order to achieve high glycerol conversion and selectivity for triacetin.

Acetalization of glycerol - Glycerol acetals seem to be important chemical intermediates mainly for the production of 1,3 DHA and 1,3 propanediol and as oxygenates in fuels. Acetalization of glycerol with aldehydes and ketones was conventionally carried out using classical homogeneous acid catalysts.



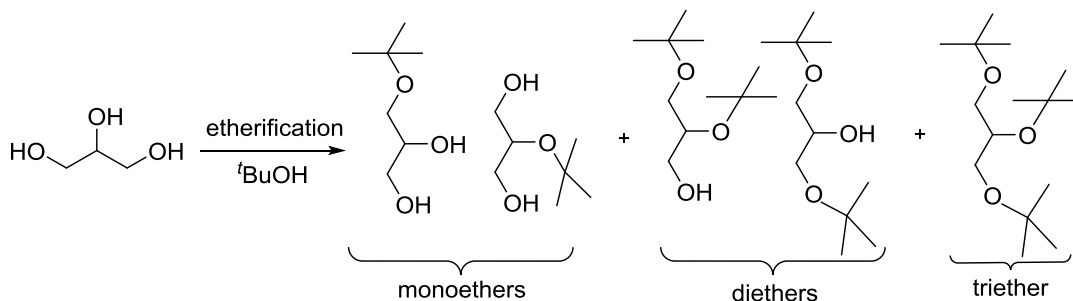
Scheme 1.9. Acetalization of aldehydes with glycerol

However these pathways were not selective because of the concomitant formation of five membered and six membered acetals (Scheme 1.9). Also, the formation of salts during the neutralization step of the homogeneous catalyst resulted in complex work up procedures. In order to overcome these problems, use of various solid acid catalysts like amberlyst, nafion, zeolites, montmorillonite, supported heteropoly acid, supported metal oxides have been reported and various parameters have been studied to control the selectivities of the desired product.^[42,45] Transition metal complexes like

[Cp*IrCl₂]₂ have been reported for acetalization. However, the reaction had to be carried out under inert atmosphere and the catalyst showed poor activity due to the water formed during the reaction.^[46] Various zeolites like USY, BEA, ZSM-5, Dowex have been studied as solid acids for the acetalization of glycerol.^[47] In all the cases 5-membered acetal was obtained as a major product and a maximum glycerol conversion of 66% was obtained. The reason for low glycerol conversion and higher selectivity for 5-membered acetal was the accessibility constraints of the reactants and intermediates in the pores of the catalysts. The reaction occurred at the pore entrance and on the external surface of the catalyst which in turn led to limited access of acid sites to the reactants. Reports regarding the use of Beta and Y zeolite suggested that higher concentration of acid sites are not the only factors for the better catalytic performance, but the properties like pore size, surface area and hydrophobicity of the catalyst have to be taken into consideration.^[48] Therefore, to achieve appreciable conversion of glycerol and high selectivity for the desired products, it is necessary to study the limitations of the catalyst and design the catalyst to cope up with the drawbacks of the available catalysts.

Etherification of glycerol - The selective etherification of glycerol is an interesting pathway to value-added chemicals. The products of etherification of glycerol are alkyl glyceryl ethers (Scheme 1.10) and they find numerous applications because of their inflammatory, antibacterial, antifungal, immunological stimulation and antitumour properties. They also form chemical intermediates for the production of 1,3 dioxolan-2-one and bis (sodium sulfonate) ester type cleavable surfactants. These ethers find wide applications as fuel additives to enhance the energy efficiency and the stability of the fuel to lower the emissions when mixed with fuels including biodiesel. The glycerol ethers have proved to poses efficient burning properties with reduced pollutant and particulate matter emissions. First report on etherification of glycerol and *tert*-butyl alcohol (TBA) using heterogeneous catalyst was using acid-ion exchange resins under solvent free conditions. A lot of work has been reported on silica-supported sulfonic acid, various zeolites, supported metal oxides as solid acid catalysts. Although there have been reports on the use of heterogeneous catalysts for etherification of glycerol, many reports describe the use of iso-butene (IB) as reactant for the *t*butylation of glycerol. However there are a few problems like- IB has to be liquefied, solvent is necessary for the solubility of IB and glycerol, and there is

formation of some undesired oligomerized products. Taking these issues into consideration the use of TBA can be seen as a promising option for the etherification of glycerol.



Scheme 1.10. Etherification of glycerol with *t*BuOH

Glycerol being a large molecule (radius - 4.83 Å), in heterogeneous catalysis, the catalytic conversion of glycerol needs catalysts with a high surface area and a large pore size for the easy accessibility of the reactants to catalytically active sites as well as diffusion of the bulky intermediates formed during the reaction.

1.6. Solid catalysts for acid-catalyzed transformations of glycerol

Most of the reactions of glycerol discussed above are typically acid-catalyzed organic transformations. These reactions can be carried out using conventional homogeneous Lewis or Brønsted catalysts like AlCl₃, *p*-TSA, H₂SO₄, etc. But the use of homogeneous catalysts pose problems regarding recyclability, isolation, tedious work-up procedures, formation of undesired byproducts, etc. Therefore, the use of solid acids is preferred over homogeneous acids to overcome these problems associated with homogeneous catalysts. In recent years researchers are intensely focusing on the preparation of mesoporous inorganic materials for technological application and fundamental studies due to their advantages of good surface permeability, large specific area, low density, and high mechanical stability and tunable acidity.^[49-55] For mesoporous materials to act as potential catalysts they should possess high acidity or basicity, high stability and recyclability. Moreover, mesoporous materials like aluminosilicates have attracted attention for their potential applications as heterogeneous catalysts and catalyst supports, especially for large molecule catalysis.^[57] The important structural parameters of the catalyst that should be tuned to result in high conversion and selectivity in glycerol-based organic

transformations are the hydrophilicity and porosity of the catalysts. Therefore, for the functionalization of glycerol following approaches are to be considered during the preparation of a heterogeneous catalyst^[42] -

- (i) the preparation of porous materials,
- (ii) the control of the acidity or the basicity,
- (iii) the consideration of the surface hydrophilicity of the catalysts, a quite important property governing the adsorption of polyhydroxylated compounds and the surface coverage of the catalyst.

1.7. Scope and objective of the thesis

To develop organic processes based on the utilization of glycerol as an organic block, it is necessary to take into account a few physicochemical properties of glycerol (viz., strong hydrophilicity, three hydroxyl groups, molecular size). For increasing the conversion of glycerol and selectivity of glycerol-based products, many heterogeneous catalysts are being designed. Alongwith the advantages of heterogeneous catalysts over homogeneous catalysts, heterogeneous catalysts appear to be promising for controlling the selectivity of the products thereby overcoming the limitations in the use of glycerol in organic syntheses. Taking into consideration all the above discussed issues on the acid-catalyzed conversions of glycerol, objective of the thesis is to develop a suitable solid acid catalyst for conversion of glycerol to value-added chemicals and the objective has been achieved by carrying out the following work-

- i) Synthesis and characterization of efficient solid acid catalyst ($\text{MoO}_3/\text{SiO}_2$) with high surface area and mesoporosity.
- ii) Isolation, characterization and identification of *in situ* formed catalytically active species during various acid-catalyzed organic transformations.
- iii) The catalysts have been successfully used for acid-catalyzed transformations of glycerol like acetylation, acetalization and butylation to value-added chemicals (fuel oxygenates).

1.8. Outline of the thesis

This section gives the chapter wise distribution of the work done during the Ph.D. tenure.

Chapter 1: An overall perspective about the fast depleting fossil fuels and emphasis on the use of renewable resources as an alternative energy source has been discussed in details. The biorefinery concept has been described in brief. Availability of glycerol as byproduct of biodiesel and its possible valorization to various products has been discussed in this chapter.

Chapter 2: A novel sol-gel technique developed for the synthesis of MoO₃/SiO₂ (ranging from 1-20 mol% MoO₃) catalysts has been discussed in detail. The detailed characterization using PXRD, BET-surface area, NH₃-TPD, FTIR of adsorbed pyridine, FTIR, Raman spectroscopy and TEM has been discussed in this chapter.

Chapter 3: Sol-gel synthesized MoO₃/SiO₂ catalyst has been used as solid acid for esterification of acetic acid with ethanol and glycerol, respectively. Isolation, characterization and identification of catalytically active species in MoO₃/SiO₂ catalyst during solid acid catalyzed reactions has been discussed in this chapter.

Chapter 4: The fourth chapter deals with the use of MoO₃/SiO₂ catalyst for acetalization and etherification reactions. The chapter is divided into two sections 4A and 4B. The section 4A describes the acetalization of various aldehydes with glycerol. Reaction of benzaldehyde and glycerol was studied in detail. Various reaction parameters were studied so as to optimize the reaction conditions in order to get maximum conversion of glycerol with high selectivity for the desired product. Plausible mechanism for acetalization is also given in the chapter. In the section 4B, etherification of glycerol with TBA was studied using MoO₃/SiO₂ as solid acid catalyst. The t-butylation was also carried out with various alcohols so as to study the substrate scope.

Chapter 5: This chapter presents the summary and conclusions of the thesis work.

1.9. References

- 1 G.W. Huber, A. Corma, *Angew. Chem. Int. Ed.* **2007**, 46, 7184.
- 2 J. N. Chheda, G. W. Huber, J. A. Dumesic, *Angew. Chem. Int. Ed.* **2007**, 46, 7164.

- 3 S. R. A. Kersten, W. P. M. van Swaaij, L. Lefferts, K. Seshan, *Catalysis for Renewables: From Feedstock to Energy Production* (Eds.: G. Centi, R. A. van Santen), Wiley-VCH, Weinheim, **2007**, chap. 6, p. 119.
- 4 D. Mohan, C. U. Pittman, P. H. Steele, *Energy & Fuels* **2006**, 20, 848.
- 5 A. J. Ragauskas, C. K. Williams, B. H. Davison, G. Britovsek, J. Caine, C. A. Eckert, W. J. Frederick, Jr. J. P. Hallett, D. J. Leak, C. L. Liotta, J. R. Mielenz, R. Murphy, R. Templer, T. Tschaplinski, *Science* **2006**, 311, 484.
- 6 J. O. Metzger, *Angew. Chem. Int. Ed.* **2006**, 45, 696.
- 7 M. Hartmann, *Ergol Erdgas Kohle Oil Gas European Magazine* **2007**, 123, 362.
- 8 B. Kamm, M. Kamm, *Chem. Ing. Tech.* **2007**, 79, 592.
- 9 E. Audsley, J. E. Annetts, *Agric. Syst.* **2003**, 76, 39.
- 10 J. J. Bozel, M. K. Patel, *Feed Stocks for Future, ACS, Symposium Series, Washington* **2006**, 921, 1.
- 11 U. S. DOE report, *Energy Efficiency and Renewable Energy, Biomass Program*, **2003**.
- 12 B. Kamm, M. Kamm, *Appl. Microbiol. Biotechnol.* **2004**, 64, 137.
- 13 S. Fernando, S. Adhikari, C. Chandrapal, N. Murali, *Energy & Fuels* **2006**, 20, 1727.
- 14 J. H. Clark, V. Budarin, F. E. I. Deswarte, J. E. Hardy, F. M. Kerton, A. J. Hunt, R. Luque, D. J. Macquarrie, K. Milkowski, A. Rodriguez, O. Samuel, S. J. Tavener, R. J. White, A. J. Wilson, *Green Chem.* **2006**, 8, 853.
- 15 C-H. Zhou, J. N. Beltramini, Y-X. Fan, G. Q. Lu *Chem. Soc. Rev.* **2008**, 37, 527.
- 16 L. Ott, M. Bicker, H. Vogel, *Green Chem.* **2006**, 8, 214.
- 17 M. Heming, S. Claude, *Info. Chim. Mag.* **2006**, 474, 40.
- 18 C. H. Zhou, J. N. Beltramini, Y. X. Fan, G. Q. Lu, *Chem. Soc. Rev.* **2008**, 27, 527.
- 19 S. P. Maio, *J. Braz. Chem. Soc.* **2012**, 23, 5.
- 20 R. R. Soares, D. A. Simonetti, J. A. Dumesic, *Angew. Chem. Int. Ed.* **2006**, 45, 3982.

- 21 P. McMorn, G. Roberts, G. J. Hutchings, *Catal. Lett.* **1999**, 63, 193.
- 22 S. Carrettin, P. McMorn, P. Johnston, K. Griffin, C. J. Kiely, C. A. Attard, G. J. Hutchings, *Top. Catal.* **2004**, 27, 131.
- 23 S. Demirel-Gulen, M. Lucas, P. Claus, *Catal. Today* **2005**, 102, 166.
- 24 N. Dimitratos, J. A. Lopez-Sanchez, D. Lennon, F. Porta, L. Prati, A. Villa, *Catal. Lett.* **2006**, 108, 147.
- 25 B. N. Zope, E. Robert, J. Davis, *Top. Catal.* **2009**, 52, 269.
- 26 P. Gallezot, *Appl. Catal. A* **1995**, 133, 179.
- 27 R. Ciriminna, M. Pagliaro, *Adv. Synth. Catal.* **2003**, 345, 383.
- 28 R. Ciriminna, G. Palmisano, C. Della Pina, M. Rossi, M. Pagliaro, *Tetrahedron Lett.* **2006**, 47, 6993.
- 29 B. Katryniok, H. Kimura, E-Z Skrzynska, J-S Girardon, P. Fongarland, M. Capron, R. Ducoulombier, N. Mimura, S. Paul, F. Dumeignil, *Green Chem.* **2011**, 13, 1960.
- 30 M. Dasari, P. Kiatsimkul, W. Sutterlin, G. J. Suppes, *Appl. Catal. A: General* **2005**, 281, 225.
- 31 T. Miyazawa, Y. Kusunoki, K. Kunimori, K. Tomishige, *J. Catal.* **2006**, 240, 213.
- 32 J. L. Dubois, *WO Patent* **2012**, 010923 A1.
- 33 Small-scale production of these highly branched glycidol polymers has been commercialized in Europe by Hyperpolymers (Germany)
- 34 E. Jungermann, N. O. V. Sonntag, *Glycerin: a Key Cosmetic Ingredient*, Marcel Dekler Inc. Ed., New York, **1991**.
- 35 J. Barrault, F. Jerome, Y. Pouilloux, *Lipid Technol.* **2005**, 17, 6, 131.
- 36 M. Kloosterman, V. H. M. Elferink, J. Van Lersel, J. H. Roskam, E. M. Meijer, L. A. Hulshof, R. Sheldon, *Trends Biotechnol.* **1998**, 6, 251.
- 37 C. C. Yu, Y. S. Lee, B. S. Cheon, S. H. Lee, *Bull. Korean Chem. Soc.* **2003**, 24, 1229.
- 38 M. Ghandi, A. Mostashari, M. Karegar, M. Barzegar, *J. Am. Oil Chem. Soc.* **2007**, 84, 681.
- 39 D. G. Hayes, E. Gulari, *Biotechnol. Bioeng.* **2004**, 38, 507.
- 40 N. O. V. Sonntag, *J. Am. Oil Chem. Soc.* **1982**, 59, 795.
- 41 D. Swern, *Industrial Oil and Fat Products*, Wiley, New York, **1979**.

- 42 F. Jerome, Y. Pouilloux, J. Barrault, *ChemSusChem* **2008**, 1, 586.
- 43 X. Liao, Y. Zhu, S-G Wang, Y. Li, *Fuel Processing Technology* **2009**, 90, 988.
- 44 a) V. L. C. Goncalves, B. P. Pinto, J. C. Silva, C. J. A. Mota, *Catalysis Today* **2008**, 133-135, 673; b) S. B. Tronce, S. Wuttke, E. Kemnitz, S. M. Coman, V. I. Parvulescu, *Appl. Catal. B: Environmental* **2011**, 107, 260; c) P. S. Reddy, P. Sudarsanam, G. Raju, B. M. Reddy, *J. of Ind. and Eng. Chemistry* **2012**, 18, 648.
- 45 a) P. Ferreira, I. M. Fonseca, A. M. Ramos, J. Vital, J. E. Castanheiro, *Catal. Commun.* **2009**, 10, 481; b) P. Ferreira, I. M. Fonseca, A. M. Ramos, J. Vital, J. E. Castanheiro, *Catal. Commun.* **2011**, 12, 573.
- 46 M. Garcia-Perez, J. Shen, X. S. Wang, C. Z. Li, *Fuel Process. Technol.* **2010**, 91, 296.
- 47 C. Crotti, E. Farnetti, N. Guidolin, *Green Chem.* **2010**, 12, 2225.
- 48 H. Serafima, I. M. Fonseca, A. M. Ramos, J. Vital, J. E. Castanheiro, *Chem. Eng. J.* **2011**, 178, 291.
- 49 M. J. Climent, A. Velty, A. Corma, *Green Chem.* **2002**, 4, 565.
- 50 F. Caruso, *Chem. Eur. J.* **2000**, 6, 413.
- 51 A. B. Bourlinos, M. A. Karakassides, *Chem. Commun.* **2001**, 1, 518.
- 52 a) C. E. Fowler, D. Khushalani, S. Mann, *J. Mater. Chem.* **2001**, 11, 1968.
b) M. Ohmori, E. Matijevic, *J. Colloid Interface Sci.* **1992**, 150, 594.c)
- 53 E. Mathlowitz, J. S. Jacob, Y. S. Jong, G. P. Carino, *Nature* **1997**, 386, 410.
- 54 H. Huang, E. E. Remsen, *J. Am. Chem. Soc.* **1999**, 121, 3805.
- 55 W. Li, X. Sha, W. Dong, Z. Wang, *Chem. Commun.* **2002**, 2434.
- 56 A. Corma, *Chem. Rev.* **1997**, 97, 2373.
- 57 Z. T. Zhang, Y. Han, F. S. Xiao, S. L. Qiu, L. Zhu, R. W. Wang, Y. Yu, Z. Zhang, B. S. Zou, Y. Q. Wang, H. P. Sun, D. Y. Zhao, Y. Wei, *J. Am. Chem. Soc.* **2001**, 123, 5014.

**Chapter 2: Synthesis and characterization
of MoO₃/SiO₂ catalysts
prepared by sol-gel method**

Abstract

A series of MoO₃/SiO₂ catalysts with varying MoO₃ loadings (1-20 mol%) were prepared by sol-gel technique using ethyl silicate-40 (ETS-40) and ammonium heptamolybdate (AHM) as silica and molybdenum source, respectively. The sol-gel derived samples were calcined at 500 °C and extensively characterized using various techniques viz., XRD, BET surface area, NH₃-TPD, pyridine-FTIR, TEM, Raman and FTIR spectroscopy. The XRD of the calcined samples showed the formation of amorphous phase up to 10 mol% MoO₃ loading and at higher loading crystalline α -MoO₃ was observed on amorphous silica support. TEM analyses of the materials showed the uniform distribution of MoO₃ nanoparticles on amorphous silica support. Raman spectroscopy showed the formation of silicomolybdic acid at low Mo loading and a mixture of α -MoO₃ and polymolybdate species at high Mo loadings.

Chapter 2: Synthesis and Characterization of the MoO₃/SiO₂ catalysts by sol-gel method

2.1. Introduction

2.1.1. Catalysis

Catalysis is the single most important interdisciplinary technology in the chemical industry. Of all chemical and pharmaceutical products produced today, more than 85% products are manufactured by catalytic processes. The importance of catalytic processes, however, does not remain limited to the chemical industry. Catalysis also plays a key role in the processing of raw materials in refineries, during energy production for e.g. in fuel cells and batteries, as well as in terms of climate and environmental protection. Catalysis research is a major interdisciplinary field, and it is characterized by the fact that major economic potential is attached to the results of the research. An example worth mentioning is the Haber-Bosch ammonia process with a catalyst which has developed by Alwin Mittasch in the beginning of the last century. Today, without this process it would not have been possible to feed the world population. Currently, catalysis plays a key role in chemical synthesis, fuels, petroleum refineries and polymer industries, etc. Global dependence on catalysis is increasing by 6.3% per year. The global catalysis market is estimated to reach a cost of 17.2 billion US\$ in 2014. Usually, catalysts are categorized depending on the physical form in which they are used. Catalysis is mainly categorized in three types - biocatalysis, homogeneous and heterogeneous catalysis.

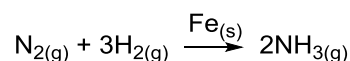
In biocatalysis the catalyst is a biologically active molecule like enzyme. Enzymes are protein molecules, the structure of which results in a very shape-specific active site. Having shapes that are optimally suited to guide the reactant molecules in the optimum configuration for reaction, enzymes are highly specific and efficient catalysts. Enzymes have been classified depending on the type of reaction to be carried out. For e.g. *Oxidoreductases* catalyze oxidation/reduction reactions, *transferases* transfer functional group (e.g. methyl group), *hydrolases* catalyze the hydrolysis of various bonds, etc. There are well-known examples of biotransformations on industrial scale such as- in pharma industry for the manufacture of drugs like ampicillin (>100 t.p.a.), in polymer industry for the production of

acrylamide (>10000t.p.a.), in food industry for the production of lactose-free milk (>100,000 t.p.a.), high-fructose corn syrup (1,000,000 t.p.a.) and in asymmetric catalysis for the synthesis of *l*-DOPA, *l*-maleic acid, *l*-aspartate (>100 t.p.a.), etc. The main advantages of biocatalysts and enzymes are high selectivity or enantioselectivity in case of drug industries, high regioselectivity, transformations under mild conditions, green chemistry e.g. often water is used as solvent. However, there are a few disadvantages like often low specific activity, instability at extreme temperatures and pH values, availability for specific reactions only, prolonged procedure for development of new enzymes.

In homogeneous catalysis the sequence of reactions involve a catalyst in the same phase as the reactants. Various industrially important processes are based on homogeneous catalysis such as - hydroformylation/oxo-process (HRh(CO)(PPh₃)),^[1] Wacker process (PdCl₂,CuCl),^[2] Monsanto process (cis-[Rh(CO)₂I₂]⁻),^[3] olefin metathesis ('Mo' and 'W' alkylidene complexes),^[4] etc. Another class of homogeneous catalysts is different acid catalysts like Bronsted and Lewis acids for e.g. AlCl₃, H₂SO₄, *p*-TSA which are used in reactions like acylation, alkylations, etc. The main advantages of using homogeneous catalysts are - highly and controllable activity, chemo- and regio-, enantioselective, high TON and TOF, no mass transfer limitations, high accessibility to active sites, easy catalyst designing and mechanistic understanding, etc. However, there are major drawbacks like - poor thermal stability, isolation problems, recyclability issues, and tedious work up procedures, etc. Though there are many important industrial applications of homogeneous catalysts as discussed above, so far there are no homogeneous catalysts for processes like cracking, reforming, ammonia synthesis, etc.

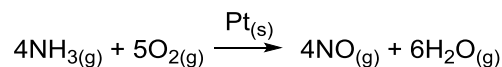
Heterogeneous catalysts dominate chemical and petrochemical industry: ~ 95% of all chemical processes use heterogeneous catalysts. Practically, majority of heterogeneous catalysts are solids and the reactants are gases or liquids. Heterogeneous catalysts are widely used in the industry because of their properties like high thermal stability, recovery and reusability, lower chances of deactivation, etc. For e.g.:

(1) Manufacture of ammonia from N₂ and H₂ by Haber-Bosch process.



Here Fe is a heterogeneous catalyst as it is present in solid phase while the reactants are in gas phase. This process is rated as the 'Process of the Millenium'.

(2) Oxidation of ammonia to nitric oxide using platinum as a catalyst.



Here Pt is a heterogeneous catalyst as it is present in solid phase and the reactants are in gas phase.

Some of the important applications of heterogeneous catalysis are - the selective oxidation of ethylene to ethylene epoxide, an important intermediate towards ethylene glycol (antifreeze) and various polyethers and polyurethanes. The catalyst used is silver promoted by small amounts of chlorine, exhibiting a selectivity of 90% with about 10% of ethylene ending up as CO₂.^[5]

Commonly, the heterogeneous catalyst is a porous high surface area material supporting an active metal or metal oxide. These reactions usually occur at the surface of the catalyst. In heterogeneous processes, the catalytic sites are part of an insoluble inorganic solid or are distributed on the surface of an insoluble support like silica, alumina or carbon, etc. To use the often-expensive materials (e.g. platinum, rhodium, etc.) in an economical way, catalysts are usually nanosized particles supported on an inert, porous structure. As heterogeneous catalysis is a surface phenomenon, crucial factor like high surface area is generally sought for. Another such important factor is controlling the pore size, as for a porous catalyst the diffusion rate of the reactants and product is a function of the pore size.

Different protocols are commonly employed for the preparation of solid catalysts (for e.g. supported metal oxides), which involve a sequence of complex processes that impart advantages and disadvantages for catalytic applications. The properties of good catalysts are determined based on the activity and selectivity to produce desired product, and their stability under reaction conditions. A few synthetic techniques have been listed as follows-

1) Precipitation method- It is a single or a multicomponent preparation in which precipitation or simultaneous precipitation of the components is carried out depending on the differences in the solubilities of the components. However a few drawbacks like the homogeneity of the reactants is difficult to maintain which thereby affects the textural properties of the catalyst.

2) Incipient wetness impregnation method- It is also called capillary impregnation, a commonly used technique for the synthesis of heterogeneous catalysts. Typically, the active metal precursor is dissolved in an aqueous or organic solution. Then the metal-containing solution is added to a catalyst support containing the same pore volume as the volume of solution which is added.

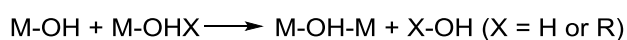
3) Deposition-precipitation method- The addition of precipitating agent to a well dispersed suspension of the support, in a solution of the active metal salt, resulting in the precipitation of the active metal precursor onto the surface of the support is known as deposition-precipitation method.

4) Sol-gel method- The sol-gel method is a homogeneous process, in which results a homogeneous sol condenses into a hydrated solid precursor called gel). Sol-gel method has been recognized for its versatility, which allows control of the texture, composition, homogeneity and structural properties of the finished solids. The synthesis and the applications of the sol-gel synthesized catalysts have been extensively reviewed.^[6,7] The method is based on the hydrolysis and gelation (for instance by controlled addition of water) of alkoxides or other reactive compounds in alcoholic solution.^[8,9] The chemistry of the processes, that occur during the formation of porous structure are controlled by changing of various parameters during preparation, such as pH, solvent and amount of water added for reaction.

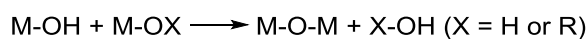
Hydrolysis (hydroxylation) of the metal alkoxides



Olation (condensation with formation of hydroxy bridges)



Oxolation (condensation with formation of oxygen bridges)



Of all these techniques, sol-gel method offers a few unique advantages over the other techniques as given below-

- (i) high purity of the materials and precise control of the composition,
- (ii) control of the structure and homogeneity at the molecular level,
- (iii) control of the texture.

The unique versatility of sol-gel chemistry is due to the large number of adjustable parameters, including nature and concentration of precursors, amount of water, temperature, solvent, pH, aging and drying conditions.

Till date, a range of catalysts have been synthesized and studied using sol-gel method. Depending on the nature of catalytic reaction to be carried out, the catalyst synthesis is done using templates or without templates. There have been reports which study the synthesis of various heterogeneous catalysts. One of such types of catalysts is supported oxides and mixed oxides. Oxides and mixed oxides have attracted considerable attention in the stream of heterogeneous catalysis, serving either as catalysts or as supports for many catalytically active species (metallic nanoparticles, oxides, organometallic complexes, enzymes, etc.). Oxides are preferred for their thermal and chemical stability, and mechanical strength when used as supports and also for their intrinsic activity (acidic, basic, redox) when employed as catalysts. Oxide like silica (SiO_2) is a largely studied support in the field of heterogeneous catalysis. Commercially, ordered or disordered SiO_2 support is synthesized using sol-gel method (with or without template) to get a high surface area mesoporous sample using tetraethyl orthosilicate (TEOS) as a SiO_2 precursor.

However, for the first time our group has successfully established the synthesis of high surface area ($896 \text{ m}^2/\text{g}$) mesoporous (average pore volume of $0.93 \text{ cm}^3/\text{g}$ and average pore diameter of 42.5 \AA) SiO_2 by sol-gel technique using ethyl silicate-40 (ETS-40) as a SiO_2 source and without using any template. From commercial point of view, ETS-40 is a cheaper SiO_2 source than TEOS.

Supported metal oxides are well known for catalyzing a large variety of reactions. Thus many studies have been devoted to the preparation and characterization of these solids. Metal oxide catalysts (viz., MoO_3 , WO_3) supported on SiO_2 , Al_2O_3 , ZrO_2 and TiO_2 have been extensively investigated because of their catalytic activity in oxidation and acid catalyzed organic reactions.

The use of mesoporous solid catalysts such as supported metal oxides and related molecular sieves has an additional benefit in organic synthesis. Furthermore, the incorporation of transition metal ions and complexes into the mesoporous supports extends their catalytic scope to redox reactions and a variety of other transition metal acid-catalyzed processes.

One such largely studied material is supported molybdenum oxide catalysts. Silica-supported molybdenum oxide ($\text{MoO}_3/\text{SiO}_2$) prepared by an impregnation

method or sol-gel method has been used as a catalyst in a variety of reactions, such as the olefin metathesis,^[10] selective oxidation,^[11] oxidative dehydrogenation of light alkanes^[12] and photocatalytic oxidation of CO.^[13] It has also been used extensively to catalyze the selective oxidation of methane to methanol.^[14-16] It also gives activity comparable to that of the commercial catalyst TS-1 for the liquid-phase epoxidation of propylene,^[17] which is an important industrial process commercialized by Sumitomo^[18] using TS-1 and cumene hydroperoxide as an oxidant. In recent years, lot of work has been carried out on the synthesis and catalytic applications of MoO₃/SiO₂ catalyst as a solid acid as well as oxidation catalyst. MoO₃/SiO₂ catalysts prepared by sol-gel method were used for nitration of simple aromatic compounds by Ma *et al.*^[19] In both the above mentioned cases, tetraethyl orthosilicate was used as silica precursor. Park *et al.*^[20] used MoO₃/SiO₂ prepared by wet impregnation technique as a catalyst for double bond migration from 2-butene to 1-butene.

In the thesis, a modified sol-gel method has been used to prepare the MoO₃/SiO₂ catalyst in which ammonium heptamolybdate (AHM) and ethylsilicate-40 (ETS-40) have been used as a molybdenum and silica source, respectively. During the sol-gel method, the structure of the gel would be affected significantly by the preparation procedure, resulting in the change in textural and catalytic properties of synthesized catalysts. In the chapter, synthesis and detailed characterization of the MoO₃/SiO₂ catalysts has been discussed.

2.2. Experimental Section

2.2.1. Material

All the reagents viz., AHM, ETS-40 (Chemplast, Chennai, CAS registry no. 18945-71-7), *iso*-propyl alcohol (IPA), 50% aqueous hydrogen peroxide, 25% ammonia solution, were of AR grade (99.8%) and were obtained from S.D. Fine, Thomas Baker, LOBA and Merck chemicals, India. The chemicals were used without further purification.

2.2.2. Catalyst Preparation

The MoO₃/SiO₂ catalyst was synthesized using a novel sol-gel technique. Two different MoO₃ precursors viz., AHM, and molybdenum oxo-peroxo species were used to prepare the catalyst. MoO₃/SiO₂ catalyst was also prepared using conventional impregnation technique to compare the properties of the sol-gel synthesized catalyst

with that prepared by impregnation method. The typical synthesis procedures are discussed below:-

a) Sol-gel synthesis of $\text{MoO}_3/\text{SiO}_2$ catalyst using (AHM) as MoO_3 precursor:

$\text{MoO}_3/\text{SiO}_2$ catalysts with varying molybdenum oxide molar concentrations (1, 5, 10, 15, and 20 mol%) were prepared. In a typical procedure, 20 mol% $\text{MoO}_3/\text{SiO}_2$ catalyst was synthesized by dissolving 14.11 g AHM in 40 mL distilled water at 80 °C. This hot solution was added drop wise to the dry IPA solution of ETS-40 (48.0 g ETS-40 in 100 mL of IPA) with constant stirring. The resultant transparent greenish gel was air dried and calcined at 500 °C in air in a muffle furnace for 5 h. Similarly catalysts with 1, 5, 10, 15 mol% molybdenum oxide loadings were prepared (Figure 2.3).

b) Sol-gel synthesis of $\text{MoO}_3/\text{SiO}_2$ catalyst using molybdenum peroxy species as precursor:

In a typical procedure, 9.1 g AHM was separately dissolved in 50% aqueous hydrogen peroxide solution to form molybdenum peroxy species, its quantity being calculated to obtain required final MoO_3 loading on the calcined oxide precursors. This solution was added drop wise to the dry IPA (100 mL) solution of ETS-40 (31.25 g) with constant stirring. The solution was kept overnight until a transparent yellowish gel was obtained. The resultant yellow gel was air dried and calcined at 500 °C in air in a muffle furnace for 5 h. The catalyst will be referred to as MSOP.

c) Sol-gel synthesis of pure silica (SiO_2) using ETS-40 as silica source:

Pure high surface area SiO_2 catalyst was prepared for comparison by adding 52 g ETS-40 to 30 g dry IPA; to this mixture 0.02 g ammonia solution (25%) was slowly added with constant stirring. The transparent white gel thus obtained was air dried and calcined in a muffle furnace at 500 °C for 5 h.

d) Synthesis of $\text{MoO}_3/\text{SiO}_2$ catalyst using AHM and ETS- 40 using conventional impregnation method:

In a beaker, 9.1 g AHM was dissolved in excess of warm distilled water. Sol-gel synthesized SiO_2 (as discussed in 'c' calcined at 500 °C, 12.5 g) was used as support. The SiO_2 was impregnated with AHM solution and the water was removed in a rotary evaporator at 60 °C until totally dried. The dried solid was calcined in muffle furnace at 500 °C for 5 h. The catalyst will be referred to as MS-imp.

2.2.3. Characterization

(a) Powder X-ray Diffraction studies

The powder X-ray diffraction data of the samples was collected on a Rigaku Miniflex diffractometer equipped with a Ni filtered CuK α radiation ($\lambda = 1.5406 \text{ \AA}$, 30 kV, 15 mA) radiation. The data was collected in the 2θ range $20\text{-}80^\circ$ with a step size of 0.02° and scan rate of $4^\circ/\text{min}$.

(b) Nitrogen Adsorption studies

The BET surface area of the calcined samples was determined by N₂ sorption at -196°C using NOVA 1200 (Quanta Chrome) equipment. Prior to N₂ adsorption, the materials were evacuated at 300°C under vacuum. The specific surface area, S_{BET} , was determined according to the BET equation.

(c) NH₃-Temperature Programmed Desorption studies

Temperature programmed desorption of ammonia (NH₃-TPD) was carried out using a Micromeritics Autocue 2910 apparatus. The catalyst was cleaned up at 500°C in a He flow and then cooled to 100°C prior to NH₃ adsorption followed by the desorption experiment carried out at the rate of $10^\circ\text{C}/\text{min}$ till 600°C .

(d) FTIR of Adsorbed Pyridine studies

The nature of the surface acid sites was studied by FTIR of adsorbed pyridine. The FT-IR spectra of chemisorbed pyridine (py-IR) were obtained in a high temperature cell (Spectra-Tech) fitted with a Zn-Se window (Shimadzu 8000 FTIR spectrophotometer). The temperature in the cell was varied from 40°C to 400°C . The sample (30 mg) was finely crushed and placed in a sample holder. Prior to pyridine adsorption, the sample was out gassed for 2 h at 400°C under N₂ flow to get rid of the adsorbed moisture. The cell was cooled to 100°C stepwise and the spectra of neat catalyst were recorded (100 scans and resolution 4 cm^{-1}) at different temperatures. The sample was dosed with two successive pulses of pyridine ($10 \mu\text{L}$ each). The temperature-programmed desorption of pyridine was studied at 100, 200, 300 and 400°C after equilibration for 30 min after attaining the temperature. The spectrum of the neat sample was subtracted from the pyridine adsorbed sample.

(e) Fourier Transform Infrared Spectroscopic studies

The Fourier transform infrared spectroscopy (FT-IR) spectra of the samples were recorded on a Thermo Nicolet Nexus 670 IR instrument at ambient conditions using KBr pellets with a resolution of 4 cm^{-1} in the range of $4000\text{-}400 \text{ cm}^{-1}$ and with 100 scans.

(f) Raman Spectroscopic studies

Raman spectra were recorded under ambient conditions on a LabRAM infinity spectrometer (Horiba-Jobin-Yvon) equipped with a liquid nitrogen detector and a frequency doubled Nd-YAG laser supplying the excitation line at 532 nm with 1-10 mW power. The spectrometer was calibrated using the Si line at 521 cm^{-1} with a spectral resolution of 3 cm^{-1} .

(g) Transmission Microscopic studies

TEM measurements were performed on a JEOL model 1200EX instrument operating at an accelerating voltage at 120 kV. Before analysis, the powders were ultrasonically dispersed in ethanol, and two drops of ethanol containing the solid were deposited on a carbon coated copper grid.

2.3. Results and discussion

Our group has successfully established the synthesis of pure SiO_2 by sol-gel technique using ETS-40 as a SiO_2 source for the first time and without the use of any surfactant template. By this method a very high surface area of $896\text{ m}^2/\text{g}$ with an average pore volume of $0.93\text{ cm}^3/\text{g}$ and average pore diameter of 42.5 \AA was obtained. The SiO_2 synthesized by this method showed a very high mesoporosity.

ETS-40 is a condensed oligomeric liquid with a siloxane backbone having the following formula as shown in Figure 2.1. The value of n varies from 3 to 5. The average value of n is 5.

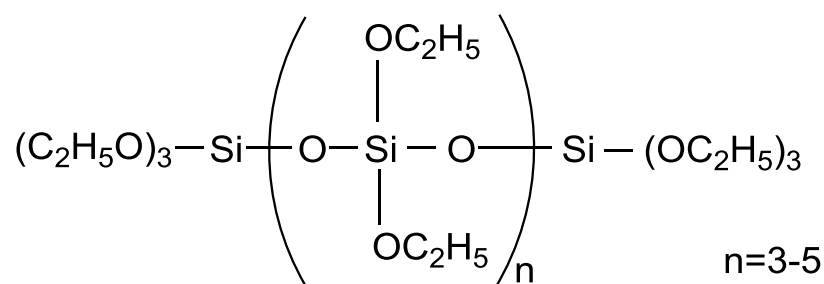


Figure 2.1. Structural formula of ethyl silicate-40 (ETS-40)

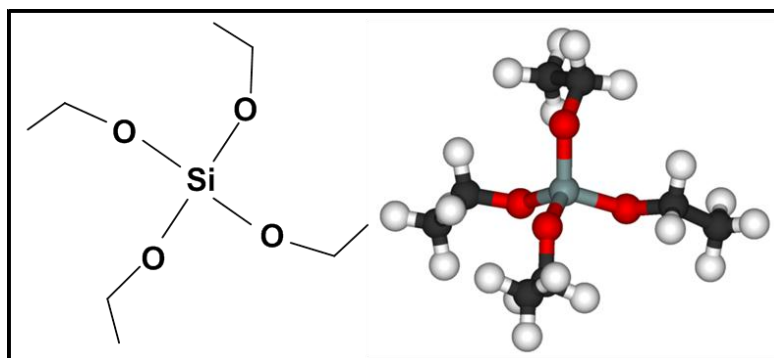


Figure 2.2. Structural formula of tetraethyl orthosilicate (TEOS)

ETS-40 is transparent liquid containing 40% silica (SiO_2) by mass, but in practice, in addition to chain condensates, it also contains branch-shaped and ring-shaped condensates. It is used in industry as foundry chemical for investment casting and is manufactured on industrial scale and is comparatively very cheap compared to TEOS (monomer) (Figure 2.2) which is conventionally used as silica source in silica based catalyst synthesis. ETS-40 is a polymeric form (trimeric and tetrameric) of TEOS monomer, which on controlled hydrolysis yields silica of a very high surface area.^[21,22] The trimeric and tetrameric silica structures restrict the growth of large particles.

This high surface area mesoporous SiO_2 was used as support for the synthesis of acid catalyst and AHM was used as MoO_3 precursor for the incorporation of acidity. When AHM solution was added to ES-40, evolution of ammonia gas was observed showing the reaction between AHM and ES-40 during the synthesis by sol-gel technique. The resulting homogeneous and transparent solution formed when kept overnight gave a transparent solid mass showing the uniform distribution of molybdenum oxide in silica matrix. The present sol-gel synthesis procedure for synthesis of $\text{MoO}_3/\text{SiO}_2$ is quite simple compared to the conventional procedure using tetraethyl silicate monomer because ES-40, being polymerized silica network forms uniform silica support for uniform dispersion of MoO_3 (Figure 2.3).

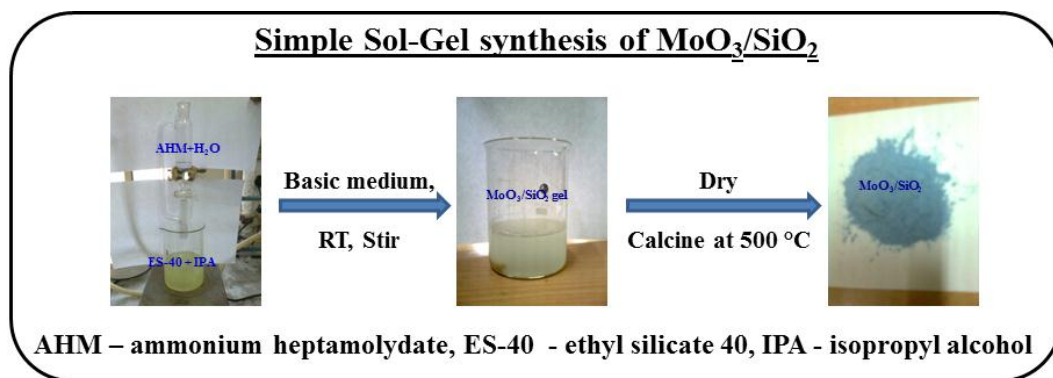


Figure 2.3. Pictorial presentation of sol-gel synthesis of $\text{MoO}_3/\text{SiO}_2$ catalyst

2.3.1. X-ray Diffraction studies

The XRD patterns of all the catalysts prepared by sol-gel are shown in Figure 2.4. For comparison, the XRD pattern of pure silica is also included (Figure 2.4a). The patterns showed the amorphous nature of the material at low Mo loadings (Figure 2.4b-d), indicating a very high dispersion of amorphous molybdenum oxo species on amorphous silica support up to 10 mol% loading of molybdenum oxide. The XRD patterns of the 15 and 20 mol% Mo loaded catalysts (Figure 2.4e and f) exhibited sharp peaks on the broad underlying peaks characteristic of the amorphous silica at $2\Theta = 24^\circ$. These intense peaks observed at $2\Theta = 12.9, 23.4, 25.8$ and 27.4° are characteristic of the α - MoO_3 orthorhombic phase.^[23] It is interesting to note that even though the MoO_3 showed the crystalline form at higher Mo loading, the silica support still retained its amorphous nature leading to the high surface area of the catalysts. From the X-ray diffraction patterns of the sol-gel synthesized solids it appeared that up to 10 mol% MoO_3 loading there is a uniform dispersion of amorphous molybdenum oxo species on silica support, however at higher loading, MoO_3 crystalline bulk phase of MoO_3 is formed on amorphous silica support.^[23]

The X-ray diffraction patterns of MS-imp and MSOP did not show any appreciable difference compared to that of 20 mol% $\text{MoO}_3/\text{SiO}_2$. The solids showed intense bands corresponding to crystalline MoO_3 albeit the SiO_2 support retained its amorphous nature (Figure 2.4 g and h).

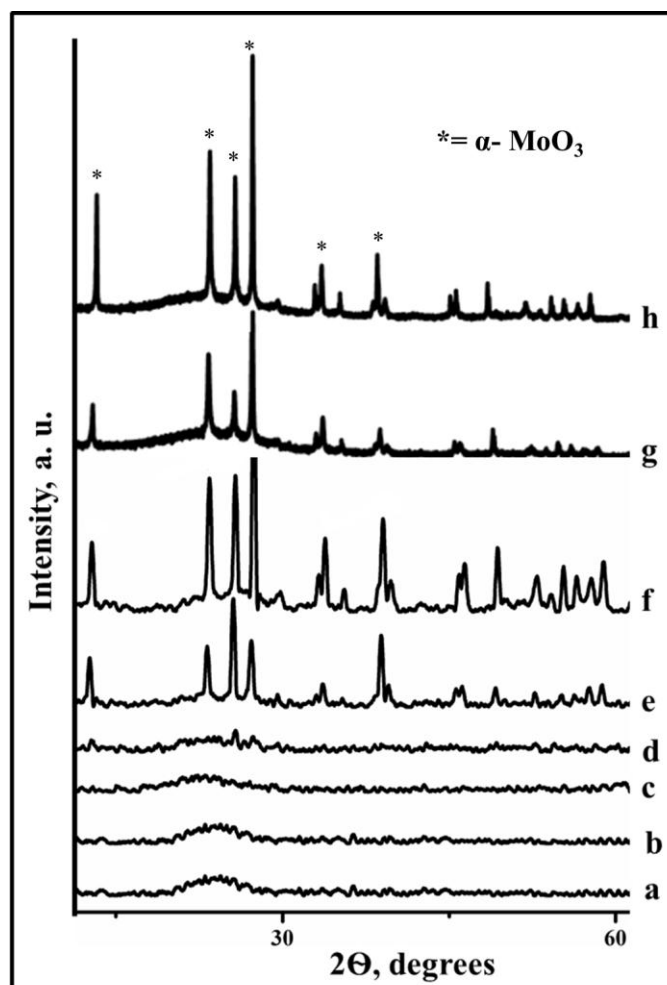


Figure 2.4. XRD of (a) pure silica, (b) 1, (c) 5, (d) 10, (e) 15, (f) 20 mol% MoO₃/SiO₂, (g) MSOP, (h) MS-imp

2.3.2. Textural Characterization

The surface areas of all the catalysts determined using BET method are given in Table 2.1. As expected, a very high surface area of 896 m²/g was observed in case of pure SiO₂ (PS) because of sol-gel technique using ETS-40 as the silica source. The surface area of the catalysts was found to decrease with increase in MoO₃ loading. During the sol-gel synthesis, an aqueous solution of AHM was added to ETS-40, which hydrolyzed ETS-40. However, the control of the rate of hydrolysis was difficult, because of the use of excess water for dissolving AHM, which led to a decrease in the surface area. It was expected that, as MoO₃ loading was increased, the crystalline molybdenum oxide clusters were formed that covered the amorphous silica support, reducing the total surface area of the catalyst. However, the catalysts prepared by sol-gel techniques showed a very high surface area as compared to the

catalysts prepared by impregnation method. For 1 mol% MoO₃ loading, the catalyst prepared by sol-gel technique showed surface area of 583 m²/g. When the MoO₃ content was increased to 20 mol% as expected the surface area decreased to 217 m²/g whereas the catalyst prepared by impregnation method showed a surface area of 149 m²/g compared to very high surface area of 896 m²/g of the pure SiO₂ support. The surface area of impregnated catalyst was appreciable compared to the surface area of the impregnated catalyst (114 m²/g) as reported in the literature.^[24] This may be because of higher surface area of silica prepared using ETS-40 as silica source on which 20 mol% MoO₃ was supported. When the surface area calculations were carried out for MSOP, no appreciable difference was observed. The surface area of MSOP was found to be 186 m²/g (Table 2.1). The mesoporosity of the catalysts was evident for all the catalysts including PS (Figure 2.5, Table 2.1). The N₂ adsorption-desorption studies were carried out for the samples synthesized by sol-gel method (Figure 2.6).

Table 2.1. Textural data and acidity of the catalysts

Catalyst	Surface Area, m ² /g	Pore Volume, cm ³ /g	Average Pore Diameter, A°	NH ₃ desorbed, mmol/g	Surface density of Mo on support (D _m), nm ⁻²
SiO ₂	896	0.93	42.5	0.03	00
1 mol% MoO ₃ /SiO ₂	583	0.63	40.7	0.18	0.0716
5 mol% MoO ₃ /SiO ₂	432	0.59	58.2	0.56	0.483
10 mol% MoO ₃ /SiO ₂	284	0.57	79.6	0.71	1.472
15 mol% MoO ₃ /SiO ₂	275	0.51	74.2	0.86	2.280
20 mol% MoO ₃ /SiO ₂	217	0.37	67.9	0.94	7.891
20 mol% MoO ₃ /SiO ₂ *	186	n.e.	n.e.	0.87	8.432
20 mol% MoO ₃ /SiO ₂ #	149	n.e.	n.e.	n.e.	10.526

* - 20 mol% MoO₃/SiO₂ synthesized using Mo peroxy sol-gel technique

- 20 mol% MoO₃/SiO₂ synthesized using conventional wet impregnation technique

n.e.- not evaluated

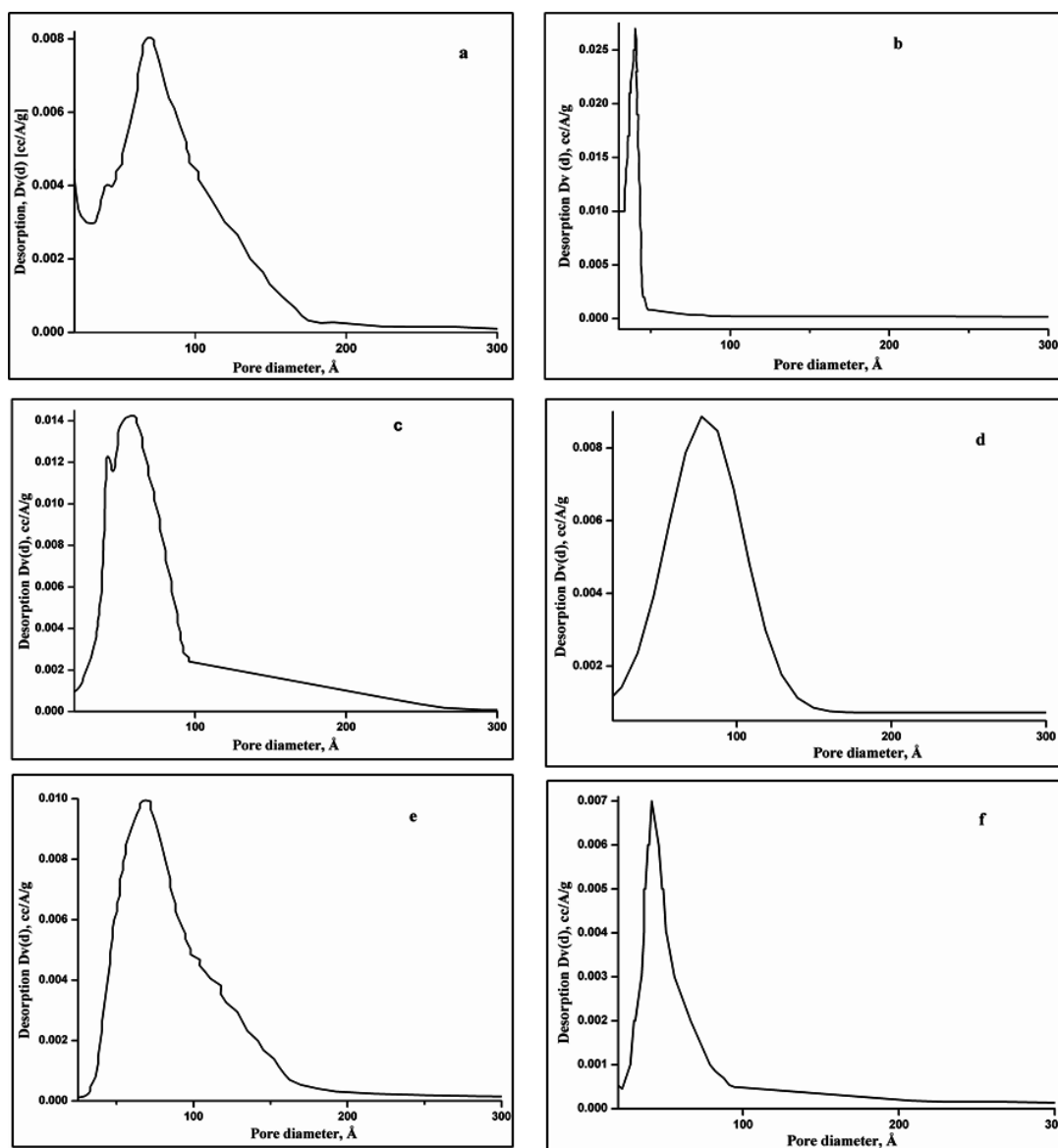


Figure 2.5. Pore size distribution of (a) SiO_2 , (b) 1, (c) 5, (d) 10, (e) 15, (f) 20 mol% $\text{MoO}_3/\text{SiO}_2$

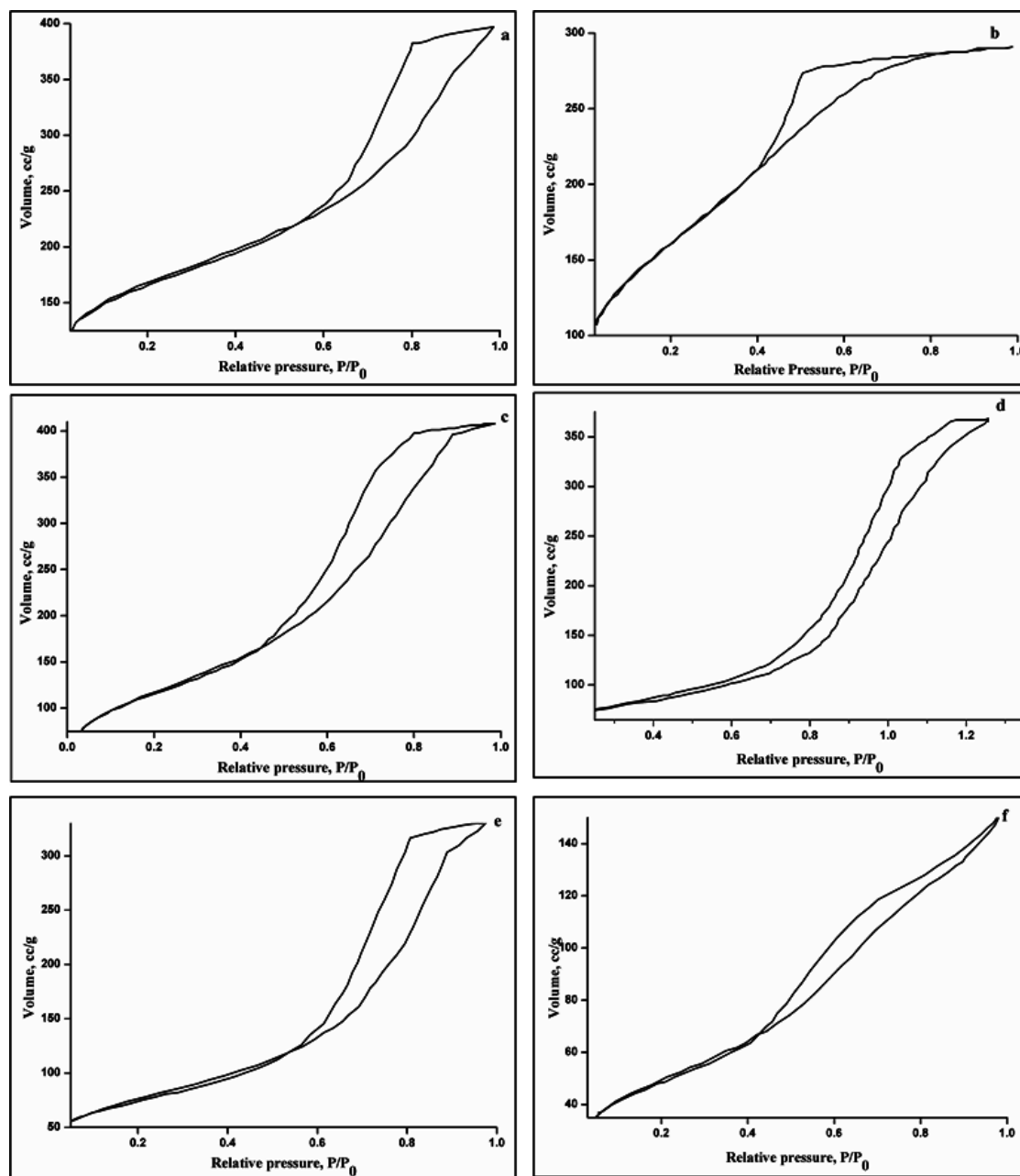


Figure 2.6. Adsorption-desorption isotherms of (a) SiO_2 , (b) 1, (c) 5, (d) 10, (e) 15, (f) 20 mol% $\text{MoO}_3/\text{SiO}_2$

‘Mo’ surface density (i. e., number of Mo atoms per square nanometer BET surface area) was evaluated from the ‘Mo’ content and surface area. Surface density is defined as the quantity of a component distributed per unit area of surface (eq. 2.1). The surface density of Mo on the SiO_2 surface was calculated as follows-

C_m = Mo content, N_m = number of Mo atoms per gram sample, D_m = Mo surface density and S_m = surface area

$$N_m = (C_m/100) \times (1/\text{Mol. Wt. of MoO}_3) \times (6.023 \times 10^{23})$$
$$D_m = N_m \times S_m \quad \text{----- (eq. 2.1)}$$

Using eq. 1 the surface density of Mo on SiO₂ could be evaluated assuming that the Mo atoms are equally distributed on the surface of SiO₂. The surface density of 'Mo' on the support increased with increase in 'Mo' content. It was 0.07 for 1 mol% MoO₃/SiO₂, which increased to 7.89 for 20 mol% MoO₃/SiO₂. This gave an idea about the optimum Mo distribution over the surface per unit area of SiO₂ assuming the uniform distribution of MoO₃ on high surface area SiO₂. This physical property is considered as a quasi-quantitative value as the calculations are valid only and only when the Mo atoms are equally distributed over the surface of the support. Owing to this, the calculations were not applicable for the catalysts with higher Mo loadings of 15 and 20 mol% as we observed the presence of both nano-sized MoO₃ particles and particles with larger size (Figures 2.4, 2.17 and 2.18).

2.3.3. Acidity Measurements

Ammonia-TPD experiments were carried out to determine the acid strength of the catalysts. The results are shown in Figure 2.7 and amount of NH₃ desorbed is given in Table 2.1. The pure silica catalyst showed the lowest acidity, with 0.0317 mmol/g of ammonia desorbed at comparatively lower temperature, indicating the presence of few weaker acid sites. Addition of 1 mol% MoO₃ to the silica support by sol-gel increased the acidity almost six times (0.183 mmol/g) with respect to the number of acid sites as well as the acid strength. The temperature for total desorption of ammonia increased (275-400 °C) with increase in MoO₃ loading showing the increase in acid strength as well as in the number of acid sites. The catalyst with 20 mol% MoO₃ loading showed maximum number of acid sites (NH₃ desorbed: 0.937 mmol/g) as well as the highest acid strength.

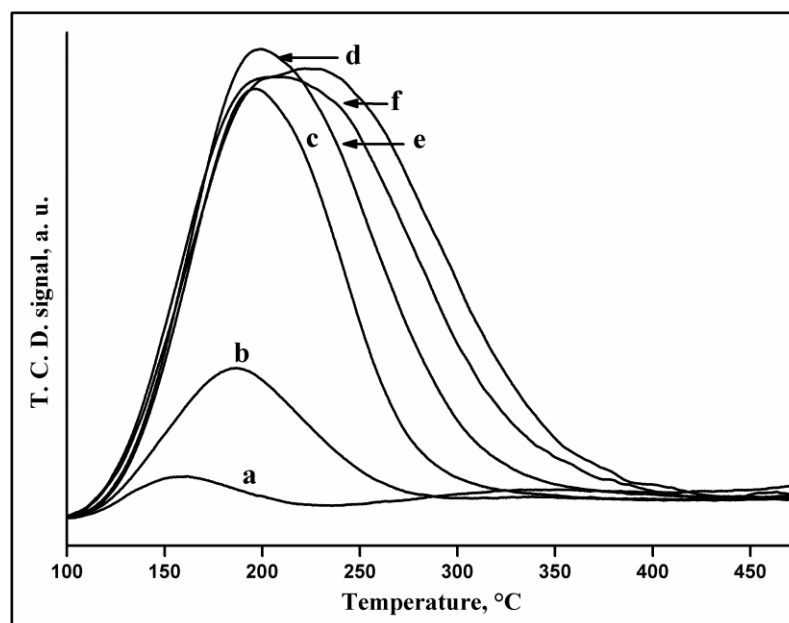


Figure 2.7. NH_3 -TPD of (a) pure silica, (b) 1, (c) 5, (d) 10, (e) 15, (f) 20 mol% $\text{MoO}_3/\text{SiO}_2$

2.3.4. FTIR of Adsorbed Pyridine

FTIR of adsorbed pyridine was studied for the determination of the nature of acidity which revealed the presence of Lewis acidity in all the catalysts as shown in Figure 2.8. Whereas, the presence of both Lewis and Brønsted acidity was observed at high ‘ MoO_3 ’ loadings. The IR spectra of adsorbed pyridine on the catalyst surface is shown in Figure 2.8. The spectrum of pure silica (Figure 2.8a) showed the presence of only Lewis acidity (peak at 1450 cm^{-1}) with low acidity; the 1 mol% $\text{MoO}_3/\text{SiO}_2$ sample (Figure 2.8b) showed increase in Lewis acidity. As the MoO_3 loading was further increased, the samples showed the presence of both Brønsted (peak at 1540 cm^{-1}) as well as Lewis acid sites (Figure 2.8c-f). The generation of Brønsted acidity may be correlated to the formation of polymolybdate Keggin structures.^[24] The observations were in good agreement with the findings from the FTIR spectra of the samples (Figure 2.9). The IR spectra of the catalyst in the framework region showed the presence of peaks at 959 and 914 cm^{-1} , which correspond to polymolybdate Keggin structures which is reported to exhibit Brønsted acidity. The oxide becomes hydrated and subsequently converts into polymolybdenic trimers.^[25,26] Such structural units are expected to show Brønsted acidity. The ratio of Brønsted to Lewis (B/L) acidity increased with increase in Mo loading. Though the Lewis acidity was found to decrease with increase in Mo loading, the Brønsted acidity observed at higher Mo

loading contributed to overall increase in the total acidity, which was seen by NH_3 -TPD. Literature reports showed the presence of only Lewis acid sites without any Brønsted acidity on $\text{MoO}_3/\text{SiO}_2$ catalysts prepared by impregnation technique. Also, the NH_3 desorption in case of impregnated catalyst takes place at much lower temperature ($<250\text{ }^\circ\text{C}$) indicating presence of weak acidity.^[27]

2.3.5. FT-IR Spectroscopic studies

The FTIR spectra of all the catalyst samples prepared by sol-gel technique are presented in Figure 2.9. The prominent band around $1300\text{--}1000\text{ cm}^{-1}$ and 800 cm^{-1} were due to the asymmetric stretching, symmetric stretching and bending of Si-O-Si, respectively. The bands at 993 , 872 and 570 cm^{-1} were observed in case of samples with higher Mo loading, which indicated the formation of $\alpha\text{-MoO}_3$. The band around 951 cm^{-1} , with a shoulder at about 908 cm^{-1} , for all the samples correspond to supported molybdenum species. However, the spectra of low MoO_3 loadings mainly showed the bands of SiO_2 .^[28]

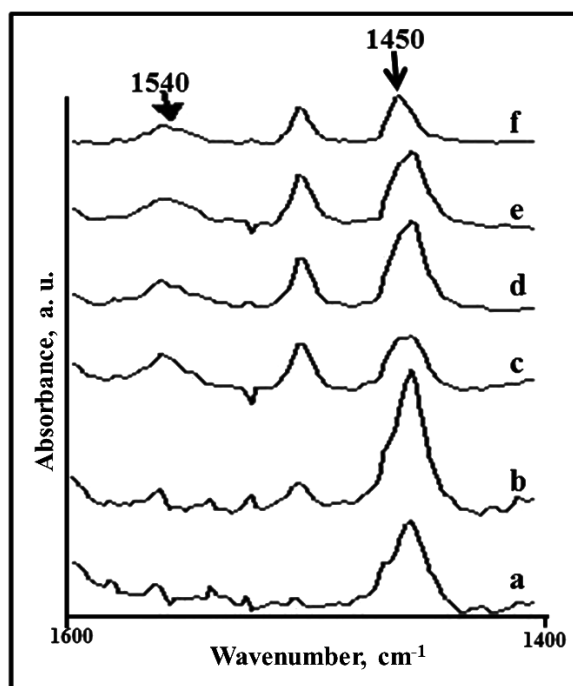


Figure 2.8. Pyridine adsorption spectra of (a) pure silica, (b) 1, (c) 5, (d) 10, (e) 15, (f) 20 mol% $\text{MoO}_3/\text{SiO}_2$ at $100\text{ }^\circ\text{C}$

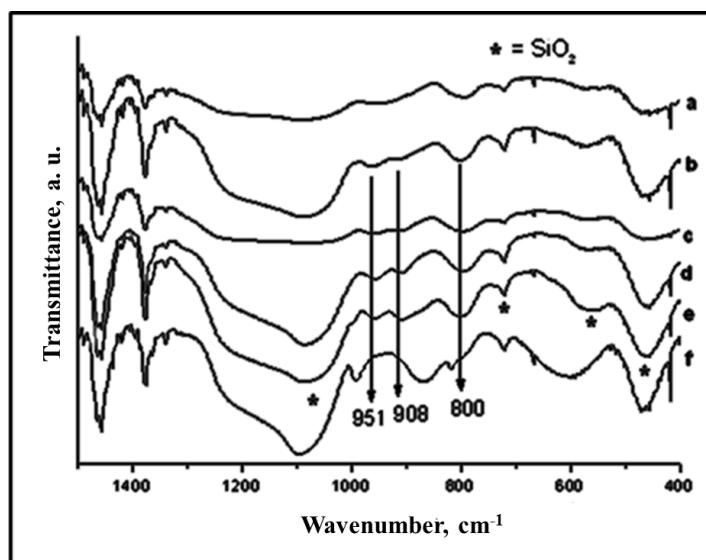


Figure 2.9. FTIR spectra of (a) pure silica, (b) 1, (c) 5, (d) 10, (e) 15, (f) 20 mol% MoO₃/SiO₂ by sol gel technique

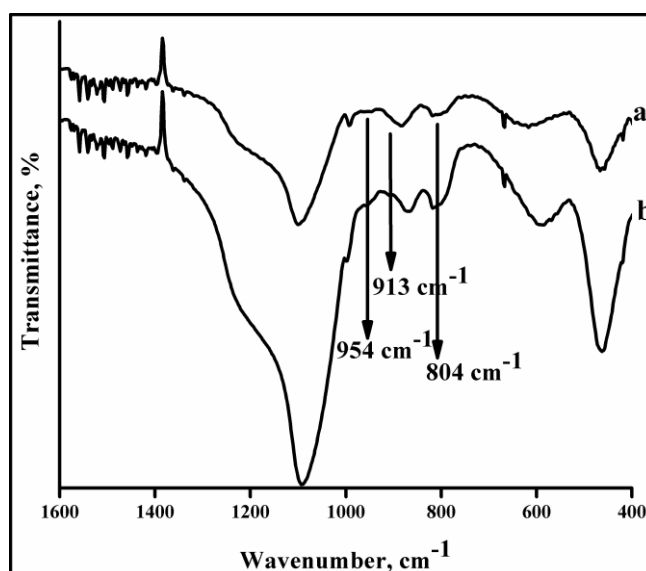


Figure 2.10. FTIR spectra (a) MSOP (b) MS-imp

The FTIR spectra of MSOP and MS-imp (Figure 2.10) showed the presence of main bands at 993, 872 and 570 cm⁻¹ (as those present in sol-gel synthesized MoO₃/SiO₂ catalysts) corresponding to α -MoO₃ and bands at 954, 913 and 804 cm⁻¹ showing the presence of oxo-molybdenum species.

2.3.6. Raman Spectroscopic studies

Raman spectroscopic analysis after calcination allowed us to have a better insight of the exact nature of deposited oxomolybdenum species. The Raman spectra of the

calcined samples prepared by sol-gel method at low (1 and 5%) and high (10, 15 and 20 mol%) loadings are, respectively shown in Figures 2.11 and 2.12. The broad line between 450-500 cm^{-1} , centered at 480 cm^{-1} (Figure 2.11a) was due to the silica support. The two samples with low Mo loading exhibited the same Raman lines at 247, 629, 961 and 981 cm^{-1} which are assigned to the silicomolybdic heteropolyanion (HPA) $[\text{SiMo}_{12}\text{O}_{40}]^{4-}$ (SMA) inside silica pores.^[29] As the Mo loading increased, new Raman lines appeared at 213, 383 and 876 cm^{-1} , the exact origin of which was not clearly established. However they were not observed at high Mo loading. At higher Mo loading, from 10 to 20 mol% MoO_3 , the Raman spectra exhibited the lines characteristic of $\alpha\text{-MoO}_3$ (161, 285, 293, 339, 381, 666, 819 and 996 cm^{-1}).^[30] However in the 10% $\text{MoO}_3/\text{SiO}_2$ spectrum (Figure 2.12c), the above mentioned features of the SMA (981, 666 and 247 cm^{-1}) were still observed together with lines at 952 and 889 cm^{-1} characteristic of well dispersed polymolybdate species by reference to literature.^[31] In the Raman spectra of the 15 and 20 mol% $\text{MoO}_3/\text{SiO}_2$, these features were no longer observed.^[32] However, a weak line was observed at 960 cm^{-1} in Figure 2.12e that could also correspond to surface polymolybdate species. In the spectrum of 15 mol% $\text{MoO}_3/\text{SiO}_2$ (Figure 2.12d) two new lines were observed at 852 and 778 cm^{-1} that were assigned to the formation of $\beta\text{-MoO}_3$.^[33,34]

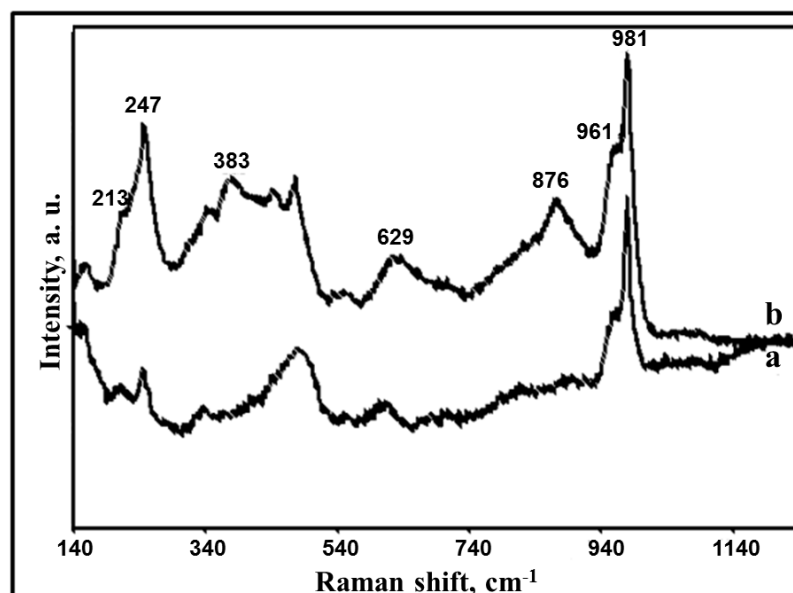


Figure 2.11. Raman spectra of a) 1 and b) 5 mol% MoO_3 supported on silica prepared by sol-gel method and calcined at 500 $^\circ\text{C}$

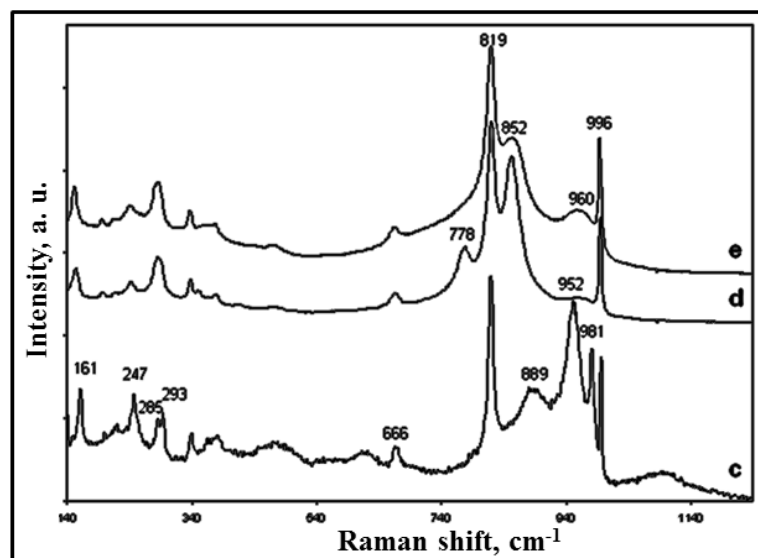


Figure 2.12. Raman spectra of c) 10, d) 15 and e) 20 mol% MoO₃ supported on silica prepared by sol-gel method and then calcined at 500 °C

The nature of the molybdenum species formed versus the Mo loading is in agreement with the evolution of the Raman spectra of the dried solids that are shown in Figure 2.13. At low Mo loading (typically 1 and 5%) they exhibit a broad line at 960 cm⁻¹ that is characteristic of a well dispersed polymolybdate phase. A shoulder is observed at 980 cm⁻¹ on its high wavenumber side that, together with the line at 626 and 248 cm⁻¹, is characteristic of the molecular silicomolybdic entities, the amount of which being very low. At higher Mo loading, the spectra (Figure 2.13c, d, e) exhibited the main lines characteristic of the AHM that transforms into α -MoO₃ upon calcination. Up to 10 mol% Mo loading presence of silicomolybdic acid as well as well dispersed polymolybdate phase was observed in the Raman spectra of the samples after calcination and transfer in air. It is well documented that hydration occurs in air^[35,36] after the calcination and it can be considered that a thin film of water covers the silica surface, which is also suggested for MoO₃/SiO₂ prepared by impregnation.^[28] The presence of SMA at low Mo loading is directly correlated to the ZPC (zero point of charge) of such silica support, which allows preservation of this HPA, which is only stable in solution at low pH values typically below 2. The increase in the Mo loading led to an increase in the pH of the solution inside the pores, which induced the presence of a well dispersed surface polymolybdate. This explained why SMA was mainly observed at low loading in the calcined solids whereas it was not observed before calcination, due to the pH of the dried gel (pH \approx 7).

The formation of this SMA heteropolyanion was not observed in the dried sample, which could be assigned to the fact that SiO_2 is not formed in dried sample and the ZPC of the amorphous gel is higher than that of the above mentioned pH stability limit. At 10 mol% MoO_3 the $\beta\text{-MoO}_3$ was evidenced by Raman spectroscopy. However the $\beta\text{-MoO}_3$ phase was not detected by the XRD technique. It should be present as microcrystallites well dispersed inside the silica framework (not observed by XRD). Thus this preparation method allowed us to stabilize this phase even after calcination at 500 °C, a temperature at which the transformation into its orthorhombic form should have been observed. At higher Mo loading (10, 15, 20 mol%) the formation of $\alpha\text{-MoO}_3$ was observed. However, this formation can be correlated to the precipitation of AHM as evidenced by the Raman spectroscopic study of the dried solids. This would lead to a lower interaction between the molybdenum oxo species and the silica and consequently to the formation of $\alpha\text{-MoO}_3$ as in the classical impregnation. This suggested that the $\beta\text{-MoO}_3$ phase could originate from the well dispersed oxomolybdate phase, and its stabilization was induced by the interaction with the support.

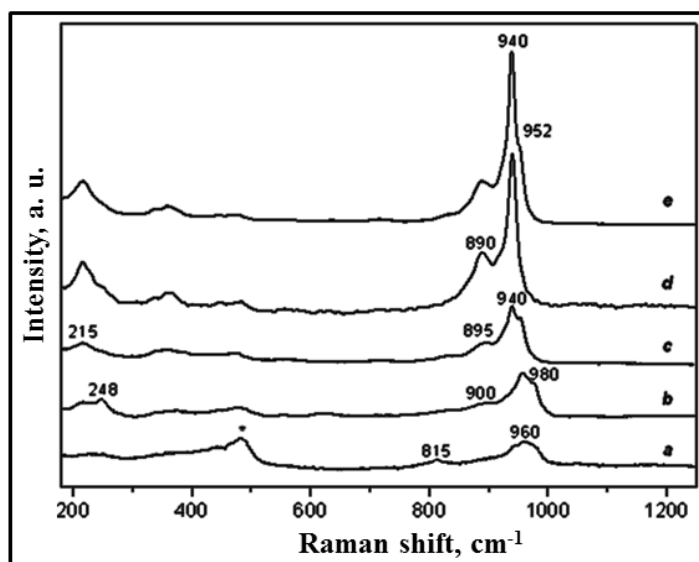


Figure 2.13. Raman spectra of a) 1, b) 5, c) 10, d) 15 and e) 20 mol% MoO_3 supported on silica prepared by sol-gel method and then dried at 100 °C

2.3.7. Transmission Electron Microscopic studies

The existence of nanosized MoO_3 particles on the mesoporous silica support is corroborated by TEM analysis (Figures 2.14-2.18). For the different Mo loadings (1-

20 mol%), TEM images showed the presence of small MoO_3 particles dispersed on the silica support, with a particle size comprised between 1 and 2 nm. The distribution of nano MoO_3 seemed to be increasing with Mo loading as seen in the TEM images of the 20 mol% MoO_3 sample in Figure 2.18b, where areas with larger particles (6-8 nm) were observed.

Together with these nanoparticles, bulk MoO_3 appeared to be present in the samples with high Mo loadings (from 10 mol%), as shown in Figures 2.16b and 2.16c. These results are in good agreement with the Raman spectroscopic study showing the presence of bulk MoO_3 on the samples with 10, 15 and 20 mol% Mo loadings, possibly resulting from AHM precipitation as mentioned before. The quantity of this compound may not be sufficient to be detected by XRD in the 10% Mo sample.

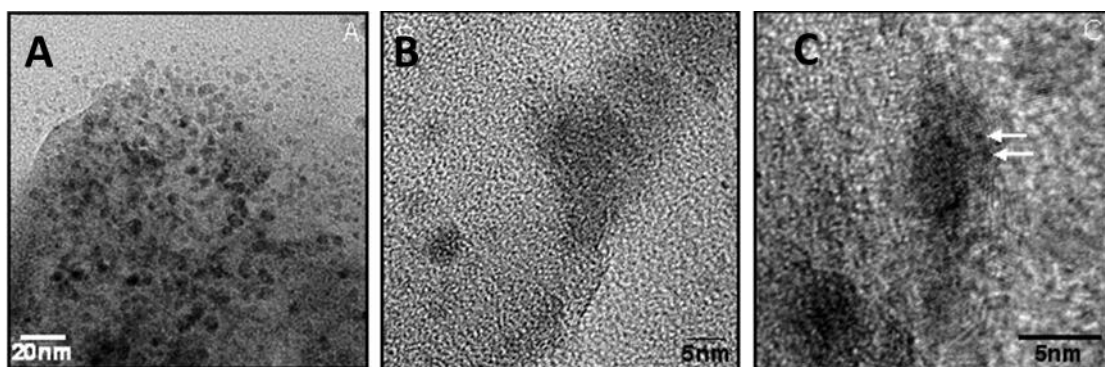


Figure 2.14. TEM micrograph of 1 mol% $\text{MoO}_3/\text{SiO}_2$ prepared by sol gel focused on different areas

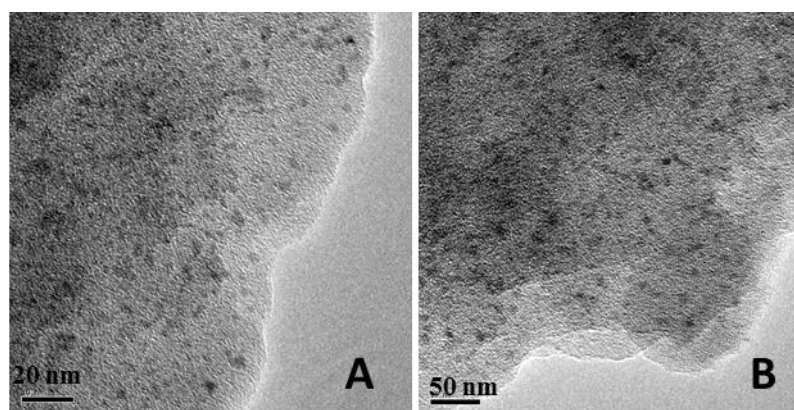


Figure 2.15. TEM micrograph of 5 mol% $\text{MoO}_3/\text{SiO}_2$ prepared by sol gel focused on different areas

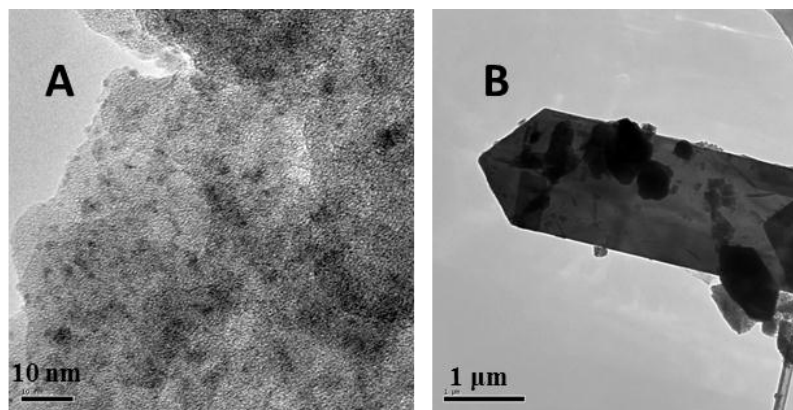


Figure 2.16. TEM micrograph of 10 mol% MoO₃/SiO₂ prepared by sol gel focused on different areas

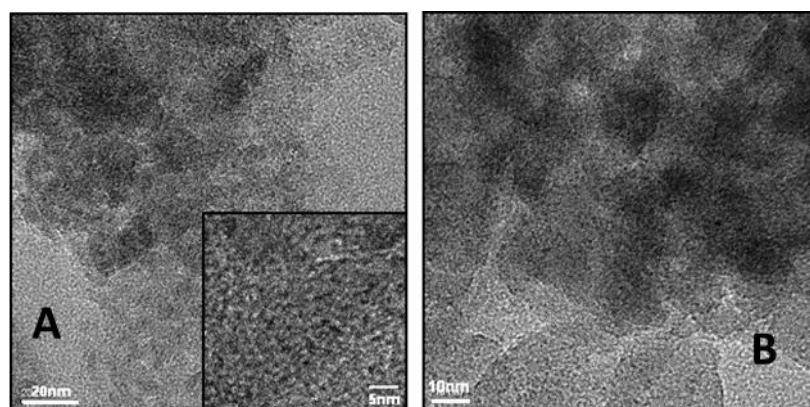


Figure 2.17. TEM micrograph of 15 mol% MoO₃/SiO₂ prepared by sol gel at different magnification and focused on different areas

The ammonia and pyridine adsorption was studied on the solids activated by a thermal treatment (preactivation at 500 and 400 °C respectively). However this treatment modified the nature of the well dispersed surface oxomolybdate species as it has been clearly shown by Raman spectroscopy.^[37] The coordination of the Mo being lower than 6, pre-activated solids would exhibit Lewis acid site rather than Brønsted ones, which is in agreement with the pyridine acidity measurement. Thus the ammonia desorption at low temperature on these solids should correspond to ammonia molecules adsorbed on Lewis acid sites. Upon increasing the Mo loading this acidity was still observed in agreement with Raman spectroscopy as the lines characteristic of the aforementioned well dispersed oxomolybdate phase were still observed. Stronger acidity is evidenced by NH₃-TPD^[38] at this high Mo loading whereas pyridine adsorption showed the existence of Brønsted sites also.

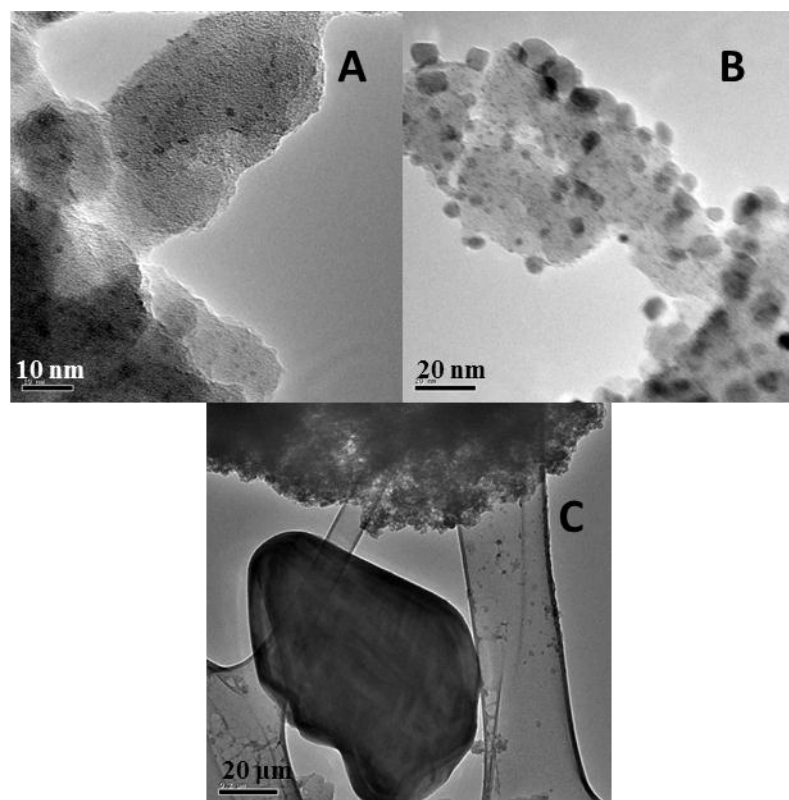


Figure 2.18. TEM micrograph of 20 mol% MoO₃/SiO₂ prepared by sol gel focused on different areas

It can be considered that the Brønsted acidity observed at higher Mo loading contributed to overall increase in the total acidity, which is seen by NH₃-TPD. Such evolution is in agreement with the Raman spectroscopic characterization, which proved the presence of the above mentioned surface oxomolybdate phase and of a mixture of α - and β - MoO₃ nanoparticles, their relative amount depending on the Mo loading. Both MoO₃ phases could be responsible for this new Brønsted acidity. This is in agreement with literature data showing that bulk MoO₃ may exhibit Brønsted acidity.

Recently, Ma *et al.*^[19] reported the synthesis of MoO₃/SiO₂ catalysts by sol-gel technique. The surface area of pure SiO₂ was 630 m²/g and that of 20 mol% MoO₃/SiO₂ was found to be 150 m²/g. Another group reported the synthesis of MoO₃/SBA-15 using impregnation technique. In this case the surface area of 10 wt% MoO₃/SiO₂ was found to be 111 m²/g, though SBA-15 is a high surface mesoporous support and the loading of MoO₃ in terms of wt% is comparatively very low than that reported in the present work (1-20 mol% MoO₃ loading). Miao *et al.*^[17] also reported the synthesis of MoO₃/SiO₂ by sol-gel method using TEOS and AHM as SiO₂ and

MoO₃ precursors, respectively. In this case, from the NH₃-TPD results, very low surface acidity was observed for the MoO₃/SiO₂ catalyst. Another recent report by Adam *et al.*^[39] showed the synthesis of MoO₃/SiO₂ by sol-gel method. However, in this case rice husk was used as SiO₂ precursor for which a very complex procedure has been reported for the extraction of SiO₂ from the husk. There are many reports on the sol-gel synthesis of MoO₃/SiO₂ catalysts. However, in many cases TEOS or commercial SiO₂ has been used as SiO₂ precursor resulting in low surface area of catalyst. In our case we have established a simple sol-gel route without using any surfactant or template for the synthesis of MoO₃/SiO₂ acid catalyst. The series of catalyst has shown very high surface area, mesoporosity and high total acidity compared to the literature reports.

2.4. Conclusions

ETS-40 was used as a novel precursor for the synthesis of high surface mesoporous SiO₂. High surface area mesoporous MoO₃/SiO₂ catalysts were prepared by sol-gel technique and characterized. The detailed characterization of the catalysts showed presence of various well dispersed entities like SMA, polymolybdate species or molybdenum oxide nanoparticles depending on the Mo loading. The present sol-gel method of preparation allowed us to increase the dispersion and the range of existence of the Mo entities with the Mo loading. It has been shown that the SMA at low Mo loading was not formed during the sol-gel process but by the rehydration of the calcined catalyst due to the presence of nanosized molybdenum oxo species supported on high surface mesoporous silica support. It has been shown that the formation of aggregates of α -MoO₃ particles at high Mo loadings originates from the AHM precipitation during the sol-gel preparation. The acidity measurements are in good agreement with this description, that well dispersed phases exhibit only Lewis acidity, whereas molybdenum oxide particles exhibit both Lewis and Brønsted acidity.

2.5. References

- 1 M. Kuil, T. Soltner, P. W. N. M. van Leeuwen, J. N. H. Reek, *J. Am. Chem. Soc.* **2006**, 128, 11344.
- 2 R. Jira, *Angew. Chem. Int. Ed.* **2009**, 48, 9034.
- 3 J. H. Jones, *Platinum Metals Rev.* **2000**, 44, 94.

- 4 D.Astruc, *New J. Chem.* **2005**, 29, 42.
- 5 I. Chorkendroff, J. W. Niemantsverdriet *Concepts of Modern Catalysis and Kinetics* Wiley-VCH **2003**.
- 6 D. P. Debecker, P. H. Mutin, *Chem. Soc. Rev.* **2012**, 41, 3624.
- 7 H. D. Gesser, P. C. Goswami, *Chem. Rev.* **1989**, 89, 765.
- 8 C. J. Brinker, G. W. Sherer, *Sol-Gel Science*, Academic Press, San Diego, **1990**, 20.
- 9 L. L. Hench, J. K. West, *Chem. Rev.* **1990**, 90, 33.
- 10 J. Handzlik, J. Ogonowski, J. Stoch, M. Mikołajczyk, P. Michorczyk, *Appl. Catal. A: General* **2006**, 312, 213.
- 11 S. Mathew, C. S. Kumara, N. Nagaraju, *J. Mol. Catal. A: Chem.* **2006**, 255, 243.
- 12 R. B. Watson, U. S. Ozkan, *J. Catal.* **2002**, 208, 124.
- 13 T. Kamegawa, R. Takeuchi, M. Matsuoka, M. Anpo, *Catal. Today* **2006**, 111, 248.
- 14 T. Sugino, A. Kido, N. Azuma, A. Ueno, Y. Udagawa, *J. Catal.* **2000**, 190, 118.
- 15 T. Ono, H. Kamisuki, H. Hisashi, H. Miyata, *J. Catal.* **1989**, 116, 303.
- 16 W. M. Zhang, A. Desikan, S. T. Oyama, *J. Phys. Chem.* **1995**, 99, 14468.
- 17 Y. Miao, G. Lu, X. Liu, Y. Guo, Y. Wang, Y. Guo, *J. of Mol. Catal. A: Chem.* **2009**, 306, 17.
- 18 J. M. Bregeault, *Dalton Trans.* **2003**, 17, 3289.
- 19 X. Ma, B. Li, C. Lv, M. Lu, J. Wu, L. Liang, *Catal. Lett.* **2011**, 141, 1814.
- 20 Y. K. Park, S. J. Kim, N. You, J. Cho, S. J. Lee, J. H. Lee, J. K. Jeon, *J. of Ind. and Eng. Chem.*, **2011**, 17, 186.
- 21 A. V. Biradar, S. B. Umbarkar, M. K. Dongare, *Appl. Catal. A* **2005**, 285, 190.
- 22 R. Deliche, A. Auissi, M. M. Bettahar, S. Launey, M. Fournier, *J. Catal.* **1996**, 164, 16.
- 23 A. Cesar, D. S. Ferreira, J. C. Barbe, A. Bertrand, *J. Agric. Food Chem.* **2002**, 50, 2560.
- 24 A. Kido, H. Iwamoto, N. Azuma, A. Ueno, *Catal. Surv. Asia* **2002**, 6, 45.
- 25 J. M. Bialon, *Appl. Catal. A* **2004**, 273, 47.
- 26 M. Pagliaro, R. Ciriminna, H. Kimura, M. Rossi, C. Della Pina, *Angew. Chem.*

- Int. Ed.* **2007**, 46, 4434.
- 27 G. Cherkaev, S. A. Timonin, G. F. Yakovleva, L. Shutikova, A. S. Mikhailova, L. D. Shapiro, *SU Patent* **1987**, 1, 337.
- 28 M. J. Ashton, C. Lawrence, J. A. Karlsson, K. A. J. Stuttle, C. G. Newton, B. Y. J. Vacher, S. Webber, M. J. Withnall, *J. Med. Chem.* **1996**, 39, 4888.
- 29 X. Ma, J. Gong, S. Wang, N. Gao, D. Wang, X. Yang, F. He, *Catal. Commun.* **2004**, 5, 101.
- 30 C. Martin, G. Plazenet, J. Lynch, B. Rebours, E. Payen, *Micropor. Mesopor. Mater.* **2004**, 80, 275.
- 31 L. lebihan, L. Duhamel, C. Mauchausse, E. Payen, J. Grimblot, *J. Sol-Gel Sci. Technol.* **1994**, 2, 837.
- 32 J. H. Prish, E. M. Carron, R. V. Dreele, J. A. Goldstone, *J. Solid-State Chem.* **1991**, 93, 13.
- 33 J. Stencel, *Raman Spectroscopy for Catalysis*, Van Nostrend Reinhold, NewYork, **1990**, p. 53.
- 34 L. Seguin, M. Figlarz, R. Cavagnat, J. C. Lassègues, *Spect. Chem. Acta A* **1995**. 51, 1323.
- 35 E. M. McCarron, *Chem. Commun.* **1986**, 336.
- 36 E. Payen, J. Grimblot, J. C. Lerelley, R. Datuier, F. Mauge, *Handbook of Vibrational Spectroscopy*, p. 4.
- 37 J. N. Chalmers, P. R. Griffiths, *John Wiley and Sons Ltd.* **2001**, p. 2036.
- 38 S. D. Kohler, J. G. Ekerdt, D. S. Kim, I. E. Wachs, *Catal. Lett.* **1992**, 16, 231.
- 39 F. Adam, A. Iqbal, *Micro. and Meso. Mat.* **2011**, 141, 119.

**Chapter 3: Sol-gel synthesized
MoO₃/SiO₂ catalyst for
esterification reactions**

Abstract

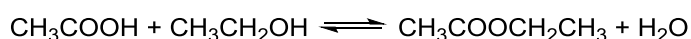
Esterification of acetic acid with ethanol was studied using $\text{MoO}_3/\text{SiO}_2$ as solid acid catalyst. A very high conversion of acetic acid and 100% selectivity for ethyl acetate was observed. The catalyst showed no deactivation when the esterification of acetic acid and ethanol was carried out on continuous mode. In order to understand the nature of catalytically active species formed during the esterification reaction, the catalytically active species were isolated, dried and characterized by FT-IR, Raman, PXRD, BET-Surface area, NH_3 -TPD, EDAX and TEM. Additionally, esterification of glycerol with various acids was investigated using sol-gel synthesized $\text{MoO}_3/\text{SiO}_2$ solid catalysts. Acetylation of glycerol with acetic acid was studied in details to achieve maximum conversion of glycerol and high selectivity for triacetin.

Chapter 3: Sol-gel synthesized MoO₃/SiO₂ as Solid Acid Catalyst for Esterification reactions

3.1. Introduction

Esterification of carboxylic acids is one of the fundamental reactions in synthetic organic chemistry, a technique to protect carboxylic acid group in a molecule and an important method for production of various esters.^[1] Organic esters play a vital role as intermediates in the synthesis of fine chemicals, drugs, plasticisers, food preservatives, pharmaceuticals, solvents, perfumes, cosmetics and chiral auxiliaries.^[2] Esterification of acetic acid with ethanol to ethyl acetate is one such industrially important reaction. Ethyl acetate is extensively used as solvent in paints, coatings, inks and adhesives.

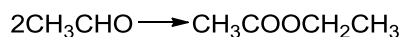
Conventionally, esterification of acetic acid and ethanol is carried out using homogeneous catalysts like sulfuric acid or *p*-toluene sulfonic acid (*p*-TSA).^[3] The use of these catalysts has been recognized commercially as Fischer esterification process (Scheme 3.1).



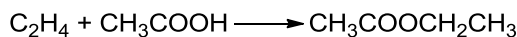
Scheme 3.1. Fischer esterification process

Although this process is used industrially, highly corrosive nature of the catalyst requires specialized material of construction increasing the overall cost of production. Secondly, the catalysts get deactivated and hence need complete or partial replacement during the reaction. The synthesis of ethyl acetate is also carried out by following methods other than the Fischer esterification method:-

The Tishchenko process^[4] which uses aluminium triethoxide as catalyst and acetaldehyde as starting material (Scheme 3.2) and Showa Denko process using ethylene and acetic acid as starting material and heteropoly acids as catalysts (Scheme 3.3).^[5]

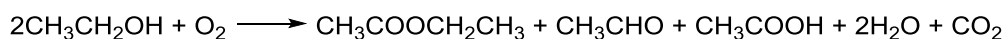


Scheme 3.2. Tishchenko process for ethyl acetate production



Scheme 3.3. Ethyl acetate production from ethylene and acetic acid

The main drawback associated with the systems is that the processes involve multi-step synthesis of ethyl acetate. Therefore, alternative processes namely- the oxidative route (Pd based catalysts)^[6] (Scheme 3.4) and the dehydrogenative route (Cu-Zn based catalysts)^[7] (Scheme 3.5) have been contemplated for the one-pot ethyl acetate production in industries. The processes involve ethanol as a starting material.



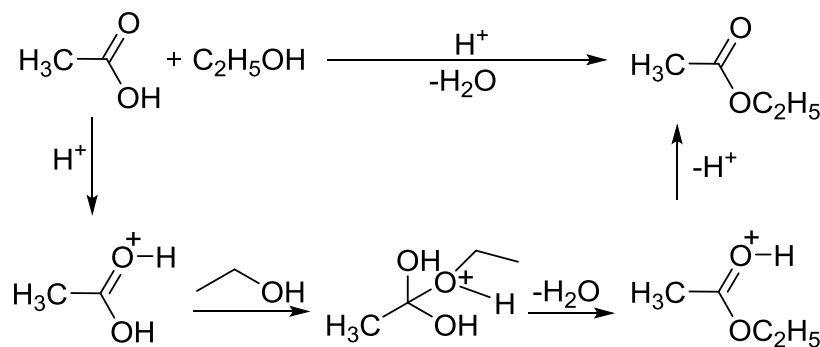
Scheme 3.4. Oxidative route for ethyl acetate production



Scheme 3.5. Dehydrogenative route for ethyl acetate production

The oxidative process (Scheme 3.4) produces acetaldehyde, acetic acid and CO_2 as the main byproducts while its main drawback is the flammability limit of the ethanol/ O_2 mixture. A simple route for the synthesis of ethyl acetate using heterogeneous catalysis for one-pot esterification of acetic acid and ethanol can be a promising alternative. Ethanol is a non-toxic and easy to handle reactant which can be considered as renewable because it is produced from biomass. General mechanism for the esterification of acetic acid and ethanol is as follows- The esterification of carboxylic acids by alcohols is catalyzed by strong acids. Their role is to protonate the carbonyl group, which makes it far more electrophilic and reactive towards the alcohol (Scheme 3.6).

To overcome the drawbacks of using homogeneous catalysts as discussed above, steps are being taken to use heterogeneous solid acid catalysts for esterification reactions. There are a few literature reports which deal with the application of solid acids as efficient catalysts for esterification reaction. A few have been discussed herein.



Scheme 3.6. General mechanism for the esterification of acetic acid and ethanol using acid catalyst

A literature report describes the use of solid acid catalysts like MCM-22, MCM-49, MCM-56, ZSM-5, zeolite-beta for esterification.^[8] In a recent report, Bedard *et al.*^[9] studied the steady-state catalytic reactions of acetic acid with ethanol over H-BEA, H-FER, H-MFI, and H-MOR at 50-110 °C and showed that esterification reactions produced ethyl acetate with more than 90% selectivity on all four zeolites. The esterification of acetic acid and ethanol using onium (γ -propyl-*N*-pyridinium, γ -propyl-*N*-methyl and γ -propyl-*N*-butyl-imidazolium) silica-immobilized-keggin acids as heterogeneous catalysts has been reported by Kovalchuk *et al.*^[10] In this case, best results (68% acid conversion) were obtained when the reaction was carried out at 60 °C for 20 h. Various supported metal oxides have been reported as catalyst for esterification reactions. Recently, Said *et al.*^[11] studied the surface properties and catalytic behavior of impregnated MoO₃/SiO₂ catalyst for esterification of acetic acid with ethanol. In this case it was observed that catalyst with 20 wt% MoO₃ loading was the most active and selective one, emphasizing the importance of the surface sites together with the surface area of the catalysts. Although there are many reports which describe the synthesis of MoO₃/SiO₂ catalysts with various techniques and their catalytic activity for various acid catalyzed and oxidation reactions, so far not many studies have been carried out which describe the nature of catalytically active species formed on MoO₃/SiO₂ in various organic transformations. The present work deals with the detailed studies on the esterification of acetic acid and ethanol to investigate nature of catalytically active species formed during acid catalyzed reactions using MoO₃/SiO₂ catalyst prepared by sol-gel route. A detailed study on isolation, characterization and identification of *in situ* generated catalytically active species was carried out.

Glycerol Esterification

The application of sol-gel synthesized MoO₃/SiO₂ catalysts was extended to study the esterification of glycerol with acetic acid to achieve maximum glycerol conversion with high selectivity for triacetin. In recent times, valorization of glycerol into fuel oxygenates by means of esterification is gaining considerable attention, of which the esterification of glycerol with acetic acid is one of the important alternatives. The products of the reaction are monoacetin, diacetin and triacetin (Scheme 3.10) which find multitude of industrial applications. The triacetin has a range of applications from cosmetics to fuel additives.^[12,13] The monoacetin and diacetin are commercially employed in cryogenics and as raw material for the production of biodegradable polyesters.^[14] Traditionally, the acetylation of glycerol is carried out over mineral acids as homogeneous catalyst. In that case the effluent disposal leads to environmental hazards. These problems can be overcome by using heterogeneous catalysts. There are reports which describe the use of solid acid catalysts including zeolites, amberlyst and niobic acid for acetylation of glycerol.^[15] Goncalves *et al.*^[16] reported the use of acid exchange resin, amberlyst-15 which showed 97% conversion of glycerol in 30 min at 110 °C with maximum selectivity for monoacetin. Other solid catalysts like K-10 montmorillonite, HZSM-5 and HUSY were used for the reaction. In each case, hydroxyacetone was obtained as a byproduct. Melero *et al.*^[17] showed the use of sulfonic acid functionalized mesoporous silica providing up to 90% glycerol conversion and over 80% of combined selectivity for di- and triacetin in 4 h at 125 °C when acetic acid to glycerol molar ratio of 9:1 was used. In a recent report the use of dodecamolybdophosphoric acid encapsulated in USY zeolite was studied for acetylation of glycerol. In this case, the catalytic activity increased with the increase in the amount of heteropolyacid immobilized on USY zeolite.^[18] Studies on the use of dodecatungstophosphoric acid immobilized in the silica matrix for acetylation reaction was also reported by Ferreira *et al.*^[19] In this case acetic acid to glycerol molar ratio was 1:16 and the reaction temperature was 120 °C. Maximum selectivity was observed for diacetin with 87% conversion of glycerol in 7 h. A very high selectivity for triacetin of 87% was reported by Lu and Ma^[20] using acidic ion exchange resin and MgSO₄ at room temperature for 72 h. Yang and Lu^[21] used SO₄²⁻/ZrO₂-TiO₂, and obtained >85% yield for triacetin, referring the best activity of the catalyst at 450 °C. Another literature reported a very high yield of 93.6% was for triacetin at 130 °C using sulfated zirconia as solid acid.^[22] Liu *et al.*^[23]

used *p*-toluenesulfonic acid/C and obtained triacetin yield of 92%, Li *et al.*^[24] used ionic liquids ($[\text{HSO}_3\text{-pmim}][\text{PTSA}]$) and the optimum operating conditions were glycerol/acetic acid ratio of 1:8, catalyst amount of 10.5% of the total weight of reactants, 6 h reaction time and reaction temperature was 120 °C. There are also several patents that report about the appreciable selectivity for triacetin using solid acid catalysts.^[25-29]

To evaluate the wider applicability of sol-gel synthesized $\text{MoO}_3/\text{SiO}_2$ catalyst for the esterification; acetylation of glycerol with acetic acid was studied in details.

3.2. Experimental Section

3.2.1. Material

All the reagents viz., acids, ethanol (absolute) and glycerol of AR grade (99.8%) were obtained from Thomas Baker, India. The chemicals were used without further purification.

3.2.2. Typical esterification reaction

a) Esterification of acetic acid and ethanol in batch mode

The esterification of acetic acid and ethanol was carried out in a 250 mL two necked round bottom flask fitted with reflux condenser and a magnetic stirrer. The flask was charged with acetic acid (1 mol, 100 g), ethanol (1.2 mol, 96 g) and 20 mol% $\text{MoO}_3/\text{SiO}_2$ (MSF) as catalyst (10% by weight of acetic acid). The reaction was carried out at 75 °C for 8 h.

b) Esterification of acetic acid and ethanol in continuous mode

The continuous esterification reaction of acetic acid and ethanol was carried out in a 500 mL two necked round bottom flask fitted with a reactive distillation column and a magnetic stirrer (Figure 3.1). The flask was charged with acetic acid (1 mol), ethanol (1.2 mol) and MSF as catalyst (10 g). The azeotropic mixture of ethyl acetate: ethanol: water was distilled out continuously at 70 °C with intermittent addition of fresh charge of ethanol (1.2 mol) and acetic acid (1 mol) to the reaction mixture after every 8 h.

c) Esterification of glycerol with acids

The esterification of glycerol with various acids was carried out in a 50 mL round bottom flask fitted with a reflux condenser. In a typical esterification experiment the

reactor was charged with glycerol (1 mmol), acid (3 mmol) and catalyst (10 wt% w.r.t. wt. of glycerol). The reaction was carried out at 100 °C for 8 h.

3.2.3. *Catalyst Separation and investigation of the different catalytic species*

After completion of the esterification of ethanol and acetic acid (as in section 3.2.2a) the catalyst fractions were isolated as follows: The reaction mixture was decanted and the solid residue was separated and was denoted as ‘MSR’. The decanted solution was filtered and fine suspension was collected on the filter paper and dried and this fraction was denoted as ‘MSS’. The transparent blue filtrate was concentrated under reduced pressure using rotary evaporator and was denoted as ‘MSB’.

The esterification reaction of acetic acid and ethanol was carried out using all three fractions separately as catalyst. The esterification was carried out according to the reaction conditions as discussed in the section 3.2.2a.

All the reactions were monitored by GC. Prior to use the GC method was calibrated using external standard method. Samples were withdrawn at regular time intervals and analyzed using GC - Perkin-Elmer AutoSystem XL equipped with FFAP column (50 m length, 0.25 mm internal diameter and 1 μm film thickness) and with flame ionization detector.

3.2.4. *Screening of 20 mol% $\text{MoO}_3/\text{SiO}_2$ catalyst under industrial conditions*

The sol-gel synthesized 20 mol% $\text{MoO}_3/\text{SiO}_2$ was given to an industry (Jubilant Life Sciences pvt. ltd., Delhi). The catalyst was used for the esterification of acetic acid and ethanol following the industrial procedure. A reaction mixture with composition containing 77.5% acetic acid, 15% ethyl acetate, 1% ethanol, 5% water and 1.5% (20 mol% $\text{MoO}_3/\text{SiO}_2$) catalyst was used as initial reaction charge. Same reaction charge was used to carry out the reaction using *p*-TSA (1.5%) as catalyst for comparison. The reaction charge was taken in a round bottom flask attached with SS wire mesh packed column (1m height and 25 mm diameter), dean stark apparatus and condenser. The reaction mixture was refluxed for a fixed time followed by intermittent addition of equimolar quantities of ethanol and acetic acid and the crude ethyl acetate was distilled off consequently.

3.2.5. *Characterization of catalyst fractions*

All the three fractions alongwith MSF, pure SiO_2 (PS) and silicomolybdic acid (SMA) were characterized using various characterization techniques like FTIR, Raman spectroscopy, XRD, BET surface area, NH_3 -TPD, EDAX, TEM. FT-IR

spectra of the samples were recorded on a Thermo Nicolet IR instrument as KBr pellets with resolution of 4 cm^{-1} and averaged over 100 scans. KBr pressed disk technique was used for obtaining the FTIR spectra of the catalyst samples as well as the catalyst fractions.

Raman spectra of the catalyst fractions were recorded on a HR 800 LabRAM infinity spectrometer (Horiba-Jobin-Yvon) equipped with a liquid nitrogen detector and a He-Ne laser supplying the excitation line at 632 nm with 1-10 mW power and with a resolution of 0.35 cm^{-1} .

X-ray diffraction patterns of the catalyst fractions were recorded on PAN analytical X'Pert Pro Dual Goniometer diffractometer. X'celerator solid state detector was employed for the experiments with $\text{CuK}\alpha$ (1.542 \AA) radiation and a Ni filter.

The BET surface area of the samples was determined by N_2 sorption at $-196\text{ }^\circ\text{C}$ using NOVA 1200 (Quanta Chrome) equipment. Prior to N_2 adsorption, the materials were evacuated at $300\text{ }^\circ\text{C}$ under vacuum. The specific surface area, S_{BET} , was determined according to the BET equation.

Chemical composition of the samples was obtained using FEI Quanta 200-3D Dual Beam-ESEM with EDX (Genesis) attachment. This system was equipped with a standard Si(Li) large field detector and Tungsten Filament (Thermionic emission) as electron source. The EDX was calibrated with the pure elements Cu and Al. During the EDX measurements the system was operated at 30 keV in low vacuum.

Temperature programmed desorption of ammonia (NH_3 -TPD) was carried out using a Micromeritics Autocue 2910 apparatus. The catalyst was cleaned up at $500\text{ }^\circ\text{C}$ in a He flow and then cooled to $100\text{ }^\circ\text{C}$ prior to NH_3 adsorption. Then, desorption experiment was carried out at the rate of $10\text{ }^\circ\text{C}/\text{min}$ till $600\text{ }^\circ\text{C}$.

The strength of acid sites on the catalyst was calculated by acid-base titration.^[30] Firstly, aqueous NaOH solution (0.01 mol/L , 25 mL) was added to a catalyst (0.022 g). The mixture was then stirred for 2 h at room temperature (RT). After centrifugal separation, one drop of phenolphthalein solution was added to the filtrate and titrated with HCl (0.01 mol/L) to neutrality.

TEM measurements were performed on a Tecnai G2-20 FEI instrument operating at an accelerating voltage at 200 kV. Before analysis, the powders were ultrasonically

dispersed in ethanol, and two drops of ethanol containing the solid were deposited on a carbon coated copper grid.

UV-Visible spectra of the materials were recorded on Perkin Elmer 650 Lambda model using BaSO_4 powder as a reference.

3.3. Results and discussion

Esterification of ethanol and acetic acid (Scheme 3.1) was initially carried out in batch mode without removal of water by azeotropic distillation at 75 °C and very high acid conversion of 83.7% was obtained after 8 h showing high efficiency of the catalyst.

Further, to study the utility of the catalyst for esterification on continuous mode and to study stability of the catalyst, esterification of acetic acid and ethanol was carried out using continuous mode using MSF under reactive distillation conditions (Figure 3.1). Reactive distillation involves simultaneous chemical reaction and azeotropic distillation. In the present case, the azeotropic mixture containing ethyl acetate: ethanol: water in the ratio of 93:4:3 was distilled (at 70 °C) out continuously even up to 60 h of reaction time with intermittent addition (after 8 h) of fresh charge of ethanol and acetic acid. High acid conversion (65%) was achieved. There was no change in the ratio of the distilled components ($\text{EtOAc}/\text{EtOH}/\text{H}_2\text{O}$, 93/4/3) observed even after 60 h with no change in the acetic acid conversion showing the stability of the catalyst under reaction environment. However, lower acid conversion was obtained in continuous mode compared to batch mode due to the lower reaction time compared to batch mode. This can also be correlated to the loss of reactant ethanol during azeotropic distillation which in turn may reduce the conversion.

The fresh $\text{MoO}_3/\text{SiO}_2$ (MSF) catalyst is greenish white in color which turned blue during the reaction indicating the reduction of molybdenum species during the reaction. The catalyst formed a blue suspension in the reaction medium during the course of reaction. In order to identify the different catalytic species formed during the esterification, the catalyst fractions were isolated from the reaction mixture. After completion of the reaction, the reaction mixture was decanted to separate the solid catalyst as residue denoted as 'MSR' ($\text{MoO}_3/\text{SiO}_2$ residue). It was observed that the blue colored decanted solution consisted of the suspended fine particles and

transparent blue fraction. These suspended particles were separated from the blue reaction mixture by filtration denoted as ‘MSS’ ($\text{MoO}_3/\text{SiO}_2$ suspended particles) and the remaining homogeneous blue filtrate was concentrated to blue colored solid ‘MSB’ ($\text{MoO}_3/\text{SiO}_2$ blue). Three fractions thus obtained were weighed and the weights of three fractions, MSR, MSS and MSB were 8.73 g, 0.91 g and 0.27 g respectively when initial catalyst used was 10 g (94.45% recovery).

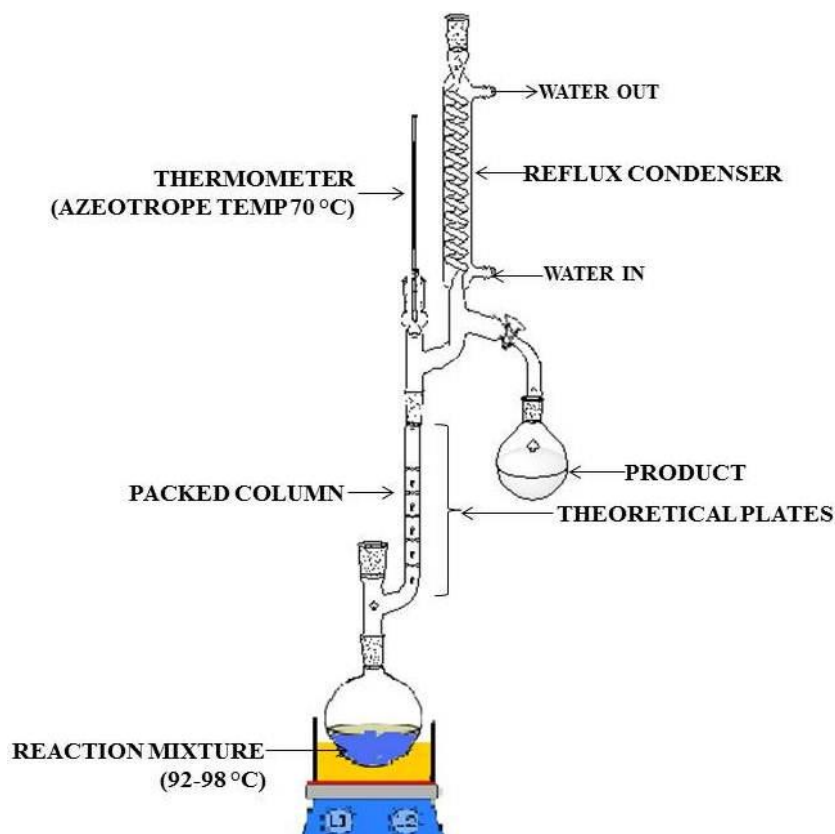


Figure 3.1. Typical azeotropic distillation assembly for esterification reaction in continuous mode

The isolated catalyst fractions were used for esterification reaction separately to compare the activity of each fraction with that of the fresh catalyst (MSF) for batch mode esterification and the results are shown in Figure 3.2. For comparison the reaction was also carried out with pure silicomolybdic acid (SMA). The catalyst loading for MSR, MSS and MSB used was equal to the each fraction obtained from the 10 wt% MSF used for the same charge of the reaction. For 10 g acetic acid charge 1 g MSF was used. From 1 g MSF - 0.87 g MSR, 0.09 g MSS and 0.03 g MSB was

obtained, hence for 10 g acetic acid batch 0.87 g MSR, 0.09 g MSS or 0.03 g MSB was used for esterification.

All the catalyst fractions showed appreciable activity for the esterification reaction. Acetic acid conversion obtained was 77% for MSF, 73% for pure SMA, 67% for MSB, 51% for MSS whereas 60% for MSR. MSB was found to be the most active catalyst fraction of the three.

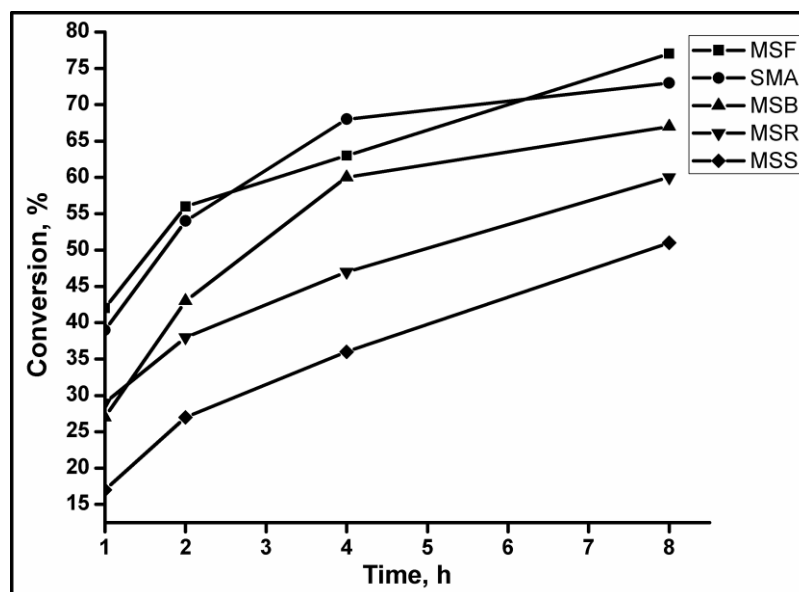


Figure 3.2. Esterification reaction of acetic acid and ethanol using the isolated catalyst fractions

Reaction conditions: AcOH:EtOH-1:1.2 (molar ratio), AcOH-10 g, Temperature-75 °C, Time-8 h, MSF-1 g, SMA-0.03 g, MSB-0.03 g, MSR-0.87 g, MSS-0.09 g

In order to understand the nature of catalytic active species present in three different fractions, a detailed characterization of all these fractions was carried out separately.

The IR spectrum of SMA (Figure 3.3c) exhibited the main peaks characteristic of Keggin structures at 906 and 956 cm^{-1} .^[31] These bands were assigned to the vibrations of the terminal Mo-O-Si and Mo=O bonds, respectively. The band at 756 cm^{-1} was assigned to Mo-O-Mo vibrations. These three bands were observed in case of the IR spectra of MSR, MSS, MSB and MSF (Figure 3.3) with band intensity comparatively lower than that of SMA. The peaks observed in case of MSB matched very well with that of authentic SMA indicating the *in situ* formation of SMA. An additional broad band at 1080 cm^{-1} observed in case of MSB matched with Si-O-Si bond in SiO_2

suggesting presence of silica support associated with *in situ* formed SMA. In case of MSS and MSR additional bands at 993 cm^{-1} , 870 cm^{-1} and 570 cm^{-1} were observed corresponding to $\alpha\text{-MoO}_3$. The Table 3.1 shows the prominent IR bands in silicomolybdic acid.^[32]

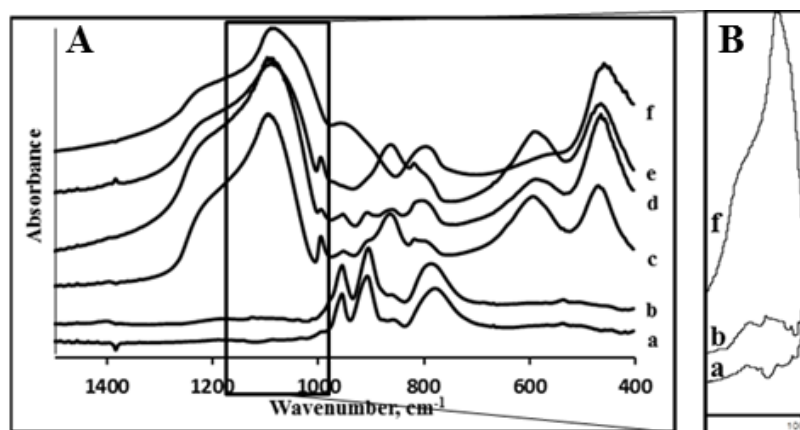


Figure 3.3. FTIR spectra of a) SMA, b) MSB, c) MSS, d) MSR, e) MSF, f) PS in the range: **A**- $1500\text{-}400\text{ cm}^{-1}$ and **B**- $980\text{-}1180\text{ cm}^{-1}$

Table 3.1. Infrared bands of silicomolybdic acid

Wavenumbers, cm^{-1}	Attribution of bands
993	ν_s Mo-O _{terminal}
956	ν_{as} Mo-O _{terminal}
906	ν_{as} Si-O
870	ν_{as} Mo-O-Mo
570	δ O-Si-O

Raman spectra of the $\text{MoO}_3/\text{SiO}_2$ catalyst reported earlier which presence of silicomolybdic heteropolyanions.^[33] Hence the Raman spectra of the catalyst fractions were recorded along with PS and SMA and were compared with the earlier reported spectra (Figure 3.4). The presence of intense bands at 989 ($\nu_{\text{Mo=O}}$ terminal stretching mode), 820 (bulk MoO_3 species), 654 ($\nu_{\text{Mo-O-Mo}}$ symmetric stretching mode) and 275 cm^{-1} ($\nu_{\text{Mo-O-Mo}}$ deformation mode) correspond to $[\text{SiMo}_{12}\text{O}_{40}]^{4-}$ (SMA). Pure SiO_2 showed broad bands at 424 , 480 and 717 cm^{-1} . The presence of silicomolybdic heteropolyanions was observed in case of MSS, MSR and MSB. The Raman shifts

observed in case of MSB were in good agreement with the values obtained in case of pure SMA.

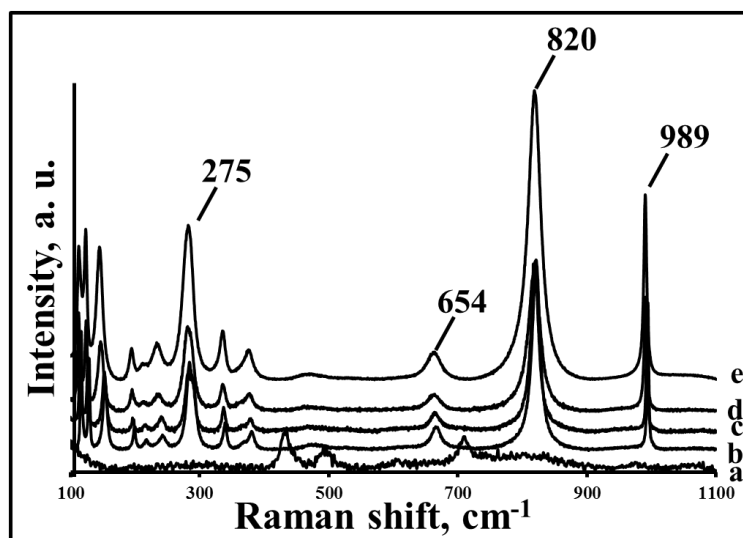


Figure 3.4. Raman spectra of a) PS b) MSR c) MSS d) MSB e) SMA

XRD patterns of MSR, MSS and MSB along with MSF for comparison were recorded and are shown in Figure 3.5. The XRD patterns of MSR and MSS showed the presence of peaks at $2\theta = 12.9, 23.4, 25.8$ and 27.4° corresponding to $\alpha\text{-MoO}_3$ species similar to that of the fresh catalyst MSF, which is in good agreement with the observation in FTIR studies. The diffraction pattern of MSB (Figure 3.5c) showed the peaks at $2\theta = 10.2, 25.4, 33.5^\circ$ which are in well agreement with the peaks corresponding to keggin heteropolyanions.^[31] It is interesting to note that the SiO_2 support retained its amorphous nature despite of the formation of keggin heteropolyanions on the surface of the support. This was confirmed by the presence of broad peak characteristic of the amorphous silica at $2\theta = 24^\circ$.

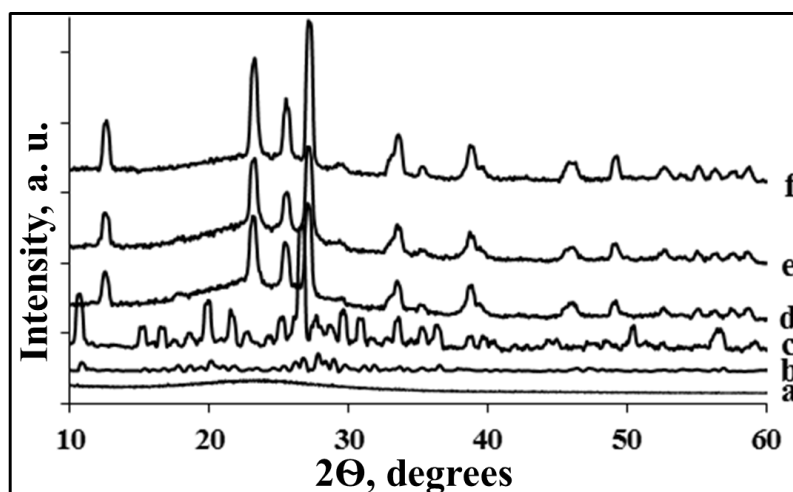


Figure 3.5. XRD patterns of a) PS, b) SMA, c) MSB, d) MSS, e) MSR, f) MSF

To investigate the textural properties of different fractions, a detailed surface characterization was carried out and the results are given in the Table 3.2. The specific surface area of the catalyst fractions MSR and MSS slightly decreased to $169 \text{ m}^2/\text{g}$ and $198 \text{ m}^2/\text{g}$ respectively from $217 \text{ m}^2/\text{g}$ for MSF. However the mesoporosity of the catalyst was retained even after the reaction. Acidity of all the fractions was evaluated by NH_3 -TPD and the total acidity of the fractions MSR and MSS were found to be 0.54 and 0.3 mmol/g respectively, which was lesser than that of MSF (0.9 mmol/g).

Table 3.2. Textural data, acidity, and EDAX analysis of the fresh and spent catalyst fractions

Catalyst	Surface area, m^2/g	Pore volume, cm^3/g	Average Pore Diameter, \AA	Number of acid sites, mmol/g^*	Total acidity $^{\text{a}}$, mmol/g	EDAX analysis (wt%)		
						Mo	Si	O
PS	896	0.94	42.0	1.4	0.03	0.0	46.6	53.4
MSF	217	0.37	67.9	4.6	0.9	23.5	31.5	46
MSR	169	0.31	73.5	5.2	0.3	10	34.2	55.7
MSS	198	0.36	72.7	5.3	0.54	16.4	41.6	41.9
MSB	--	--	--	9.3	--	60	2.5	37.6
(SMA)				(9.8)				

*Acid strength of the samples determined by acid-base titration method; @ Total acidity by NH_3 -TPD

The homogeneous nature of MSB restricted the textural analysis and acidity measurements at higher temperatures as the sample was not stable and could be easily decomposed. Therefore, the acid strengths of all the catalyst fractions were evaluated using acid-base titration method.^[30] The acidity of MSB (9.38 mmol/g) matched very well with pure SMA (9.85 mmol/g). The acidity of the fractions MSF, MSR and MSS ranged from 4.57 to 5.30 mmol/g. However the acidity of PS was found to be 1.37 mmol/g which can be attributed to the dissolution of silica in NaOH. The spot EDAX analyses of the three catalyst fractions were carried out and results are given in Table 3.2. EDAX analyses revealed that the molybdenum content in the fractions decreased in the order MSB>MSF>MSS>MSR showing removal of Mo from MSF due to which MSR showed least Mo content. In case of MSS, SMA formation can be on large silica particles due to which the Mo content was lower. The percentages of 'Mo', 'Si' and 'O' in MSB were slightly different from the calculated percentages of the elements in SMA, (Mo=63%, Si =1.5%, O=35% in pure SMA) 'Si' being slightly higher which can be attributed to formation of SMA on fine silica nano particles.

To investigate this fact, HRTEM studies were carried out (Figure 3.6-3.8). The HRTEM image of MSR (Figure 3.6) showed highly dispersed ' MoO_3 ' particles which are in the range of 1-2 nm on mesoporous silica support. Interestingly, the TEM image of MSB showed particles of 13.2 to 24.6 nm supported on silica nanoparticles. The TEM image of MSB showed the dark image of SMA in the centre surrounded by less dark image corresponding to amorphous SiO_2 (Figure 3.8C) referred as Stobber silica.^[34] The formation of Stobber silica in the presence of ethanol and water mixture has been reported by Asefa *et al.*^[35] This specially leads to a formation of SiO_2 with low surface area. The formation of Stobber silica was also observed in case of MSS and MSR which could be the reason for the decrease in the surface area of these catalyst fractions. Spot diffraction patterns in Figure 3.8C showed a modulation in the streak intensity, giving rise to diffused maxima and minima corresponding to the amorphous SiO_2 support. Depending on the particle size of silica support reacting with MoO_3 , the fraction appeared as either suspension as in MSS when particle size is comparatively bigger or appeared as solution when the particle size is very small as in MSB.

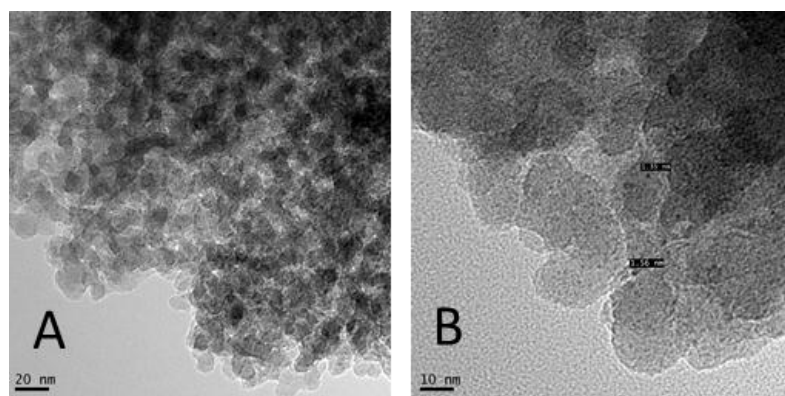


Figure 3.6. TEM images of MSR focused on different area

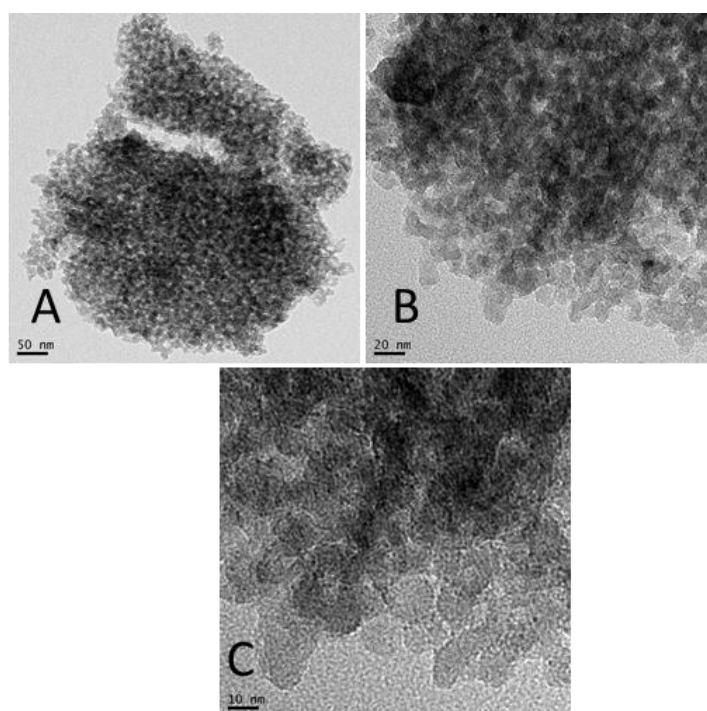


Figure 3.7. TEM images of MSS at different magnification

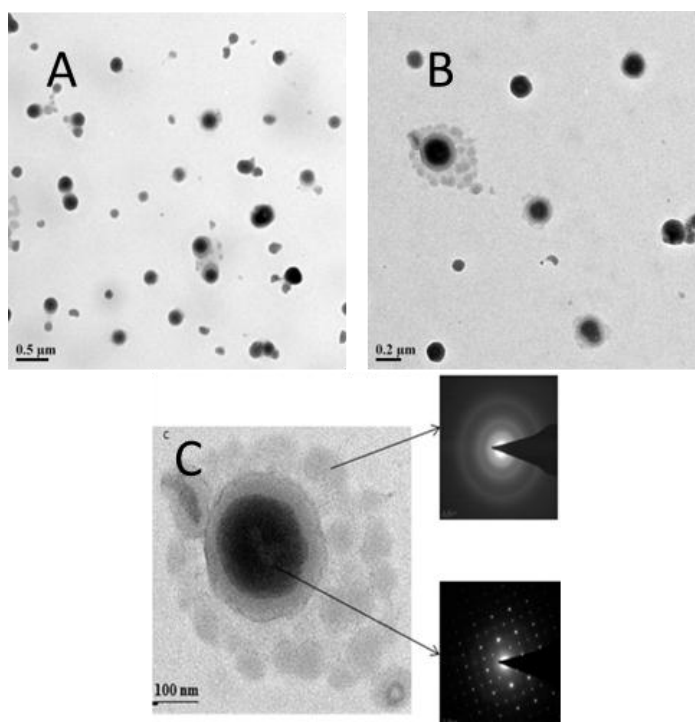


Figure 3.8. TEM images of MSB focused on different area

Although the EDAX analysis and the FTIR spectra of the samples showed the *in situ* formation of SMA on the silica support, and the blue color indicates the formation of reduced SMA species. This observation was correlated with the UV-visible spectroscopic studies (Figure 3.9).

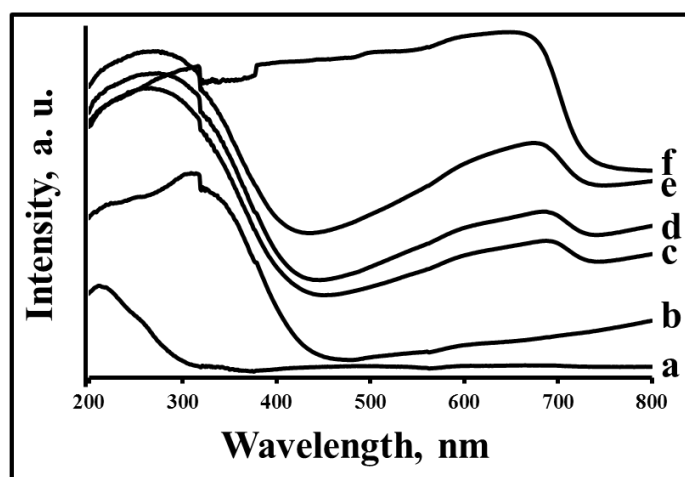
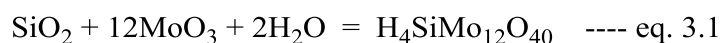


Figure 3.9. UV-Vis spectra of a) PS b) Pure MoO_3 c) MSF d) MSR e) MSS f) MSB

Torok *et al.* ^[36] have studied using UV-Vis spectroscopy the redox transformation of homogeneous SMA in electrophilic reactions and reported one electron reduction

of Mo(VI) to Mo(V) leading to color change from yellow to blue. The reduction was the consequence of a one-electron transfer, which altered the valence state of a single molybdenum ion in the Keggin-type cluster of molybdenum, denoted as Mo(VI) to Mo(V). The change in the valence state of molybdenum led to the formation of dark blue colored solid. The observed blue shift in the UV-Vis spectra of MSB in the 600-800 nm region (band at 720 nm) clearly indicated the formation of Mo (V) centers. Additionally, the crystal field (d-d) bands of Mo⁵⁺ centers (shoulder at 325 nm) were observed as well as the intervallic bands resulting from the optical excitation Mo⁵⁺...O...Mo⁶⁺ to Mo⁶⁺...O... Mo⁵⁺. The UV-Vis spectra of MSF, MSS and MSR showed the presence of the two shoulders at 720 and 325 nm, however the width of the bands decreased in the order MSB>MSS>MSR>MSF (Figure 3.9c-f). Presence of such bands was not observed in the UV-Vis spectra of PS and pure MoO₃ (Figure 3.9a, b).

The detailed characterization of different catalyst fractions indicated *in situ* formation of SMA supported on mesoporous silica which is known to get reduced in presence of water/alcohol. The formation of molybdenum oxide nanoparticles on mesoporous silica support in the present simple sol-gel synthesis may be correlated to the polymeric nature of ETS-40 and its reaction with AHM during sol-gel synthesis. The *in situ* generation of silicomolybdic acid under mild reaction conditions in presence of water may be due to formation of MoO₃ nanoparticles which are highly reactive. As SMA is highly soluble in water as soon as it forms on silica surface it dissolves in the aqueous reaction medium along with silica nanoparticles associated with it and acts as catalytically active species for esterification reaction. The *in situ* formation of reduced SMA during esterification reaction where MoO₃ nano particles reacting with water which is formed as byproduct, can be represented by equation 3.1 given below:

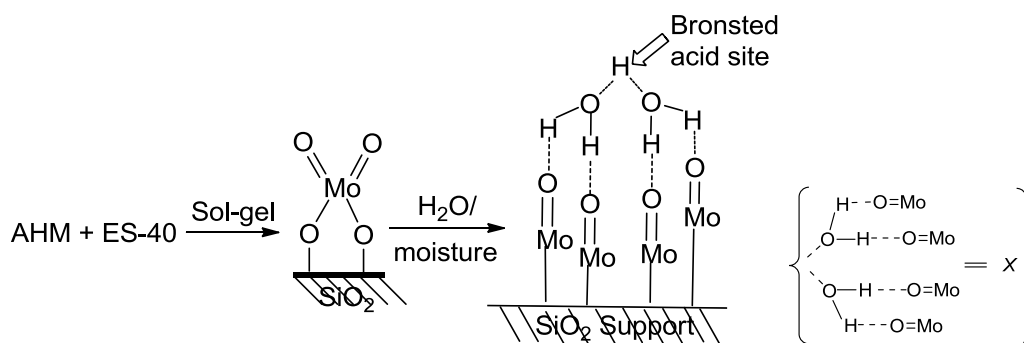


It was observed that during esterification all the MoO₃ in MSF was not converted to SMA and EDAX analysis showed the presence of 'Mo' in MSS as well as MSR. This may be due to limited quantity of water available in the reaction mixture. In order to check the amount of MSB formation with respect to water, 2 g MSF was heated in excess of water (20 mL) for 5 h. The blue suspension formed was filtered

after cooling and the filtrate was concentrated to give 0.7 g of blue colored solid (MSB1) which was analyzed by FTIR. The spectrum of blue solid matched well with SMA. This isolated quantity equaled to almost 90% conversion of MoO_3 present in MSF to SMA. It was observed that all MoO_3 present in the fresh catalyst comes out as reduced SMA (blue color) and white colored silica remained as residue denoted as RS. When this residual silica (RS) was characterized using BET analysis, considerable increase in the surface area and pore volume was observed compared to fresh catalyst. The surface area increased from $217 \text{ m}^2/\text{g}$ for MSF to $373 \text{ m}^2/\text{g}$ for RS with corresponding increase in the pore volume from 0.37 to 0.57 cc/g. The residual SiO_2 did not possess any acidity (0.006 mmol/g) when NH_3 -TPD was carried out for the solid. This clearly indicates that MoO_3 in MSF reacts with silica in presence of water to form SMA which is soluble in water generating pores on the silica support thereby increasing the pore volume as well as surface area. The weight of the blue fraction thus obtained was corresponding to weight of SMA if all MoO_3 in MSF converts to SMA. This may be considered a simple procedure to prepare good quality reduced SMA.

HPAs on various supports have been prepared earlier by wet impregnation technique. Deltcheff *et al.*^[37] reported that anchoring of SMA on various supports could be obtained using molybdic acid. The generation and stability of silicomolybdic acid on silica-supported molybdenum oxide catalysts prepared by incipient-wetness impregnation method has been reported earlier.^[38] The catalyst was used for the selective oxidation of methanol to formaldehyde at temperature from 300-600 °C. However the surface SMA species were unstable above 300 °C and transformed to $\beta\text{-MoO}_3$. Vapor phase partial oxidation of methane to methanol and formaldehyde was studied by Sugino *et al.*^[39] using silica supported MoO_3 (maximum 2 wt% loading) and silica supported SMA (6-36 wt% loading) prepared by wet impregnation method and the activity of both the catalysts was compared. Excess amount of water vapor was added for the generation of SMA on the catalyst surface. Further, Kido *et al.*^[40] reported the partial oxidation of methane using silica-supported SMA and decomposition of SMA to SiO_2 and MoO_3 at temperatures beyond 300 °C and the regeneration of SMA species by adding excess water. In context with these literature reports and their speculations on the formation of the species, we have successfully isolated and extensively characterized the *in situ* formed catalytically active species

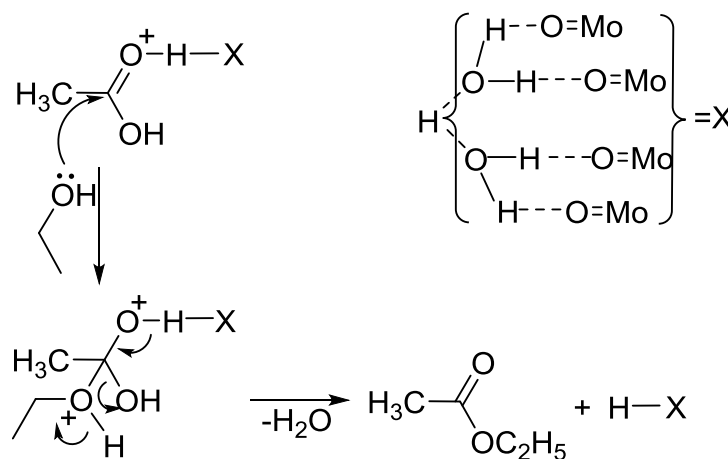
formed during the acid catalyzed reactions. The *in situ* formation of SiO_2 supported SMA can be schematically presented as shown in Scheme 3.7.



Scheme 3.7. *In situ* formation of SiO_2 supported SMA in presence of moisture or water

The *in situ* generation of silicomolybdic acid during esterification reaction may be due to the higher reactivity of molybdenum oxide and silica nanoparticles formed, during the present modified sol-gel method in presence of water in the reaction mixture were found to be catalytically active species for esterification reaction.

Plausible mechanism of the esterification using *in situ* generated SMA on SiO_2 support is shown in Scheme 3.8.



Scheme 3.8. Plausible mechanism of esterification reaction on *in situ* formed SiO_2 supported SMA

Industrial trials for esterification

Industrial lab trials were conducted for esterification of ethanol with acetic acid using MSF under the reaction conditions used for ethyl acetate production using *p*-TSA catalyst. The results obtained were compared with that of *p*-TSA (Table 3.3). The analysis of the crude ethyl acetate fraction for both the catalysts was compared. In case of *p*-TSA catalyst the composition was 95.14% ethyl acetate, 0.011% ethanol and 2.8% water, whereas for MSF it was 81.94% ethyl acetate, 0.019% ethanol and 7.31% water. It is interesting to note that the catalyst loading in both the cases was same though *p*-TSA is typical homogeneous catalyst and MSF is heterogeneous catalyst. Activity of MSF was comparable with that of *p*-TSA though used in such small quantities, which shows the potential of this catalyst for industrial process for the production of ethyl acetate. The typical disadvantage of *p*-TSA for industrial use is catalyst deactivation after certain time interval due to which it needs to be replaced with a fresh batch of the catalyst. However, in our lab we have carried out the continuous esterification of ethanol and acetic acid using MSF for 60 h and there was no catalyst deactivation confirming the catalyst stability under reaction conditions for ethyl acetate production.

Table 3.3. Results of industrial lab trials for esterification of acetic acid and ethanol using 20 mol% MoO₃/SiO₂

Entry	Component	Composition of crude ethyl acetate fraction using	
		MSF, %	<i>p</i> -TSA, %
1	Acetic acid	10.71	1.94
2	Ethyl acetate	81.94	95.14
3	Ethanol	0.019	0.011
4	Water	7.31	2.8

Glycerol esterification

In continuation to these studies, the study of the esterification of glycerol was carried out using various acids. As presented in the scheme 3.9, the esterification of glycerol occurs through consecutive reaction steps initially from monoglyceryl ester to di and ultimately to triglyceryl ester. Sol-gel synthesized 20 mol% MoO₃/SiO₂ was used as catalyst for the esterification of glycerol, owing to its high Brønsted acidity

and high catalytic activity towards esterification of ethanol and acetic acid as observed in our earlier studies. The results are shown in Table 3.4.



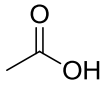
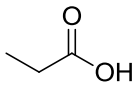
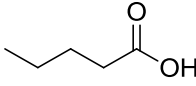
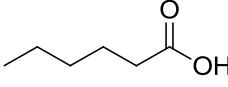
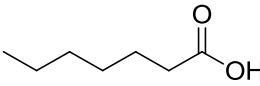
Scheme 3.9. Esterification of glycerol with acid

The conversion of glycerol and selectivity for the products were calculated as shown in equations 3.2 and 3.3 respectively.

$$\text{Conversion of glycerol (\%)} = \frac{\text{Number of moles of glycerol reacted}}{\text{Number of moles of glycerol taken}} \times 100 \quad \text{--- eq. 3.2}$$

$$\text{Selectivity of the product (\%)} = \frac{\text{Number of moles of desired product}}{\text{Number of moles of glycerol reacted}} \times 100 \quad \text{--- eq. 3.3}$$

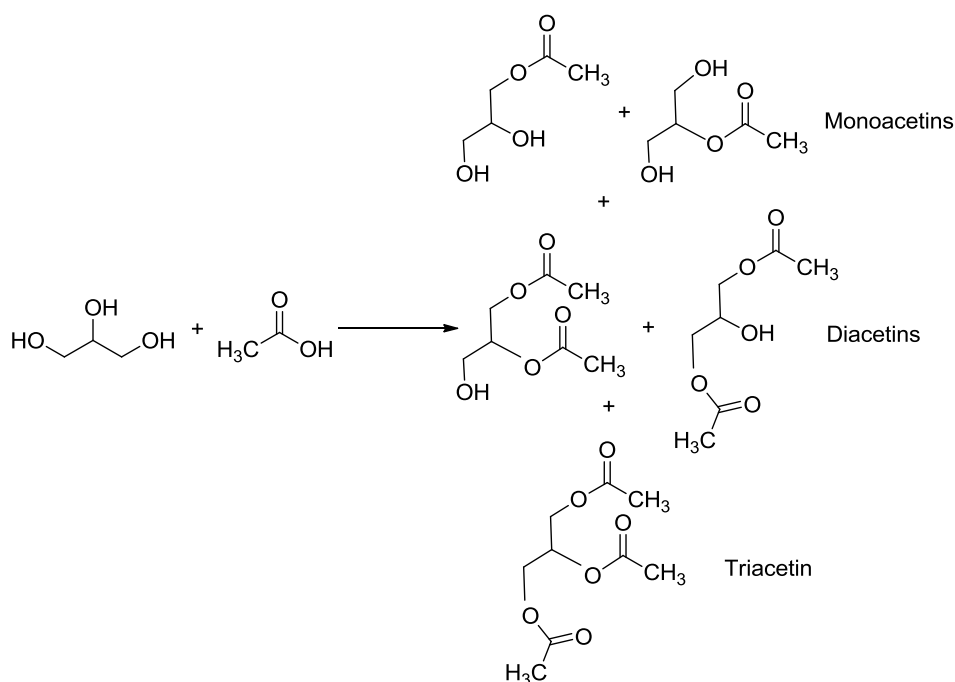
Table 3.4. Esterification of glycerol with various acids using 20 mol% MoO₃/SiO₂ as catalyst[#]

Entry	Acid	Glycerol Conv., %	Glyceride selectivity, %		
			Mono-	Di-	Tri-
1		68	81.3	16.5	2.2
2		41	100	---	---
3		39	100	---	---
4		35	100	---	---
5		30	100	---	---

Reaction conditions: Acid:glycerol-3:1 (molar ratio), Temperature-100 °C, Time-8 h, Catalyst-10% w.r.t. wt. of glycerol.

When the esterification of glycerol was carried out with acetic acid it showed maximum conversion of 68% with maximum selectivity of 81.3% for monoacetin. Moreover, the formation of di- and tri-ester was observed with a very low selectivity of 16.5% and 2.2% respectively. In case of other acids, the conversion decreased slightly with 100% selectivity for monoester. The acid conversion decreased in the series acetic acid > propionic acid > pentanoic acid > hexanoic acid > heptanoic acid. The reason for this can be attributed to the +I effect of the alkyl group which increases with increase in the chain length. It thereby reduces the electropositivity of the carbonyl carbon which in turn decreases the activity of the substrate. In all the cases 100% selectivity for monoester was obtained, except for acetic acid.

Esterification of glycerol with acetic acid was carried out (Scheme 3.10) to achieve maximum selectivity for the tri acetylated product (triacetin), which is the most interesting products from a fuel-application point of view, since it can be formulated with petrol-derived fuels to improve either cold and viscosity properties (biodiesel)^[41] or antiknocking properties (gasoline).^[42] The effect of various reaction parameters such as molar ratio of acetic acid to glycerol, catalyst loading and temperature were studied to optimize the reaction conditions in order to get maximum selectivity for triacetin.



Initially, the effect of molar ratio of acetic acid to glycerol was studied on glycerol conversion and selectivity for mono-, di- and triacetin products. The results are discussed in Table 3.5.

Table 3.5. Effect of mole ratio of acetic acid to glycerol on acetylation of glycerol over 20 mol% $\text{MoO}_3/\text{SiO}_2$ catalyst*

Entry	Molar ratio (AcOH:Gly)	Glycerol Conv., %	Acetin Selectivity, %		
			Mono-	Di-	Tri-
1	3:1	67	81	16	3
2	5:1	91	51	30	19
3	10:1	100	17	33	50

*Reaction conditions: Catalyst-10 wt% (w.r.t. glycerol), Temperature-100 °C, Time-8 h.

It was observed that even at low AcOH:glycerol molar ratio of 3:1 and 5:1, appreciable glycerol conversion of 67% and 91% was obtained in 8 h, respectively. However, 100% glycerol conversion was achieved at a higher AcOH:glycerol molar ratio of 10:1. It was interesting to note that the selectivity distribution of acetins for

different AcOH:glycerol molar ratio was altogether different. At AcOH:glycerol molar ratio of 3:1, a very high selectivity of 81% was achieved for monoacetin whereas only 16% and 3% selectivity was obtained for diacetin and triacetin respectively. As expected the selectivity of diacetin and triacetin increased to 30% and 19% respectively with decrease in the selectivity for monoacetin (51%) when AcOH:glycerol molar ratio of 5:1 was used. In order to achieve maximum selectivity for triacetin, the AcOH:glycerol molar ratio was increased to 10:1. In this case a very high triacetin selectivity of 50% was obtained compared to lower AcOH:glycerol molar ratio. Therefore all the further studies were carried out using AcOH:glycerol molar ratio of 10:1. All the above discussed reactions were carried out using 10 wt% (w.r.t. glycerol) catalyst loading. When the reaction was carried out using 5 wt% catalyst (w.r.t. weight of glycerol) only 78% conversion of glycerol was obtained with 73% selectivity for monoacetin. This showed that catalyst loading played an important role to attain maximum glycerol conversion and high selectivity for triacetin. To carry out the further parametric studies, 10 wt% catalyst (w.r.t. wt. of glycerol) was used for the acetylation reaction.

The effect of MoO_3 loading on SiO_2 support was studied on the acetylation reaction and the results are shown in Table 3.6. The acetylation of glycerol was also carried out without catalyst for comparison. The esterification occurred in absence of the catalyst, although the glycerol conversion remained much lower compared to the case when $\text{MoO}_3/\text{SiO}_2$ was used as catalyst. In absence of catalyst, the esterification led only to higher selectivity for monoacetin (92%) and 8% of diacetin. Formation of triacetin was not observed. The esterification was carried out using pure SiO_2 as catalyst and it was found that the glycerol conversion was only 44% with 86% monoacetin and 11% diacetin. Traces of triacetin were observed in this case. Further the reaction was carried out using series of $\text{MoO}_3/\text{SiO}_2$ catalysts with different MoO_3 loadings on SiO_2 and it was observed that 100% glycerol conversion was obtained with 1 mol% and 10 mol% MoO_3 loading but there was a notable difference in the selectivity pattern of mono-, di- and triacetin. Only 17% triacetin was obtained when 1 mol% $\text{MoO}_3/\text{SiO}_2$ was used as catalyst (Table 3.6, entry 3). However, selectivity for triacetin increased to 33% with gradual decrease in selectivity for monoacetin (36%) and an almost equal amount of diacetin (31%) was obtained when 10 mol% $\text{MoO}_3/\text{SiO}_2$ was used as catalyst (Table 3.6, entry 4).

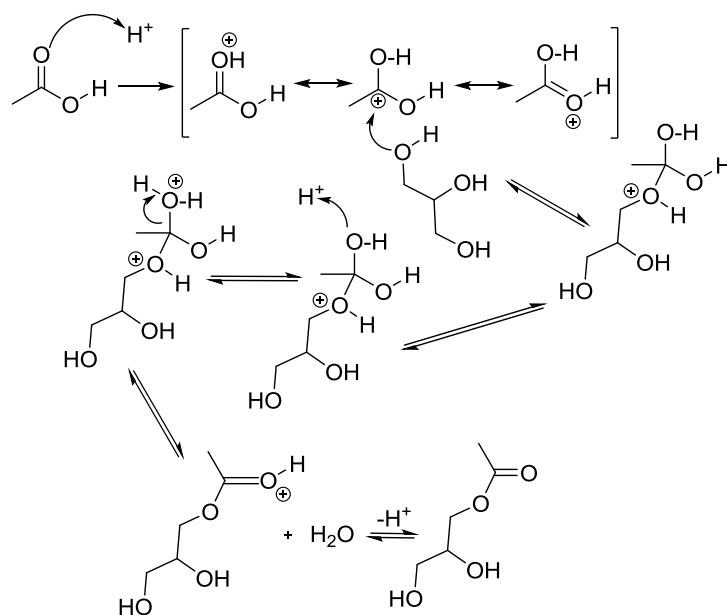
Table 3.6. Acetylation of glycerol with acetic acid using different loadings of $\text{MoO}_3/\text{SiO}_2$ [§]

Entry	Catalyst	Glycerol Conv., %	Acetin Selectivity, %		
			Mono-	Di-	Tri-
1	--	36	92	08	00
2	SiO_2	44	86	11	3
3	1 mol% $\text{MoO}_3/\text{SiO}_2$	100	56	28	17
4	10 mol% $\text{MoO}_3/\text{SiO}_2$	100	36	31	33
5	20 mol% $\text{MoO}_3/\text{SiO}_2$	100	17	33	50

[§] Reaction conditions: Acetic acid:glycerol-10:1 (molar ratio), Catalyst-10 wt% (w.r.t. glycerol), Temperature-100 °C, Time-8 h.

A maximum selectivity of 50% was obtained for triacetin when 20 mol% $\text{MoO}_3/\text{SiO}_2$ was used as catalyst (Table 3.6 entry 5). The main function of the catalyst in this reaction should be to direct the selectivity to the desired product i.e. triacetin. In this case increase in MoO_3 loading on SiO_2 increased the rate of spontaneous reaction of converting mono- to di- and ultimately to triacetin. We can assume that the traditional Fisher esterification mechanism is operating in case of blank reaction (without catalyst) and the reaction with SiO_2 as catalyst (Scheme 3.11).

Owing to the appreciable reactivity of $\text{MoO}_3/\text{SiO}_2$ for acetylation of glycerol, acidity seemed to have a dominant influence on the catalytic behavior in this reaction. NH_3 -TPD showed the global increase in acid strength with increase in MoO_3 loading on SiO_2 from 1 mol% to 20 mol% (Chapter 2, Table 2.1).



Scheme 3.11. Fisher esterification mechanism of glycerol with acetic acid to monoacetin

Moreover, from the pyridine adsorption studies it was seen that, Lewis acidity increased with incorporation of MoO_3 on SiO_2 and at higher MoO_3 loadings (10, 15, 20 mol%) the formation of Brønsted acid sites was observed which increased in the order $10 < 15 < 20$ mol% MoO_3 . This showed that both Lewis and Brønsted acid sites co-exist in the catalyst. Melero *et al.*^[43] showed a direct correlation between the selectivity of di- and triacetin and the strength of the acid sites of the sulfonic acid functionalized mesostructured materials: the strongest Brønsted acid sites caused the highest selectivity for di- and triacetin. In our case, highest selectivity for triacetin was obtained when 20 mol% $\text{MoO}_3/\text{SiO}_2$ was used as a catalyst. This catalyst showed highest acid strength (0.9 mmol/g) (NH_3 -TPD experiments) with a very high population of Brønsted acid sites (observed from the pyridine adsorption studies) directly correlated to the *in situ* formation of silicomolybdic heteropolyanions. The results are in good agreement with the earlier reported literature. This shows that acid strength and nature of acid sites are an important factor for the product distribution in the acetylation of glycerol.

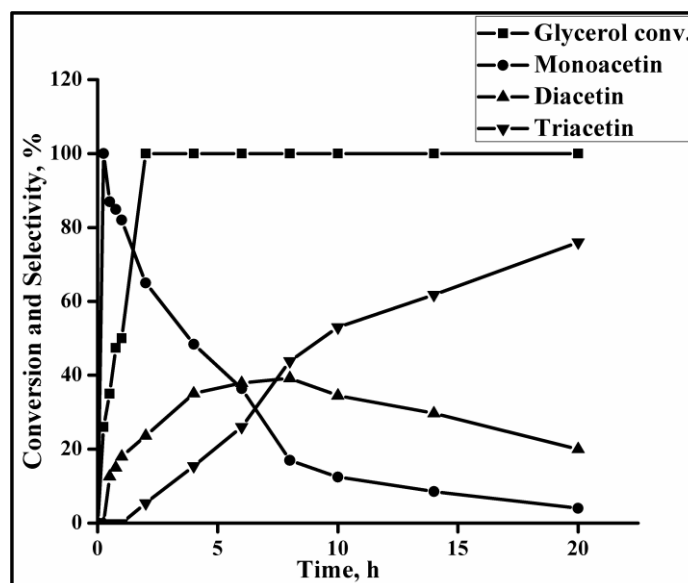


Figure 3.10. Acetylation of glycerol using 20 mol% $\text{MoO}_3/\text{SiO}_2$ as catalyst
 Reaction conditions: Glycerol-0.0108 mol, Glycerol:acetic acid-1:10 (molar ratio),
 Catalyst-0.1 g, Temperature-118 °C

The 20 mol% $\text{MoO}_3/\text{SiO}_2$ showed best results for acetylation of glycerol in comparison to that of the other $\text{MoO}_3/\text{SiO}_2$ catalysts in the series. This catalyst was further used to study the effect of temperature and time-on-stream parameter for the reaction. The reaction of glycerol and acetic acid was carried out at increased temperature of 118 °C with all other reaction conditions constant and the progress of the reaction was monitored at different time intervals till 20 h and the results are presented in Figure 3.10. The results were compared with that of the reaction carried out at 100 °C (Figure 3.11).

It was observed that in 15 min, 26% glycerol conversion was obtained with 100% selectivity for monoacetin. With time glycerol conversion increased to 47.4% after 45 min with 15% selectivity for diacetin without any formation of triacetin. Within 2 h, 100% glycerol conversion was achieved. The selectivity for monoacetin decreased with time with corresponding increase in di- and triacetin selectivity because di- and triacetin products were formed through consecutive esterification reactions. Though 100% conversion was achieved in 2 h, the reaction was continued further up to 20 h to attain maximum selectivity for triacetin. After 20 h of the reaction a very high selectivity of 76% was obtained for triacetin. When these results were compared with that of the reaction carried out at 100 °C (Figure 3.11), keeping the rest of the parameters constant, it was observed that 83% glycerol conversion was obtained in 2

h with 67% monoacetin and 26% and 7% of di- and triacetin, respectively. Maximum glycerol conversion of 97% was achieved after 8 h and there was no appreciable selectivity for triacetin.

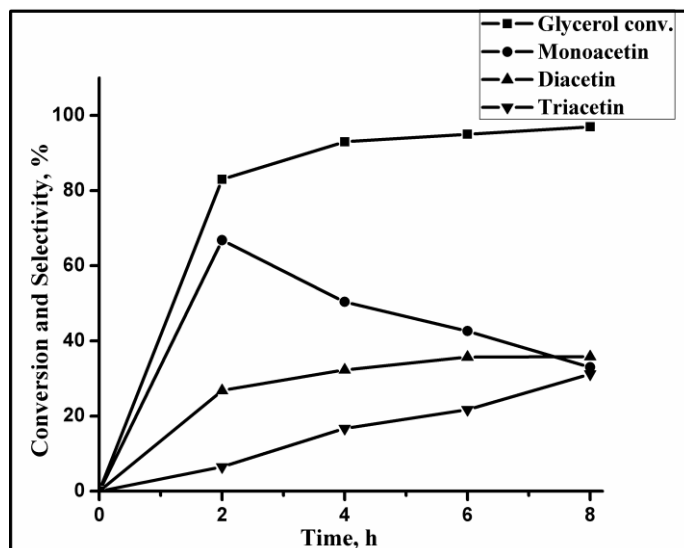


Figure 3.11. Acetylation of glycerol using 20 mol% $\text{MoO}_3/\text{SiO}_2$ as catalyst
Reaction conditions: Glycerol-0.0108 mol, Glycerol:acetic acid-1:10 (molar ratio),
Catalyst-0.1 g, Temperature-100 °C

Recently, a literature report describes the use of microwave or ultra sound conditions and achieved >90% glycerol conversion and ~85% selectivity for di- and triacetin collectively. Hydroxylated Mg fluorides were used as catalysts in this case and the reaction was carried out at 100 °C.^[44] Reddy *et al.*^[45] reported the $\text{SO}_4^{2-}/\text{CeO}_2\text{-ZrO}_2$ as promising catalyst for acetylation of glycerol when the reaction was carried out at 120 °C reaction temperature, 6:1 acetic acid to glycerol molar ratio and 5 wt% catalyst. However, in this >85% selectivity for triacetin was achieved in 40 h reaction time. Heteropoly acids supported on activated carbon were reported for the acylation of glycerol.^[46] In this case phosphotungstic acid (4.9 wt%) on activated carbon showed highest catalytic activity of 85% glycerol conversion in 3 h, although the reaction was carried out at 120 °C with glycerol:acetic acid molar ratio of 1:16. Diacetin was obtained with maximum selectivity in this case. In many literature reports for acetylation of glycerol, 100% conversion of glycerol was achieved in longer reaction time and in majority cases higher selectivity for diacetin is obtained.

In present case, 100% glycerol conversion was obtained in 2 h and triacetin was obtained with >75% selectivity at milder reaction conditions than discussed above.

3.4. Conclusion

The sol-gel synthesized MoO₃/SiO₂ catalyst was very efficient and stable for continuous esterification of ethanol with acetic acid for ethyl acetate formation. The catalyst was stable up to 60 h without any deactivation. Isolation and characterization of different catalytic species formed during the reaction showed the formation of SMA supported on nanosized silica to be catalytically active species responsible for high activity and high acidity of the catalyst. In presence of excess water almost 90% MoO₃ present in the catalyst was converted to SMA. This may be considered a simple procedure to prepare good quality reduced SMA. Industrial trials showed the activity of MoO₃/SiO₂ comparable with that of conventional homogeneous *p*-TSA. The catalyst showed appreciable activity for the acetylation of glycerol and acetic acid with 100% glycerol conversion in 2 h and 76% selectivity for triacetin at glycerol to acetic acid ratio of 1:10.

3.5. References

- 1 R. C. Larock, *Comprehensive organic transformations*, VCH publishers, NY, **1989**, Chap. 9.
- 2 M. A. Ogliaruso, J. F. Wolfe, *Synthesis of carboxylic acids esters and their derivatives*, Wiley, NY, **1991**.
- 3 a) Y. Izumi, R. Hasebe, K. Urabe, *J. Catal.* **1983**, 84, 402; b) Y. Izumi, K. Urabe, *Chem. Lett.* **1981**, 10, 663; c) I. Mochida, Y. Anju, A. Kato, T. Seiyama, *J. Catal.* **1971**, 21, 263; d) A. Corma, H. Garcia, S. Iborra, J. Primo, *J. Catal.* **1989**, 120, 78.
- 4 W.J. Tishchenko, *J. Russ. Phys. Chem. Soc.* **1906**, 38, 398.
- 5 Y. Obana, H. Uchida, K-I. Sano, *US Patent* **2005**, 006867164B2.
- 6 F. H. A. Bolder, *Ind. Eng. Chem. Res.* **2008**, 47, 7496.
- 7 a) G. Carotenuto, R. Tesser, M. Di Serio, E. Santacesaria *Catal. Today* **2013**, 203, 202; b) K. Inui, T. Kurabayashi and S. Sato, *Appl. Catal. A: General*, 2002, **237**, 53.
- 8 R. A. Crane, S. H. Brown, L. DeCaul, *US Patent* **1999**, 5973193

- 9 J. Bedard, H. Chiang, A. Bhan, *J. Catal.* **2012**, 290, 210.
- 10 T. V. Kovalchuk, J. N. Kochkin, H. Sfihi, V. N. Zaitsev, J. Fraissard, *J. Catal.* **2009**, 263, 247.
- 11 A. E-A. A. Said, M. MM A. El-Wahab, *J. Chem. Technol. Biotechnol.* **2006**, 81, 329.
- 12 H. Nabeshima, K. Ito, *JP Patent* **1995**, 276787.
- 13 S. Nomura, T. Hyoshi, *JP Patent* **1995**, 203429.
- 14 Y. Taguchi, A. Oishi, Y. Ikeda, K. Fujita, T. Masuda, *JP Patent* **2000**, 298099.
- 15 I. V. Kozhevnikov, *Chem. Rev.* **1998**, 98, 171.
- 16 V. L. C. Goncalves, B. P. Pinto, J. C. Silva, C. J. A. Mota, *Catal. Today* **2008**, 133-135, 673.
- 17 J. A. Melero, R. Grieken, G. Morales, M. Paniagua, *Energy Fuels* **2007**, 21, 1782.
- 18 P. Ferreira, I. M. Fonseca, A. M. Ramos, J. Vital, J. E. Castanheiro, *Catal. Commun.* **2009**, 10, 481.
- 19 P. Ferreira, I. M. Fonseca, A. M. Ramos, J. Vital, J. E. Castanheiro, *Appl. Catal. B: Environmental* **2009**, 91, 416.
- 20 L. Li, S. T. Yu, C. X. Xie, F. S. Liu, H. J. Li, *J. Chem. Tech. and Biotech.* **2009**, 84, 1649.
- 21 S. Yang, B. Lu, *Xibei Shifan Daxue Xuebao Ziran Kexueban* **1996**, 32, 43.
- 22 H. Wu, B. Yu, S. Ge, *Huagong Jinzhan* **2007**, 26, 1041.
- 23 H. Liu, Y. Lu, S. Gong, *Hebei Gongye Keji* **2007**, 24, 21.
- 24 H. L. Li, S. T. Yu, F. H. Liu, C. X. Xie, *Catal. Commun.* **2007**, 8, 1759.
- 25 N. Bremus, G. Dieckelmann, L. Jeromin, W. Rupilius, H. Schuett, *DE Patent* **1981**, 3004660.
- 26 A. Gawrikow, M. Hein, D. Reklat, K. Thoms, *DD Patent* **1982**, 1568038.
- 27 Y. G. Pecheney, M. A. Savinova, V. A. Ankudimov, N. I. Bastrakov, P. I. Fedotov, T. A. Dmitrieva, *RU Patent* **1995**, 2047596.
- 28 Y. Mitsuya, Y. Ogawa, *JP Patent* **1996**, 08027061, 3.
- 29 S. Mhaskar, K. Yeshwant, M. Sadguru, *IN Patent* **2002**, 188658, 12.
- 30 H. Wang, C. Zhang, H. He, L. Wang, *J. of Environmental Sciences* **2012**, 24, 473.

- 31 M. H. Tran, H. Okhita, T. Mizushima, N. Kakuta, *Appl. Catal. A* **2005**, 287, 129.
- 32 A. Griboval, P. Blanchard, E. Payen, M. Fournier, J. L. Dubois, J. R. Bernard, *Appl. Catal. A: General* **2001**, 217, 173.
- 33 S. B. Umbarkar, T. V. Kotbagi, A. V. Biradar, R. Pasricha, J. Chanale, M. K. Dongare, A. Mamede, C. Lancelot, E. Payen, *J.Mol. Catal. A: Chem.* **2009**, 310, 150.
- 34 W. Stober, A. Fink, E. Bohn, *J. Colloid Interface Sci.* **1968**, 26, 62.
- 35 A. A. Biradar, A. V. Biradar, T. Asefa, *ChemCatChem* **2010**, 2, 1004.
- 36 B. Torok, A. Molnar, N. Balogh, I. Kiricsi, I. Palinko, L. I. Horvath, *Appl.Catal. A* **1997**, 158, L17.
- 37 C. R. Deltcheff, M. Fournier, R. Franck, R. Thouvenot, *Inorg. Chem.* **1983**, 22, 207.
- 38 M. A. Banares, H. Hu, I. E. Wachs, *J. Catal.* **1995**, 155, 249.
- 39 T. Sugino, A. Kido, N. Azuma, A. Ueno, Y. Udagawa, *J. Catal.* **2000**, 190, 118.
- 40 A. Kido, H. Iwamoto, N. Azuma, A. Ueno, *Catal. Surv. Jpn.* **2002**, 6, 45.
- 41 J. Delgado, *SP Patent* **2002**, 2201894.
- 42 R. Wessendorf, *Petrochemia* **1995**, 48, 138.
- 43 J. A. Melero, R. van Grieken, G. Morales, M. Paniagua, *Energy & Fuels* **2007**, 21, 1782.
- 44 S. B. Troncea, S. Wuttke, E. Kemnitz, S. M. Coman, V. I. Parvulescu, *Appl. Catal. B: Environmental* **2011**, 107, 260.
- 45 P. S. Reddy, P. Sudarsanam, G. Raju, B. M. Reddy, *J. Ind. and Eng. Chem.* **2012**, 18, 648.
- 46 P. Ferreira, I. M. Fonseca, A. M. Ramos, J. Vital, J. E. Castanheiro, *Catal. Commun.* **2011**, 12, 573.

**Chapter 4: Acetalization and
Etherification of glycerol using
MoO₃/SiO₂ solid acid catalyst**

Abstract

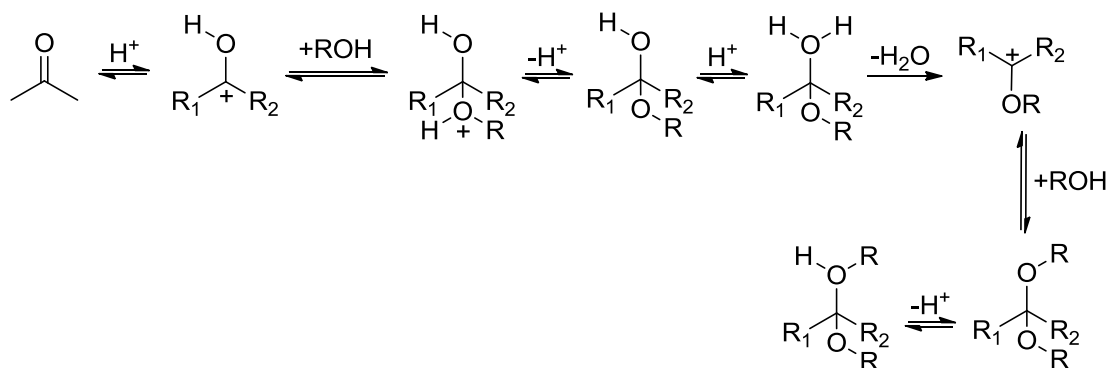
Acetalization of various aldehydes with glycerol and etherification of tert-butyl alcohol with glycerol has been carried out using series of mesoporous $\text{MoO}_3/\text{SiO}_2$ as solid acid catalyst. Maximum conversion of benzaldehyde (72%) was obtained in 8 h at 100 °C with 60% selectivity for the six-membered acetal using 20 mol% $\text{MoO}_3/\text{SiO}_2$ catalyst. However, with substituted benzaldehydes under identical reaction conditions the conversion of aldehydes decreased with increase in selectivity for six-membered acetals. The etherification of glycerol and various alcohols with tert-butyl alcohol (TBA) was carried out using 20 mol% $\text{MoO}_3/\text{SiO}_2$ as solid acid catalyst. Appreciable glycerol conversion of 67% was obtained in 8 h at 100 °C with 72% selectivity for tri-tert-butyl glyceryl ether (TTGE).

Section 4A: Acetalization of Glycerol using $\text{MoO}_3/\text{SiO}_2$ Solid Acid Catalyst

4A.1. Introduction

Acetalization reaction is one of the important methods used to protect carbonyl groups in the presence of other functional groups during the manipulation of multifunctional organic molecules.^[1] Acetals are generally stable to bases, Grignard reagents, hydrogenation reagents, metal hydrides, oxidants, bromination and esterification reagents. Besides the interest of acetals as protecting groups, many of them have direct applications as fragrances (eg. blossom orange scent-2-methyl-2-naphthyl-4-methyl-1,3-dioxolane), in cosmetics, food and beverage additives (eg. acetaldehyde diethyl acetal), pharmaceuticals, detergents, lacquer industries, as ignition accelerators, as antiknock additives in combustion engines^[2-5] and in port wine production (4/5-hydroxymethyl-2-methyl-1,3-dioxolane isomers).^[6,7] Sometimes, several acetals named as ‘potential fragrances’ (which exhibit little or no odour) are introduced into different formulations and, on contact with the skin the products are hydrolysed and the odorous molecules are released.^[8] It is known that the conversion of a carbonyl compound to an acetal, profoundly changes its vapour pressure, solubility, aroma characteristics and generally attenuates or alters its flavour impact. For eg., propylene glycol of vanillin is used as vanilla flavours because it causes flavour attenuation.^[9] Glycerol acetals can also be used as the intermediates for surfactants (alkoxyalkyl glycerol acetals).^[10,11]

Acetal formation is a reversible reaction (formation of water favours reversibility of the reaction) which proceeds by a two-step mechanism (Scheme 4A.1). The first step is the formation of a hemiacetal, followed by the removal of a water molecule. Acetal or ketal formation is strongly affected by electronic and steric factors, but it is generally accepted that the rate determining step of acetalization is the formation of a cation from the protonated hemiacetal. In order to compensate for the low rate of hemiacetal formation, the reaction media must be sufficiently acidic to promote effective protonation of any hemiacetal formed, and sufficiently polar to allow stabilization of the cationic intermediate.



Scheme 4A.1. Mechanism for acetalization of aldehydes or ketones by acid catalyst

Acetalization of aldehydes or ketones with glycerol leads to the formation of two isomeric cyclic products—six-membered 1,3 dioxane (**1**) and five-membered 1,3 dioxalane (**2**) (Figure 4A.1). Six-membered cyclic acetals are potential precursors for the production of green platform chemicals 1,3-dihydroxyacetone and 1,3-propanediol.^[12] In the acetalization reaction usually 50% of each five- and six-membered acetals are obtained. This phenomenon seems to be related to nearly identical reactivity of the primary and secondary hydroxyl group in glycerol and to similar tendencies for the formation of the 5- and 6-membered rings in **2** and **1**. Aksenes *et al.*^[13] carried out the direct separation of an isomeric mixture (**1**+**2**) into their components on a small scale with preparative gas chromatography. An isolation of one or both of the compounds on a large scale is feasible by converting the mixed isomers **1** and **2** into derivatives with sufficiently different physical properties (i.e., boiling point, polarity, solubility). However, this procedure is disadvantageous because of expensive purification steps and results in considerable loss of the target product.^[14,15] Hence efforts are being taken to change and control this ratio by varying the reaction parameters such as temperature, aldehyde or ketone to glycerol ratio and the choice of solvent.

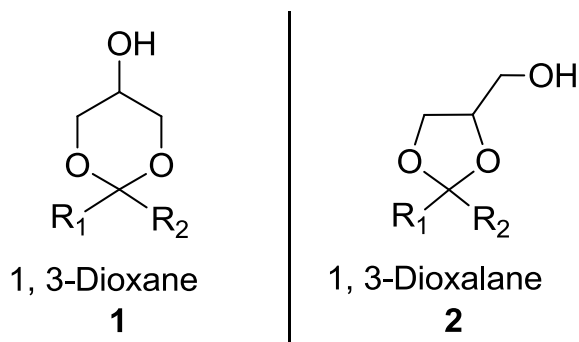


Figure 4A.1. The cyclic acetals formed by the condensation of glycerol with aldehydes or ketones

The conventional method for the synthesis of acetals is by treating carbonyl compounds with an alcohol or an orthoester in the presence of acid catalysts. Acetalization of aldehydes can be performed in the presence of weak acids, while ketones need stronger acids like sulfuric, hydrochloric or *p*-toluenesulfonic acid and larger amounts of catalyst. However, methods mentioned above present limitations such as use of expensive reagents, tedious work-up procedure and necessity of neutralization of the strongly acidic media leading to production of undesired wastes. Hence synthetic zeolites appear to be promising catalysts with the obvious advantages over conventional Brønsted or Lewis acids of easy separation from the reaction mixture, shape selectivity, and reusability.^[16,17] A number of acetalization procedures include the use of protic acids, Lewis acids (zinc chloride),^[18] alumina,^[19] montmorillonite,^[20,21] zeolites,^[22-25] mesoporous aluminosilicates^[26,27] and ion exchange resins.^[28,29] Supported metal oxides are well known for catalyzing a large variety of reactions. Thus many studies have been devoted to the preparation and characterization of these solids. Molybdenum oxide catalysts supported on SiO_2 , Al_2O_3 and TiO_2 have been extensively investigated because of their catalytic activity in oxidation and acid catalyzed organic reactions.^[30-34]

Till date, the condensation of glycerol with aldehydes or ketones, and especially possible influences on the reaction product ratio **1:2**, has not yet been investigated systematically. In continuation of our efforts to explore wider applicability of the $\text{MoO}_3/\text{SiO}_2$ catalysts for acid catalyzed organic transformations, acetalization of glycerol with various aldehydes was carried out. Based on the characterization results the catalyst activity has been correlated with the structural features of the catalyst and the results are discussed in this section.

4A.2. Experimental Section

4A.2.1. Material

All the reagents viz., glycerol, aldehydes, toluene of AR grade (99.8%) were obtained from S.D. Fine, LOBA and Merck chemicals, Thomas Baker, India. The chemicals were used without further purification.

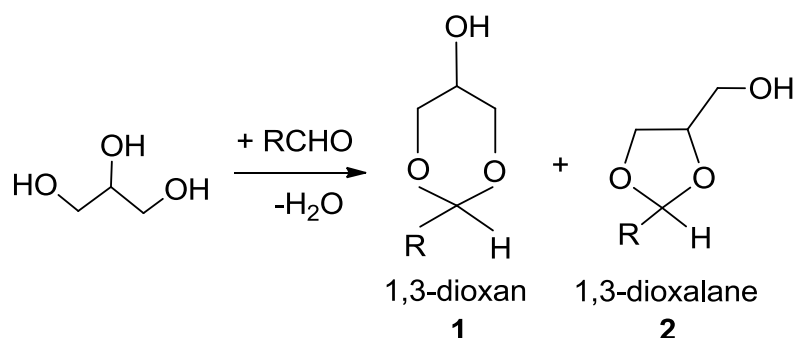
4A.2.2. Typical acetalization procedure

A typical acetalization of aldehydes with glycerol was carried out in a 50 mL two-necked round bottom flask fitted with a dean-stark apparatus. The flask was charged with glycerol (0.11 mol), aldehyde (0.1 mol), catalyst (10% by weight of glycerol) and solvent (15 g). The reaction mixture was vigorously stirred at 100 °C and reaction was continued till maximum conversion was achieved. Reaction was monitored by GC. Samples were withdrawn at regular time intervals and analyzed using a Hewlett-Packard GC model HP6890 with HP-5 (5% cross-linked polyethylene siloxane) column (diameter: 0.53 mm, film thickness: 1 µm, length: 60 m). After completion of the reaction, reaction mixture was cooled and filtered. The products were confirmed by GC-MS (model GC Agilent 6890N with HP-5 and MS Agilent 5973 network MSD, fitted with 30m capillary column).

4A.3. Results and discussion

4A.3.1. Catalytic activity

Initially, the acetalization of benzaldehyde with glycerol was studied as model reaction (Scheme 4A.2). The reaction was carried using a Dean-Stark apparatus. The Dean-stark apparatus was used to remove the water formed during the acetalization as azeotropic mixture with toluene as a solvent.



Scheme 4A.2. Acetalization of aldehyde with glycerol

Acetalization of benzaldehyde with glycerol was carried out using series of MoO₃/SiO₂ catalysts with different MoO₃ molar loadings on silica and the results are given in Table 4A.1. The reaction was carried out without catalyst, with the conventional catalyst *p*-TSA and pure SiO₂ for comparison. Benzaldehyde conversion with 1 and 10 mol% MoO₃ loading was 38% and 45% (Table 4A.1, entry 4 and 5), respectively, which increased to 72% with 20 mol% MoO₃/SiO₂ (Table 4A.1, entry 6). The conversion with MoO₃/SiO₂ catalysts was much higher compared to blank reaction (20%) and reaction using pure SiO₂ as catalyst (23%), thereby confirming the role of 'MoO₃' containing catalyst for the reaction. The benzaldehyde conversion using 20 mol% MoO₃/SiO₂ was marginally less (72%) compared to conventional homogeneous catalyst *p*-TSA (81%) under identical conditions proving the high efficiency of acidic MoO₃/SiO₂ for acetalization reaction. In all the cases selectivity for six-membered and five-membered acetals was 60% and 40%, respectively. The results clearly showed that the activity increased with increase in the MoO₃ loading and the maximum catalytic activity was obtained with 20 mol% MoO₃/SiO₂.

Table 4A.1. Acetalization of glycerol with benzaldehyde using different loadings of MoO₃/SiO₂[§]

Entry	Catalyst	Benzaldehyde conv., %	Selectivity, %		TON
			6-membered acetal	5-membered Acetal	
1	Blank	20	49	51	-
2	<i>p</i> -toluene sulfonic acid*	81	63	37	-
3	Pure SiO ₂	23	50	50	-
4	1 mol% MoO ₃ / SiO ₂	37	63	37	2476
5	10 mol% MoO ₃ / SiO ₂	43	62	38	324
6	20 mol% MoO ₃ / SiO ₂	72	60	40	304

[§] Reaction conditions: Glycerol-0.11 mol, Benzaldehyde-0.1 mol, Catalyst-10 wt% w.r.t. wt. of glycerol, Temperature-100 °C, Solvent (toluene)-15 g, Time-8 h.

*benzaldehyde: *p*-TSA-500:1.

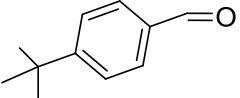
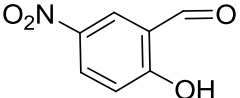
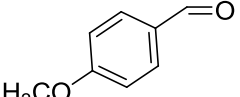
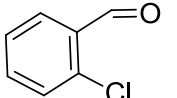
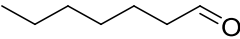
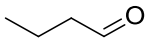
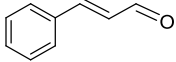
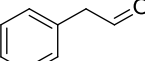
As 20 mol% MoO₃/SiO₂ showed maximum catalytic activity, acetalization of various aldehydes with glycerol was carried out using this catalyst, the results of which are shown in Table 4A.2. As discussed in Chapter 2 (Table 2.1, Figure 2.7) it was observed that the total acidity of the catalyst increased with increase in MoO₃ loading, 20 mol% MoO₃/SiO₂ showing the highest acidity among the series (0.9 mmol/g). From FTIR of pyridine adsorption it showed that catalysts with lower MoO₃ loading showed the presence of only Lewis acid sites, whereas MoO₃/SiO₂ catalyst with higher loadings 10, 15, and 20 mol% showed the co-existence of Lewis and Brønsted acidity (Chapter 2, Figure 2.8). The presence of Brønsted acidity is due to the formation of silicomolybdic (SMA) heteropolyanions in presence of moisture and water as observed from Raman spectroscopic studies (Chapter 2, Figure 2.11, 2.12). *In situ* formation of SMA on mesoporous SiO₂ support was found to be the catalytically active species for acid catalyzed reactions as discussed in Chapter 3. Therefore, the formation of SMA on SiO₂ support accounts for the high Brønsted acidity of the catalyst. Owing to these reasons, although 1 mol% MoO₃/SiO₂ catalyst showed the highest TON value, 20 mol% MoO₃/SiO₂ catalyst showed the highest activity. The TON for 1 mol% MoO₃/SiO₂ was 2476 (Table 4A.1, entry 4) whereas TON for 10 mol% MoO₃/SiO₂ and 20 mol% MoO₃/SiO₂ was found to be 324 and 304, respectively (Table 4A.1, entry 5 and 6). The highest TON in the case of 1 mol% MoO₃/SiO₂ might be because the finest particle size (0.5-1.6 nm) (Chapter 2, Figure 2.14) of molybdenum oxo species were uniformly dispersed on the SiO₂ support. The low TON for 20 mol% MoO₃/SiO₂ indicates that number of metal atoms taking part in the acetalization reaction are higher in 1 mol% MoO₃/SiO₂ than those compared to 10 mol% and 20 mol% MoO₃/SiO₂. Such behaviour may be ideally explained only if we take into consideration limited accessibility of the acid surface sites as result of physical blocking of a part of the active sites by the glycerol molecules strongly chemisorbed onto the surface. However, in this case the high activity of 20 mol% MoO₃/SiO₂ could be directly correlated to the formation of active SMA species on the surface of the catalyst thereby increasing the Brønsted acidity of the catalyst unlike that of 1 mol% MoO₃/SiO₂. This shows that the conversion of the substrate depends on the formation of active SMA species on the support which in turn enhances the acidity of the catalyst.

When the substrate scope was studied it was observed that in case of substituted benzaldehydes electron donating or electron withdrawing substitution on phenyl ring

led to decrease in glycerol conversion but with increase in selectivity for six-membered acetal. The drastic decrease in the conversion (23%) was observed in case of nitro and hydroxyl substitution at *meta*- and *ortho*-position, respectively (Table 4A.2, entry 2). In case of chloro- or other electron withdrawing substitution the conversion did not decrease significantly (Table 4A.2, entry 4). However, in case of *trans*-cinnamaldehyde very low conversion of only 10% was obtained (Table 4A.2, entry 7). This may be due to the unsaturation leading to decrease in the electrophilic character of carbonyl carbon. Aliphatic aldehydes gave higher conversions compared to aromatic aldehydes.

Corma and co-workers^[35] have reported acetalization of glycerol with phenyl acetaldehyde using various zeolites at higher temperature (~150 °C). USY-2 zeolite has showed up to 95% conversion and the selectivity for 1,3-dioxane/1,3-dioxolane 64/31 and in case of beta-2 and PTSA >90% conversion was obtained. However with modernite and MCM-41 as well as ZSM-5 the conversion decreased drastically up to 35% and 54%, respectively. In all the cases selectivity for five-membered acetal was slightly higher. When same zeolites were used for acetalization of propylene glycol with vanillin the yields obtained were in the range of 81-91%. In this work the glycerol or glycol was used in excess (2.5 equivalent). In the present work the selectivity for six-membered acetal was always higher and at lower conversions 100% selectivity for 1,3-dioxane was obtained using 20 mol% MoO₃/SiO₂ catalyst. Recently, Adam *et al.*^[36] reported ionic liquid (RHABIm-HSO₄) catalysed acetalization of benzaldehyde with glycerol and 75% conversion of benzaldehyde was achieved in 6 h with high selectivity for the five-membered acetal. Another recent report showed the use of niobia catalysts for the liquid-phase acetalization of glycerol with acetone without using any solvent to obtain solketal.^[37] Both the products were obtained in equivalent amounts. Deutsch *et al.*^[29] have used amberlyst-36 resin, nafion, H-beta and montmorillinite K-10 as catalysts for condensation of glycerol with different carbonyl compounds like benzaldehyde, formaldehyde and acetone. In case of glycerol and benzaldehyde maximum yield obtained for mixture of dioxolane and dioxane was 94% with the selectivity for dioxane/dioxolane in the range of 64/39 to 48/52. In this report very high selectivity for any particular isomer could not be achieved although very high conversions were attained.

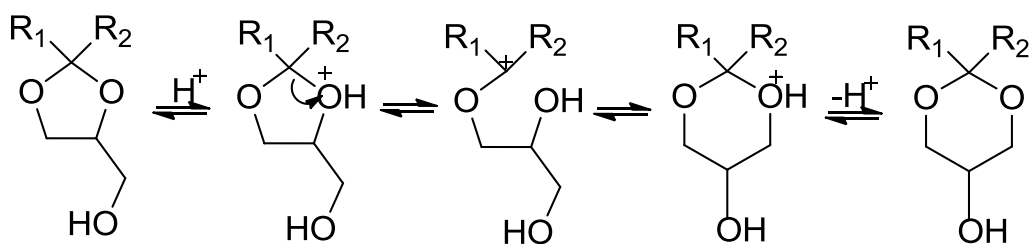
Table 4A.2. Acetalization of glycerol with various aldehydes[#]

Entry	Aldehyde	Aldehyde conv., %	Selectivity, %		TON
			6-membered Acetal	5-membered Acetal	
1		54	62	38	208
2		23	60	40	88
3		45	99	01	176
4		61 70 ^a	72 70	28 30	232
5		78	62	38	296
6		69	66	34	264
7		10	100	00	38.4
8		56	91	09	216

[#] Reaction conditions: Glycerol-0.11 mol, Aldehyde-0.1 mol, Time-8 h, Catalyst (20 mol% MoO₃/SiO₂)-10 wt% w.r.t. to wt. of glycerol, Temperature-100 °C, Solvent (toluene)-15 g, ^a-conversion after 16 h.

In all the previous reports very high selectivity for either of the isomer could not be achieved, whereas using MoO₃/SiO₂ high selectivity for six-membered acetal was achieved at lower conversion. It is proven fact that 1,3-dioxolane (**2**) is favored

kinetically, and isomerizes to the thermodynamically more stable 1,3-dioxane (**1**) as shown in Scheme 4A.3.^[4]



Scheme 4A.3. Mechanism of isomerization of 1,3-dioxolane to 1,3-dioxane catalyzed by Brønsted acid

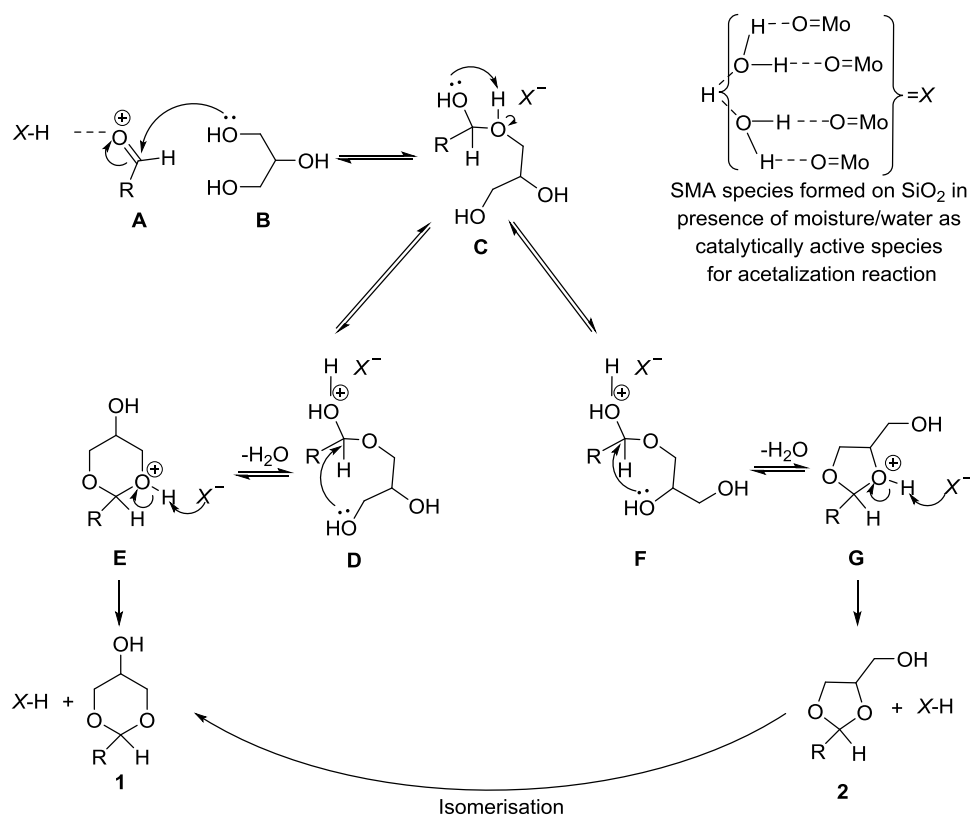
Climent *et al.*^[4] have carried out the kinetic studies for the acetalization of glycerol with phenylacetaldehyde using ZSM-5 and MOR and have achieved maximum selectivity for 1,3-dioxolane. In case of medium pore zeolite such as ZSM-5 or even for a large pore unidirectional zeolite as MOR the products might face a diffusional restriction that will be more severe for the formation of the transition state for converting 1,3-dioxolane to 1,3-dioxane. In case of 20 mol% MoO₃/SiO₂ as catalyst, the reaction could take place inside the large pores of 20 mol% MoO₃/SiO₂ (Table 4A.1, entry 6). Due to the mesoporous nature of the present catalyst the catalytically active sites were easily accessible to the reactants and the faster diffusion of the intermediates and the products into the pores of the catalyst, favored the formation of transition state for converting the 1,3-dioxolane (**2**) to 1,3-dioxane (**1**).

4A.3.2. Plausible mechanism for acetalization reaction

The suggested mechanism for acetalization of aldehyde using acid involves protonation of carbonyl group which needs Brønsted acidity. A very recent report by Baithy *et al.*^[38] suggested the mechanism of acetalization in presence of Mo and W catalysts supported on SnO₂. In this case it was observed that a large number of Brønsted acid sites on the catalyst compared to Lewis acid sites were responsible for the acetalization of carbonyl compounds like acetone and furfural with glycerol. In our case, owing to the protophilic nature of carbonyl carbon of the aldehyde and the high Brønsted acidity of the 20 mol% MoO₃/SiO₂ catalyst favours protonation which in turn increases the conversion of the reactants. Taking into account the *in situ*

formation of SMA species from MoO₃/SiO₂ catalysts, a plausible mechanism for the acetalization of aldehyde with glycerol can be put forth as shown in Scheme 4A.4.

Proton from the *in situ* formed SMA protonates the carbonyl 'O' of aldehyde (C). Then the less sterically hindered terminal hydroxy -OH of glycerol attacks carbonyl 'C' of the aldehyde to form C-O bond followed by the proton shift. The second -OH of glycerol attacks the quaternary carbon of aldehyde (D/F) with loss of one water molecule to regenerate the catalyst (E/G). In the acetalization reaction, the reactants will follow two different routes to yield 6-membered (1) and 5-membered acetals (2) as shown in the Scheme 4A.4. Five-membered acetal isomerizes to more stable six-membered acetal.



Scheme 4A.4. Plausible mechanism for the acetalization reaction by *in situ* formed SiO₂ supported SMA

4A.4. Conclusion

MoO₃/SiO₂ catalysts prepared by sol-gel technique were successfully used for acetalization of glycerol with various aldehydes. High conversion up to 78% was obtained for aliphatic aldehydes. Very high selectivity (up to 100%) for six-membered

acetal was obtained at lower conversions (10%); however, up to 70% selectivity for six-membered acetal was obtained at 70% conversion for *o*-chloro benzaldehyde. MoO₃/SiO₂ catalysts with 20 mol% Mo loading was found to be most active catalyst in the series. In each case, 6-membered acetal was achieved with maximum selectivity compared to 5-membered acetal.

Section 4B: Glycerol etherification using MoO₃/SiO₂ Solid Acid Catalyst

4B.1. Introduction

In the pursuit of value-addition of glycerol and considering innumerable routes to convert the glycerol to commodity materials, an interesting alternative is the transformation of glycerol molecule into oxygenated components for fuels. Other than acetalization, an attractive way is the etherification of glycerol with various alcohols mainly *tert*-butyl alcohol (TBA) or iso-butene (IB) to produce mono-, di-, and tri alkyl glyceryl ethers which act as fuel oxygenates. These ether derivatives of glycerol when attuned with diesel and biodiesel form excellent components for fuels. These ethers have very high octane numbers and therefore can be used as an alternative to gasoline blending oxygenates.^[39] These components enhance the energy efficiency and the stability of the fuel to lower the emissions when mixed with biodiesel. The glycerol ethers have proved to poses efficient burning properties with reduced pollutant and particulate matter emissions. Other than the applications as fuel additives,^[40] glycerol ethers have many potential uses, such as solvents,^[41] cryogenics,^[42] and anti-bacterial agents.^[43] There are many reports on the etherification of glycerol using IB to obtain a mixture of *tert*-butyl glyceryl ethers. However, use of IB has few disadvantages- a) IB is an expensive gas b) liquefaction of IB needs energy and the process thereby does not remain cost effective. Some oligomerization of IB is also reported to cause some decrease of ether selectivity based on converted IB. Another major limitation of the formation of glycerol ethers during this etherification reaction is the very low solubility of IB in glycerol.^[44,45] Alternatively, etherification of glycerol with TBA is an easy route for the production of *tert*-ethers of glycerol. Important superiorities of TBA over IB are- it is in liquid state and glycerol is easily miscible with TBA. Solvent is not required when TBA is used and the reaction can even be performed at atmospheric pressure. The etherification of glycerol can be carried out using homogeneous acid catalysts (e.g., *p*-TSA^[46] or ionic liquids with Brønsted acidity,^[47] but from an environmental point of view, heterogeneous catalysts are preferred. Different solid catalysts have been employed in the literature, mainly acid ion-exchange resins (e.g., Amberlyst 15^[48,49]

or Amberlyst 35,^[50] sulfonic acid-modified mesostructured silicas,^[51] large-pore zeolites (e.g., H-Y and H-β),^[50] and others (e.g., sulfonated peanut shell).^[52]

Herein, we have tried to extend the applicability of sol-gel synthesized MoO₃/SiO₂ catalyst as solid acid for etherification of glycerol and various alcohols with TBA and the results are discussed in this section.

4B.2. Experimental Section

4B.2.1. Material

Glycerol (>99%) was purchased from Thomas Baker, India ltd. All the alcohols were procured from Loba chemie pvt. ltd. All these chemicals were used without any further purification.

4B.2.2. Typical etherification procedure

a) Open reflux system-

The etherification reaction was carried out in 50 mL two-necked round-bottom flask fitted with a reflux condenser. The flask was charged with glycerol, an alcohol and 20 mol% MoO₃/SiO₂ catalyst (10 wt% w.r.t. wt. of glycerol). The reaction mixture was vigorously stirred at reflux temperature (80 °C).

b) Closed system-

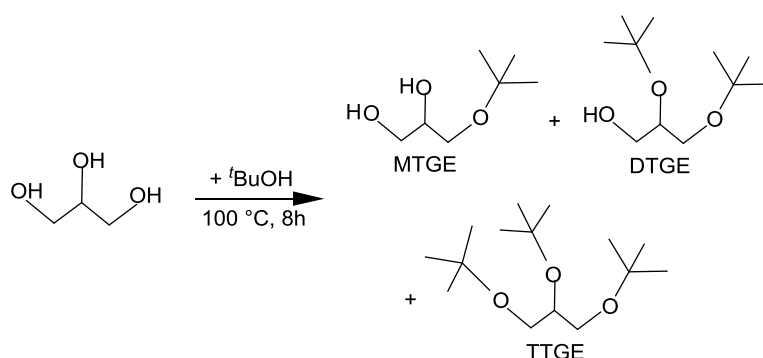
The etherification reaction was carried out in a 100 mL PARR 4343 SS 316 lab autoclave by Parr equipment pvt. ltd. The autoclave was equipped with a magnedrive, turbine stirrer, thermowell and a heating and cooling jacket located in the reactor wall. The reactions were performed at 100 °C and at autogeneous pressure.

The reactions were continued till maximum conversion was achieved. Reactions were monitored by GC. Samples were withdrawn at regular time intervals and analyzed using a Hewlett-Packard GC model HP6890 with HP-5 (5% cross-linked polyethylene siloxane) column (diameter: 0.53 mm, film thickness: 1 μm, length: 60 m).

4B.3. Results and discussion

Etherification of glycerol with TBA was studied in details using MoO₃/SiO₂ as solid acid catalyst. Like esterification, etherification of glycerol consists of three consecutive reversible steps: glycerol and TBA gives MTGE, which reacts with TBA to form DTGE and ultimately DTGE reacts with TBA leading to the formation of TTGE (Scheme 4B.1). DTGEs and TTGEs are miscible with diesel fuel and contain

high oxygen contents of 23.5% (DTGEs) and 18.5% (TTGEs), together with high octane numbers of 112-128 (blending research octane number, BRON) and 91-99 (blending motor octane number, BMON). As a result, DTGEs and TTGEs have been reported to be ignition accelerators and octane boosters, taking the place of methyl *tert*-butyl ether (MTBE). Owing to the importance of di- and tri-ethers, the objective of optimization of the reaction conditions was to achieve high glycerol conversion and low selectivity towards monoether. Therefore, a few reaction parameters have been studied considering the aim of the work. Preliminary studies were carried out at open reflux conditions.



Scheme 4B.1. Etherification of glycerol with TBA

All the etherification experiments were carried out using 20 mol% $\text{MoO}_3/\text{SiO}_2$ as solid acid catalyst, owing to its high acidity and activity as observed from earlier reactions studied in the thesis (esterification, acetalization). Effect of molar ratio of glycerol to TBA on etherification was studied and the results are given in Table 4B.1.

By stoichiometric equation, atleast three moles of TBA are required for each mole of glycerol to yield single mole of TTGE. Etherification being reversible reaction, amount of TBA should be in excess in order to drive the reaction towards the formation of DTGE and TTGE. As shown in Table 4B.1 glycerol conversion of 47% was obtained at TBA:glycerol molar ratio of 5:1. However, in all the cases MTB was obtained with 100% selectivity except for the reaction in which TBA:glycerol with molar ratio of 5:1 was used. Although the glycerol conversion increased with increasing TBA:glycerol molar ratio, the formation of DTGE and TTGE was not observed.

Table 4B.1. Effect of molar ratio of glycerol to TBA on etherification[#]

Entry	Molar ratio (TBA:Glycerol)	Glycerol Conversion, %	Selectivity, %		
			MTBE	DTBE	TTBE
1	1:1	13	100	00	00
2	3:1	26	100	00	00
3	5:1	47	93	07	00
4 [@]	5:1	67(73)	06(04)	22(24)	72
5*	5:1	52	21	43	36

[#] Reaction conditions: Catalyst (20 mol% MoO₃/SiO₂)-10 wt% w.r.t. wt. of glycerol, Temperature-80 °C, Time-8 h. [@] etherification carried out at 100 °C in an autoclave, rpm-700, autogeneous pressure; the values in bracket indicate the conversion and selectivity after 10 h. *etherification carried out at 100 °C in an autoclave using 7.5 wt% of catalyst w.r.t. wt. of glycerol.

Hence the effect of reaction temperature on etherification and product distribution was evaluated. As TBA (b.p. 80-82 °C) was one of the reactants, the etherification experiments were performed in liquid phase in an autoclave at a temperature of 100 °C. An appreciable glycerol conversion of 67% was achieved in 8 h with a very high selectivity of 72% for TTGE (Table 4B.1, entry 4). The reaction was continued up to 10 h in order to achieve maximum conversion of glycerol. However, the conversion of glycerol increased marginally to 73 % without any further increase in selectivity for TTGE. Therefore, reaction time of 8 h was found to be optimum to study further parameters. Keeping the reaction conditions as that for Table 4B.1, entry 4, and the reaction was carried out by decreasing the amount of catalyst to 7.5 wt% w.r.t. wt of glycerol. In this case, there was a drop in the conversion of glycerol from 67% to 52% in 8 h, with DTGE (43%) as a major product (Table 4B.1, entry 5).

Wider applicability of the catalyst was studied for etherification of various alcohols and diols with TBA and the results are tabulated in Table 4B.2. In the series of alcohols used for etherification, 1,2 butanediol showed the highest conversion of 39% compared to the remaining alcohols. The conversion decreased from 31% for 1,2 propanediol to 2% for ethanol. The reason for highest conversion of 1,2 butanediol

might be attributed to the presence of one -OH group on the neighbouring carbon and -CH₂-CH₃ which led to the formation of a more stable carbocation due to the induction of +I effect on the terminal carbon. This in turn enhanced the conversion of the substrate. In case of 1,2 propanediol, the respective carbocation is less stable compared to 1,2 butanediol. The conversion of 1,2 propanediol was therefore less (31%) than that of 1,2 butanediol. In case of etherification with aliphatic alcohols like *n*-propanol and ethanol only 9% and 2% conversions were obtained respectively. Thus aliphatic alcohols did not give any promising conversions. The conversions of the alcohols was in the order 1,2 butanediol>1,2 propanediol>*iso*-propanol>*n*-propanol>ethanol.

Table 4B.2. Etherification of TBA with various alcohols*

Entry	Alcohol	Conversion, %
1	1, 2 Butanediol	39
2	1,2 Propanediol	31
3	<i>Iso</i> -propanol	13
4	<i>n</i> -Propanol	9
5	Ethanol	1-2

*Reaction conditions: TBA:alcohol-5:1, Temperature-100 °C, RPM-700, Time-8 h, Autogeneous pressure.

In case of etherification of glycerol with TBA, there are many reports which describe the use of heterogeneous catalysts as solid acids. Mravec and co-workers^[48-50] reported the first heterogeneous catalytic route for the direct dehydrative etherification of glycerol with TBA under solvent-free conditions. In this report catalytic activities of different strong acid ion exchange resins were investigated. Mravec and co-workers found that the catalytic activities of acid ion-exchange resins were closely dependent on the resin structure (macroreticular or gel-type structure) and on the degree of cross-linking. In a first set of experiments, the authors studied the efficiency of two dried macroreticular acid-exchange resins (A15 and A35). Starting from a molar ratio of TBA/glycerol-2, they observed with catalyst A35 that a maximum glycerol conversion of 88% to the desired *tert*-butyl ethers was obtained at 75 °C. A further increase in the reaction temperature unfortunately led to a drop in the

reaction selectivity mainly owing to the significant byproduct formation of IB and dibutyl ethers. Catalyst A15 was less active than the solid catalyst A35 (68% conversion at 75 °C), and this phenomenon was attributed to the weaker acidity of A15. A similar phenomenon was already observed by Corma *et al.*^[53] In our case, the etherification was carried out under solvent-free conditions using 20 mol% MoO₃/SiO₂ as solid acid catalyst without formation of any side products or the oligomerized products under operating conditions. The conversions obtained were comparable with the reported literature. For effective etherification of glycerol using a solid acid, ideally the catalyst should have high stability and should possess high density of strong protonic acid sites. The cation-exchange resins and zeolites have been employed for etherification of glycerol.^[50,54] However, the major disadvantage of cation-exchange resins is poor thermal stability. For zeolites, the low density of strong protonic acid sites abates the reaction rate, and the small pore diameter leads to steric hindrance for the formation of TTGEs. Moreover, the high costs of these catalysts correspondingly increase the costs of the final products. In case of MoO₃/SiO₂ as solid acid, the formation of SMA on highly mesoporous SiO₂ support imparts it strong Brønsted acidity (as discussed in Chapter 3) with protonic sites which favors the etherification. Thereby, the sol-gel synthesized 20 mol% MoO₃/SiO₂ catalyst shows promising results for the etherification of glycerol with TBA.

4B.4. Conclusion

Sol-gel synthesized MoO₃/SiO₂ as solid acid catalyst was successfully used for the etherification of glycerol with ^tbutanol. The high stability of the catalyst and strong protonic sites of the *in situ* formed SMA on mesoporous SiO₂ support gave high glycerol conversion (67%) with 72% selectivity for TTGE in 8 h under solvent-free condition without formation of side products or oligomerization of glycerol.

4.5. References

- 1 T. W. Green, P. G. M. Wuts, *Protective Groups in Organic Synthesis*, Wiley, New York, 2nd edn. **1991**, 4, 212.
- 2 K. Bauer, D. Garbe, H. Surburg, *Common Fragrances and Flavours Materials*, 2nd edn., VCH, New York, **1990**.
- 3 D. Ballivet-Tkatchenko, S. Chambrey, R. Keiski, R. Ligabue, L. Plasseraud, P. Richard, H. Turunen, *Catal. Today* **2006**, 115, 80.
- 4 M. J. Climent, A. Corma, A. Vely, *Appl. Catal. A: Gen.* **2004**, 263, 155.
- 5 K. Woelfel, T. G. Hartman, *ACS Symp. Ser.* **1998**, 705, 193.
- 6 A. Cesar, D. S. Ferreira, J. C. Barbe, A. Bertrand, *J. Agric. Food Chem.* **2002**, 50, 2560.
- 7 K. Bauer, D. Garbe, H. Surburg, *Common Fragrances and Flavors Materials*, VCH, New York, 2nd edn., **1990**.
- 8 R. Suffis, L. B. Morton, K. Ishida, K. Sawano, A. G. Van Loveren, N. Tetsuo, C. B. Green, G. A. Reitz, R. K. L. Kang, T. Sato, *US Patent*, **1997**, 5626852.
- 9 G. A. Burdock, A. Fenarolis, *Handbook of Flavor Ingredients*, CRC, New York, 2nd edn., **1995**.
- 10 A. Piasecki, *J. of the American Oil Chemists' Soc.* **1992**, 69, 639.
- 11 M. Pagliaro, R. Ciriminna, H. Kimura, M. Rossi, C. Della Pina, *Angew. Chem. Int. Ed.* **2007**, 46, 4434.
- 12 A. J. Showler, P. A. Darley, *Chem. Rev.* **1967**, 67, 427.
- 13 G. Aksnes, P. Albrigtsen, P. Juvvik, *Acta Chem. Scand.* **1965**, 19, 920.
- 14 P. H. J. Carlsen, K. Soerbye, T. Ulven, K. Aasboe, *Acta Chem. Scand.* **1996**, 50, 185.
- 15 S. Bartoli, G. De Nicola, S. Roelens, *J. Org. Chem.* **2003**, 68, 8149.
- 16 A. Corma, L. T. Nemeth, M. Renz, S. Valencia, *Nature* **2001**, 412, 423.
- 17 A. Corma, M. Domine, L. T. Nemeth, S. Valencia, *J. Am. Chem. Soc.* **2002**, 124, 3194.
- 18 M. J. Ashton, C. Lawrence, J. A. Karlsson, K. A. J. Stuttle, C. G. Newton, B. Y. J. Vacher, S. Webber, M. J. Withnall, *J. Med. Chem.* **1996**, 39, 4888.
- 19 V. Vu Thuy, P. Maitte, *Bull. Soc. Chim. Fr.* **1975**, 9, 2558.
- 20 L. Tong-Shuang, L. Sheng-Hui, L. Ji-Tai, L. Hui-Zhang, *J. Chem. Res. (S)*,

- 1997**, 26, 18.
- 21 M. Csiba, J. Cleophax, A. Loupy, J. Malthete, S. D. Gero, *Tetrahedron Lett.* **1993**, 34, 1787.
- 22 A. Corma, M. J. Climent, H. García, J. Primo, *Appl. Catal.* **1990**, 59, 333.
- 23 R. Ballini, G. Bosica, B. Frullanti, R. Maggi, G. Sartori, F. Schroer, *Tetrahedron Lett.* **1998**, 39, 1615.
- 24 M. J. Climent, A. Corma, A. Velty, M. Susarte, *J. Catal.* **2000**, 196, 345.
- 25 A. Corma, M. J. Climent, M. Susarte, A. Velty, *Spanish Patent*, **1999** 9902439.
- 26 M. J. Climent, A. Corma, S. Iborra, M. C. Navarro, J. Primo, *J. Catal.* **1996**, 161, 783.
- 27 Y. Tanaka, N. Sawamura, M. Iwamoto, *Tetrahedron Lett.* **1998**, 39, 9457.
- 28 G. Cherkaev, S. A. Timonin, G. F. Yakovleva, L. Shutikova, A. S. Mikhailova, L. D. Shapiro, *SU Patent* **1987**, 337, 30.
- 29 J. Deutsch, A. Martin, H. Lieske, *J. Catal.* **2007**, 245, 428.
- 30 N. Ohler, A. T. Bell, *J. Catal.* **2005**, 231, 115.
- 31 S. K. Maurya, M. K. Gurjar, K. M. Malshe, P. T. Patil, M. K. Dongare, E. Kemnitz, *Green Chem.* **2003**, 5, 720.
- 32 P. T. Patil, K. M. Malshe, S. P. Dagade, M. K. Dongare, *Catal. Commun.* **2003**, 4, 429.
- 33 A. V. Biradar, S. B. Umbarkar, M. K. Dongare, *Appl. Catal. A: General* **2005**, 285, 190.
- 34 X. Ma, J. Gong, S. Wang, N. Gao, D. Wang, X. Yang, F. He, *Catal. Commun.* **2004**, 5, 101.
- 35 M. J. Climent, A. Velty, A. Corma, *Green Chem.* **2002**, 4, 565.
- 36 F. Adam, M. S. Batagarawa, K. M. Hello, S. S. Al-Juaid, *Chem. Pap.* **2012**, 66, 1048.
- 37 G. S. Nair, E. Adrijanto, A. Alsalmé, I. V. Kozhevnikov, D. J. Cooke, D. R. Brown, N. R. Shiju, *Catal. Sci. Technol.* **2012**, 2, 1173.
- 38 B. Mallesham, P. Sudarsanam, G. Raju, B. M. Reddy, *Green Chem.* **2013**, 15, 478.
- 39 R. S. Karinen, A. O. I. Krause, *Appl. Catal. A: General* **2006**, 306, 128.
- 40 C. J. A. Mota, V. L. C. Gonçalves, *Brazilian Patent* **2007**, PI 07000634.

- 41 S. Queste, P. Bauduin, D. Touraud, W. Kunz, J. M. Aubry, *Green Chem.* **2006**, 8, 822.
- 42 S. V. Koshchii, *Russ. J. Appl. Chem.* **2002**, 75, 1434.
- 43 M. P. Haynes, H. R. Buckley, M. L. Higgins, R. A. Pieringer, *Antimicrob. Agents Chemother.* **1994**, 38, 1523.
- 44 M. D. Serio, L. Casale, R. Tesser, E. Santacesaria, *Energy & Fuels* **2010**, 24, 4668.
- 45 R. S. Karinen, A. O. I. Krause, *Appl. Catal., A: General* **2006**, 306, 128.
- 46 H. J. Lee, D. Seung, I. N. Filimonov, H. Kim, *Korean J. Chem. Eng.* **2011**, 28, 756.
- 47 H. J. Lee, D. Seung, S. K. Jung, H. Kim, I. N. Filimonov, *Appl. Catal. A: General* **2010**, 390, 235.
- 48 K. Klepáčová, D. Mravec, E. Hájeková, M. Bajus, *Pet. Coal* **2003**, 45, 54.
- 49 K. Klepáčová, D. Mravec, M. Bajus, *Appl. Catal. A: General* **2005**, 294, 141.
- 50 K. Klepáčová, D. Mravec, A. Kaszonyi, M. Bajus, *Appl. Catal. A: General* **2007**, 328, 1.
- 51 J. A. Melero, G. Vicente, G. Morales, M. Paniagua, J. M. Moreno, R. Roldán, A. Ezquerro, C. Pérez, *Appl. Catal. A: General* **2008**, 346, 44.
- 52 W. Zhao, B. Yang, C. Yi, Z. Lei, J. Xu, *Ind. Eng. Chem. Res.* **2010**, 49, 12399.
- 53 A. Corma, S. Bee, S. Iborra, A. Velty, *J. Catal.* **2005**, 234, 340.
- 54 K. Klepáčová, D. Mravec, M. Bajus, *Chem. Pap.* **2006**, 60, 224.

Chapter 5: Summary and Conclusions

Abstract

This chapter delivers the overall summary of the results and highlights the key findings. The chapter wise results and discussions are briefed in the chapter to give an overview of the complete thesis.

Chapter 5: Summary and Conclusions

This chapter gives a brief summary of the results discussed in previous chapters and the overall conclusions derived from the work.

Chapter 1: Introduction

Chapter 1 gives a general discussion on the problem of depleting fossil fuels and the use of biorenewable resources as an alternative for the production of fuels and chemicals. The biorefinery concept was described in brief so as to define various breakthroughs for the conversions of bio-based materials like wood, oils, starch, lignin, cellulose/hemicellulose, proteins, etc. to number of value-added chemicals and bio-based fuels like biodiesel and bioethanol. The bioavailability, structure, versatility, chemical properties and renewability of glycerol, an important byproduct of biodiesel production, was discussed in detail. All the possible routes and industrial processes for the valorization of glycerol were described and the acid catalyzed organic transformations were emphasized. The detailed perspective on the design of solid acid catalysts for the valorization of glycerol was discussed. The scope and objective of thesis was given in detail.

Chapter 2: Synthesis and Characterization of the MoO₃/SiO₂ catalysts by sol-gel method

A simple sol-gel method was developed for the preparation of high surface area mesoporous MoO₃/SiO₂ catalysts (Mo loadings (1-20 mol%) using ammonium heptamolybdate (AHM) and ethyl silicate 40 (ETS-40) without the use of any organic template. These MoO₃/SiO₂ catalysts were characterized using XRD, BET, TEM, ammonia TPD, FTIR and Raman spectroscopy. Very high surface area of 896 m²/g with pore volume of 0.936 cc/g and the pore size distribution of 40-80 Å, was observed, indicating the mesoporous nature of silica. The XRD of the calcined samples showed the formation of amorphous phase up to 10 mol% MoO₃ loading and at higher loading crystalline α -MoO₃ on amorphous silica support. TEM analyses of the materials showed the uniform distribution of MoO₃ nanoparticles of 0.6-1.5 nm size on the silica support. The BET surface area decreased to 583 m²/g with

incorporation of 1 mol% MoO₃ and further decreased to 180 m²/g with increasing MoO₃ loading up to 20 mol%. Ammonia-TPD showed a drastic increase in acid strength after addition of 1 mol% MoO₃ compared to pure silica support and the acid strength increased with increasing MoO₃ content (0.94 mmol/g for 20 % MoO₃ loading). Raman spectroscopy showed the formation of silicomolybdic acid at low Mo loading and a mixture of α -MoO₃ and polymolybdate species at high Mo loadings.

Chapter 3: Sol-gel synthesized MoO₃/SiO₂ as Solid Acid Catalyst for Esterification reactions

Esterification of acetic acid and ethanol was carried out using sol-gel synthesized MoO₃/SiO₂ as a solid acid catalyst. An appreciably high conversion of acetic acid and selectivity for ethyl acetate was achieved for the liquid phase esterification. Deactivation of catalyst was not observed even when the esterification was carried out in continuous mode for 60 h. This clearly showed the stability of the catalyst under operating conditions. During the course of the reaction, the reaction mixture turned blue indicating the changes in the nature of catalyst under reaction condition. In order to understand the mechanistic aspects of the catalyst, the catalytic active species so formed in the reaction mixture were isolated, dried and characterized by P-XRD, BET-surface area, NH₃-TPD, FTIR, Raman, UV-Visible spectroscopy, TEM and EDAX. From the detailed characterization it was observed that there was *in situ* formation of silicomolybdic acid as catalytically active species for acid catalyzed reactions.

In continuation to our studies on esterification using MoO₃/SiO₂ as solid acid catalyst, esterification of glycerol with various acids was investigated. Acetylation of glycerol with acetic acid was studied in details to achieve maximum conversion of glycerol and high selectivity for triacetin (tri-acetylated product). The effects of various reaction parameters such as reaction temperature, molar ratio of acetic acid: glycerol, catalyst loading and time-on-stream were studied so as to optimize reaction conditions in order to achieve maximum selectivity for triacetin. The best results (100 % glycerol conversion in 2 h and 76% selectivity for triacetin in 20 h) were obtained in the presence of 20 mol% MoO₃/SiO₂ catalyst with high Brønsted acidity when the reaction was carried out at 118 °C, amount of catalyst (20 mol% MoO₃/SiO₂) used

was 10 wt% w.r.t. weight of glycerol and the acetic acid:glycerol molar ratio was 10:1.

Chapter 4: Acetalization and Etherification of glycerol using MoO₃/SiO₂ solid acid catalyst

This chapter is divided into two sections as follows-

Section 4A: This section deals with the study of acetalization of various aldehydes with glycerol using sol-gel synthesized MoO₃/SiO₂ as solid acids. Acetalization of benzaldehyde with glycerol was studied as a model reaction. The reaction was carried out using conventional *p*-TSA catalyst and pure SiO₂. The reaction was studied using different loadings of MoO₃/SiO₂. In the series, 20 mol% MoO₃/SiO₂ was the most promising catalyst for the acetalization of aldehydes with glycerol owing to its highest Brønsted acidity in the series. The activity of the catalyst was comparable with that of the conventional homogeneous *p*-TSA catalyst. A maximum of 72% benzaldehyde conversion was obtained in 8 h at 100 °C with 60% selectivity for the six-membered acetal. To study the substrate scope the reaction was carried out with a range of aliphatic and aromatic aldehydes using 20 mol% MoO₃/SiO₂ as catalyst. In all the cases 6-membered acetal was obtained with maximum selectivity. Substituted benzaldehydes with electron donating or electron withdrawing substitution on phenyl ring led to decrease in glycerol conversion but with increase in selectivity for six-membered acetal.

Section 4B: In this section the applicability of sol-gel synthesized MoO₃/SiO₂ catalyst as solid acid was extended for the etherification of glycerol. Etherification of various alcohols with *tert*-butyl alcohol (TBA) was carried out in a pressure reactor. ¹Butylation of glycerol was studied in detail. Various parameters of the reaction were studied and optimized to achieve maximum glycerol conversion and high selectivity for TTGE. A maximum of 67% glycerol conversion was obtained with 72% selectivity for TTGE at 100 °C in 8 h using 20 mol% MoO₃/SiO₂ as solid acid. Therefore the catalyst showed appreciable conversion and selectivity for etherification of glycerol.

List of publications and patents

1. **T. V. Kotbagi**, A. V. Biradar, S. B. Umbarkar, M. K. Dongare, “*Isolation, characterization and identification of catalytically active species in MoO₃/SiO₂ catalyst during solid acid catalyzed reactions*”, accepted for publication in ChemCatChem DOI: 10.1002/cctc.201200662.
2. S. B. Umbarkar, **T. V. Kotbagi**, A. V. Biradar, R. Pasricha, J. Chanale, Mohan K. Dongare, A. S. Mamede, C. Lancelot, E. Payen, “*Acetalization of glycerol using mesoporous MoO₃/SiO₂ solid acid catalyst*”, Journal of Molecular Catalysis A: Chemical **2009**, 310, 150-158. (rated 3rd in Top 25 hottest articles- October to December 2009)

Other publications

1. S. L. Pandhare, **T. V. Kotbagi**, M. K. Dongare, S. B. Umbarkar “*Copper-exchanged SiO₂/Al₂O₃ prepared by sol-gel method for intermolecular hydroamination of terminal alkynes*” *Current Catalysis*, 2, 2013, 62-69.
2. **T. V. Kotbagi**, D. L. Nguyen, C. Lancelot, C. Lamonier, K. A. Thavornprasert, Z. Wenli, M. Capron, L. Jalowiecki-Duhamel, S. B. Umbarkar, M. K. Dongare, F. Dumeignil “*Transesterification of diethyl oxalate with phenol over Sol-Gel MoO₃/TiO₂ catalysts*” *ChemSusChem* **2012**, 5, 1467-1473. Covered in *Chemistry Views* (http://www.chemistryviews.org/details/ezone/2360461/New_Sol-Gel_technique_for_the_Synthesis_of_MoxTi_Catalysts.html)
3. M. G. Chandagude, A. V. Biradar, **T. V. Kotbagi**, V. G. Puranik, M. K. Dongare, S. B. Umbarkar “*Selective oxidation of nonrefractory and refractory sulfides by cyclopentadienyl molybdenum acetylide complexes as efficient catalysts*” *Catalysis Letters* **2012**, 142, 1352-1360.
4. D.L. Nguyen, S. Gillot, D. O. Souza, P. Blanchard, C. Lamonier, E. Berrier, **T. V. Kotbagi**, M. K. Dongare, S. B. Umbarkar, S. Cristol, E. Payen, C. Lancelot “*One-pot sol-gel preparation for efficient cobalt molybdenum-TiO₂ hydrotreating catalysts*” *ChemCatChem* **2012**, 4, 2112-2120.
5. S. V. Bhosale, M. B. Kalyankar, S. V. Nalage, D. S. Bhosale, S. L. Pandhare, **T. V. Kotbagi**, S. B. Umbarkar, M. K. Dongare “*One-pot*

- synthesis of 2, 4, 5-trisubstituted imidazoles using MoO₃/SiO₂, an efficient and recyclable catalyst” Syn. Commun. 2011, 41, 762-769.*
6. A. V. Biradar, **T. V. Kotbagi**, M. K. Dongare, S. B. Umbarkar “*Selective N-oxidation of aromatic amines to nitroso derivatives using a molybdenum acetylide oxo-peroxo complex as catalyst*” Tetrahedron Lett. **2008**, 49, 3616-3619. (*highlighted in Catalysts and Catalyzed Reactions RSC Publications July 2008*)

Presentations at symposia

1. *Oral presentation at 2nd Indo-French Bilateral symposium on 'Catalysis for sustainable and environmental chemistry' at Univ. of Lille, Lille, France (11th-13th July 2012). Topic-"Transesterification of diethyl oxalate with phenol over sol-gel MoO₃/TiO₂ catalysts."*
2. *Best Poster award on National Science Day at NCL, Pune (26th February 2011). Topic-"A simple sol-gel synthesis of MoO₃/SiO₂ catalysts for various acid-catalyzed reactions."*
3. *Presented poster at 20th National Symposium on Catalysis (NSC-2010), NCCR, IIT-Madras, Chennai (19th-22nd December, 2010). Topic-"A simple sol-gel synthesis of MoO₃/SiO₂ catalysts for various acid-catalyzed reactions."*
4. *Oral presentation at 2nd Indo-French Bilateral symposium on 'Catalysis for sustainable and environmental chemistry' at NCL, Pune, India (11th-13th July 2010). Topic-"New sol-gel based preparation method for (cobalt-) molybdenum-TiO₂ catalysts."*
5. *Presented poster on National Science Day at NCL, Pune (26th February 2009). Topic-"Acetalization of glycerol using supported heteropolyacids as solid acid catalysts."*
6. *Oral presentation at 19th National Symposium on Catalysis (NSC-2009), NCL, Pune (19th-22nd January, 2009). Topic-"Oxidation of sulfides to sulfoxides and sulfones using CpMo(CO)₃CCPh as homogeneous catalyst."*

